

Investigation of MIMO Communications

By: William Tran

Patrick Kezer

Jeannie Whitmore

Rodrigo Mendez

Advisor: Dennis Derickson

California Polytechnic State University

San Luis Obispo, CA

June 2017

Table of Contents

List of Tables and Figures	iii
Acknowledgements	ix
Abstract	x
Chapter 1: Introduction to MIMO	1
1.1 Digital Communications	1
1.2 OFDM	5
1.3 Multipath and Fading	8
1.4 MIMO Overview	12
1.6 How Adding Antennas Improves Data Transmission	15
1.7 Beamforming	27
1.8 Precoding	29
1.9 Diversity Coding	29
1.10 Spatial Multiplexing	32
1.11 MIMO In Wi-Fi	34
Chapter 2: Keysight VSA/VSG Overview	35
2.1 VSG Overview	35
2.2 VSA Overview	35
2.3 Testing Hardware	36
2.4 Testing Software	39
Multi-Channel PXIe Config Utility	39
Multi-Channel Demo Tool	40
89600 VSA	40
Waveform Creator	40
2.5 Configuration Generation Walkthrough	41
2.6 Using C# to Generate Testing Environment	44
Chapter 3: Antennas and Pre-Amplifiers	55
3.1 Antennas Overview	56
Frequency	56
Radiation Pattern	57
Field Regions	59
Directivity	60
Efficiency	60
Gain	60
Beamwidth	61
Bandwidth	62

Polarization	62
Temperature	63
Friis Transmission Equation & the Wireless Domain	64
3.2 Anechoic Chamber Overview	66
3.3 Antenna Hardware	69
Antenna Overview	69
Antenna Implementation	70
Patch Antenna Overview	77
Patch Antenna Implementation	79
3.4 Preamplifiers Overview and Implementation	91
Overview	91
Implementation	92
Chapter 4: Test Data	98
4.1 SISO	98
SISO Experiment 1:	98
Purpose:	98
Procedure	98
Data	100
Discussion	103
SISO Experiment 2: Relationship between EVM and SNR	104
Purpose	104
Procedure	104
Discussion	110
SISO Experiment 3: Effects of modulation on EVM and SNR	110
Purpose	110
Procedure	110
Data	113
Discussion	118
4.2 MISO	119
Purpose:	119
Procedure	119
Data	121
Discussion	123
4.3 SIMO	124
Purpose:	124
Procedure	124
Data	126
Discussion	128
4.4 2x2 MIMO	128
Purpose:	128

Procedure:	128
Data:	130
Discussion:	133
Chapter 5: Conclusion and Recommendations	134
Appendix A: Senior Project Analysis	135
1. Summary of Functional Requirements:	135
2. Primary Constraints:	136
3. Economic:	136
4. If Manufactured on a Commercial Basis:	136
5. Environmental:	137
6. Manufacturability:	137
7. Sustainability:	137
8. Ethics:	138
9. Health and Safety:	138
10. Social and Political:	139
11. Development:	139
12. Bill of Materials:	140
Appendix B: References	141
MIMO Resources	141
Keysight and VSA/VSG resources	142
Antenna and Preamplifier Resources	144
Appendix C: Vector Signal Generator C# Code	145

List of Tables and Figures

Figures

Chapter 1: Introduction to MIMO

Figure 1.1: BPSK Data Stream	1
Figure 1.2: QPSK Constellation Diagram	2
Figure 1.3: 16-Point Constellation Diagram	3
Figure 1.4: Graphical Interpretation of Error Vector Magnitude (EVM)	4
Figure 1.5: FFT/IFFT Linearity	6
Figure 1.6: OFDM Communication Link	8
Figure 1.7: Probability Density Function of a Rayleigh Distribution	9
Figure 1.8: Doppler Shift Effect on Rayleigh Faded Signal	10
Figure 1.9: Probability Density Function of a Rice Distribution	11
Figure 1.10: Channel Capacity of SISO	14
Figure 1.11: 2x1 MISO Link	16
Figure 1.12: 1x2 SIMO Link	17
Figure 1.14: Waterfall Curve Example	24
Figure 1.15: BER Performance for Different Diversities	25
Figure 1.16: Increased Channel Diversity From Figure 1.15	26
Figure 1.17: Simplified Convolutional Encoder	30
Figure 1.18: Convolutional Encoded BPSK vs. Uncoded BPSK	31

Chapter 2: Keysight VSA/VSG Overview

Figure 2.1: Block Diagram of the M9381A VSG module from Keysight M9381A datasheet	37
Figure 2.2: Block Diagram of M9391A PXIe VSA module from Keysight M9381A datasheet	39
Figure 2.3: Shared LO wiring and module locations	41
Figure 2.4: Creating Driver Instances	46
Figure 2.5: VSG 1 and 2 Resource Names	46
Figure 2.6: Initialization	47
Figure 2.7: Configuring external triggers	48
Figure 2.8: Setting the Modulation Frequency	48
Figure 2.9: Uploading an Arbitrary Waveform	50
Figure 2.10: User Prompts	50
Figure 2.11: How to open Configurations	51
Figure 2.12: Configuration Window	52
Figure 2.13: VSA Instrument Selection	52
Figure 2.14: Channel Configuration	54
Figure 2.15: WLAN_11ac_256QAM_80MHz.setx	54
Figure 2.16: Change Measurement Type	55

Chapter 3: Antennas and Pre-Amplifiers

Figure 3.1: Frequency bands	57
Figure 3.2: Radiation pattern example	57
Figure 3.3: Types of radiation patterns	58
Figure 3.4: Visualizing Field Regions	59
Figure 3.5: Lobes visualized	61
Figure 3.6: Atmospheric attenuation, based on frequency	65
Figure 3.7: Block diagram of anechoic chamber	66
Figure 3.8: Anechoic chamber.	67
Figure 3.9: Inside of anechoic chamber	68
Figure 3.10: Transmit antenna for anechoic chamber.	68
Figure 3.11: The vector network analyzer used for antenna pattern measurements	68
Figure 3.12: Waveguide propagating modes visualized	69
Figure 3.13: Cantenna with SMA feed installed	71
Figure 3.14: Feed length, untuned	72
Figure 3.15: Uncalibrated feed, poor return loss and efficiency	72
Figure 3.16: Feed length, tuned	73
Figure 3.17: Calibrated feed, better return loss and efficiency	73
Figure 3.18: Cantenna Radiation Patterns, E-co and E-cross	75
Figure 3.19: Cantenna Radiation Patterns, H-Co and H-Cross	76
Figure 3.20: Differing microstip patch elements	77
Figure 3.21: Differing feed methods	78
Figure 3.22: Design dimensions of patch antenna. A transmission line feed is chosen.	80
Figure 3.23: 3-D view of patch antenna.	81
Figure 3.24: 3-D Radiation pattern of patch antenna.	81
Figure 3.25: Return loss of patch antenna.	82
Figure 3.26: Power characteristics of patch antenna.	82
Figure 3.27: Field characteristics of patch antenna.	83
Figure 3.28: Polarization characteristics of patch antenna.	83
Figure 3.29: Circuit board utilized	84
Figure 3.30: Othermill Pro milling machine	84
Figure 3.31: First prototype of the designed patch antennas..	85
Figure 3.32: First prototype return loss.	87
Figure 3.33: Second prototype of patch antennas.	88
Figure 3.34: Second prototype of patch antennas.	89
Figure 3.35: Radiation Pattern, E-Co and E-Cross	90
Figure 3.36: Radiation Pattern, H-Co and H-Cross	91
Figure 3.37: ERA-3+ Datasheet 1/3	93
Figure 3.38: ERA-3+ Datasheet 2/3	94
Figure 3.39: ERA-3+ Layout and Materials List 3/3	95
Figure 3.40: ERA-3+ first prototype implementation.	95

Figure 3.41: ERA-3+ characterization of the first prototype	96
Figure 3.42: ERA-3+ second prototype implementation	96
Figure 3.43: ERA-3+ second characterization	97
Chapter 4: Test Data	
Figure 4.1: SISO Experiment Setup	99
Figure 4.2: SISO Experiment Physical Setup	99
Figure 4.3: An instance of the IQ diagram, spectrum analyzer view, error vector spectrum	100
Figure 4.4: An instance of error vector summary, impulse response, and channel freq resp.	101
Figure 4.5: 2nd instance of IQ diagram, spectrum analyzer view, error vector spectrum	102
Figure 4.6: 2nd instance of error vector summary, impulse response, and channel freq resp	103
Figure 4.7: EVM-SNR Experiment Setup	105
Figure 4.8: QPSK 5 MHz bandwidth, center frequency at 1.28 GHz at 1 meter separation.	105
Figure 4.9: QPSK 5 MHz bandwidth, center frequency at 1.28 GHz at 2 meter separation.	106
Figure 4.10: QPSK 5 MHz bandwidth, center frequency at 1.28 GHz at 3 meter separation.	106
Figure 4.11: QPSK 5 MHz bandwidth, center frequency at 1.28 GHz at 4 meter separation.	107
Figure 4.12: QPSK 5 MHz bandwidth, center frequency at 1.28 GHz at 5 meter separation.	107
Figure 4.13: QPSK 5 MHz bandwidth, center frequency at 1.28 GHz at 6 meter separation.	108
Figure 4.14: SNR versus distance.	109
Figure 4.15: EVM versus SNR	109
Figure 4.16: Modulation experiment setup	111
Figure 4.17: Modulation experiment physical setup	111
Figure 4.18: Transmitter and receiver, along with amplifier	112
Figure 4.19: QPSK test case	113
Figure 4.20: 16 QAM test case	113
Figure 4.21: 64QAM test case	114
Figure 4.22: 128 QAM test case	114
Figure 4.23: 256 QAM test case	115
Figure 4.24: 512 QAM test case	115
Figure 4.25: 1024 QAM test case	116
Figure 4.26: 2048 QAM test case	116
Figure 4.27: EVM vs QAM Modulation relationship.	117
Figure 4.28: MISO experimental setup	120
Figure 4.29: MISO experiment physical setup	120
Figure 4.30: MISO 10 cm horizontal separation case	121
Figure 4.31: MISO 40 cm horizontal separation case	121
Figure 4.32: MISO no separation case	122
Figure 4.33: MISO 16 cm separation case	122
Figure 4.34: MISO experimental setup	125
Figure 4.35: MISO experiment physical setup	125
Figure 4.36: SIMO test case results.	126
Figure 4.37: SIMO test case results.	127

Figure 4.38: MIMO experimental setup	129
Figure 4.39: 802.11n OFDM 64 QAM Constellation Diagram	130
Figure 4.40: OFDM Error Summary	130
Figure 4.41: Channel 1 Spectrum	131
Figure 4.42: Channel 2 Spectrum	131
Figure 4.43: OFDM MIMO Channel Information Matrix	132

Equations

Chapter 1: Introduction to MIMO

Equation 1.1: Fast Fourier Transform (FFT) and Inverse Fast Fourier Transform (IFFT)	6
Equation 1.2: Received signal in a Rician faded channel.	11
Equation:1.3: Information in event with probability Pi	13
Equation 1.4: Information transmission equation	13
Equation 1.5: Mutual Information Function	13
Equation 1.6: Shannon Capacity	14
Equation 1.7: Channel Capacity of MISO	16
Equation 1.8: Channel Capacity of SIMO	17
Equation 1.9: Channel Capacity of SIMO, adjusted	17
Equation 1.10: Channel Capacity of MIMO	19
Equation 1.11: Direct Transmission Model	20
Equation 1.12: Channel State Matrix	20
Equation 1.13: Direct Transmission Model, substituted	21
Equation 1.14: Channel Capacity of MIMO, simplified	21
Equation 1.15: Spatial Multiplexing Gain	33

Chapter 3: Antennas and Pre-Amplifiers

Equation 3.1: Thermal Noise Equation	63
Equation 3.2: Friis Transmission Equation	64
Equation 3.3: Friis Transmission Equation, logarithmic form	64
Equation 3.4: Friis Transmission Equation, polarization factor	65
Equation 3.5: Circular waveguide cutoff wavelength	70
Equation 3.6: Relative permittivity adjusted half wavelength	79
Equation 3.7: Friis Noise Equation	92

Chapter 4: Test Data

Equation 4.1: EVM-SNR theoretical equation	104
Equation 4.2: EVM-SNR theoretical equation, 64 QAM	104

Tables

Chapter 3: Antennas and Pre-Amplifiers

Table 3.1: Transverse magnetic field mode constants	70
Table 3.2: Transverse electric field mode constants	70
Table 3.3: Computing cutoff wavelengths for TM modes	70
Table 3.4: Computing cutoff wavelengths for TE modes	70
Table 3.5: Physical dimensions of simulation-tuned patch antenna	80

Chapter 4: Test Data

Table 4.1: Compiled data of SNR-EVM experiment	108
Table 4.2: Compiled modulation	117
Table 4.3: Compiled MISO cases	123
Table 4.4: Compiled cases of EVM: SISO through MIMO	132

Acknowledgements

We would like to first thank all our family for their support and understanding. We would also like to thank Dr. Clay McKell, Dr. Dean Arakaki, and Dr. Tina Smilkstein for their tutorage in covering the topics of MIMO. We cannot forget the help and support from the staff at Keysight Technologies, as they have provided the equipment in the Advanced Communications Laboratory necessary to complete this project. And last but not least, we would like to thank Dr. Dennis Derickson for accepting to be our senior project advisor and encouraging us to push forward when the project goals seemed unreachable.

Abstract

The goal of this project is to investigate the multiple input multiple output (MIMO) wireless communication technique by incorporating multiple antennas to develop a 2x2 MIMO link. This consists of multiple antennas at both ends of the link, 2 transmitting and 2 receiving. The MIMO system should then be able to send and receive a message signal. Additionally, at various constructions of the system, data can be acquired to observe exactly how the increase in the number of antennas affects the performance of the system to form an overall base of performance, from start to finish. The various stages of the system are single input single output (SISO), single input multiple output (SIMO) and multiple input single output (MISO) systems. MIMO addresses the capacity (capacity = b/s/Hz) issue with these various systems. The capabilities of MIMO communication systems are a linear improvement in capacity without increasing transmit power, the trade-off being complexity introduced through the multiple transmitters and receivers. In MIMO communication, the transmit power is evenly split between the antennas of the system. Furthermore, MIMO enhances the dimensions of communication through the use of multiple channels, so that bits can be sent in a parallel fashion. By using multiple channels, the same data can be sent through these channels to increase probability of successful transmission should one of the channels fail. An understanding of all these concepts is the scope of this project through research, implementation and measurements. MIMO is an important topic for communications as 4G, LTE, and 5G all apply this idea.

Chapter 1: Introduction to MIMO

1.1 Digital Communications

Before we talk about the most common methods for MIMO modulation, it is important to first look at how digital communication works. The most primitive form of digital modulation is called Binary Phase-Shift Keying, more commonly referred to as BPSK. In BPSK a binary data stream is modulated with a sine wave carrier signal. The binary data stream has values of either '1', to represent a binary 1, or '-1', to represent a binary 0. Figure 1.1 shows where BPSK gets its name from; the sine of the carrier signal undergoes a 180° phase shift when the data stream goes from a binary 0 to a binary 1.

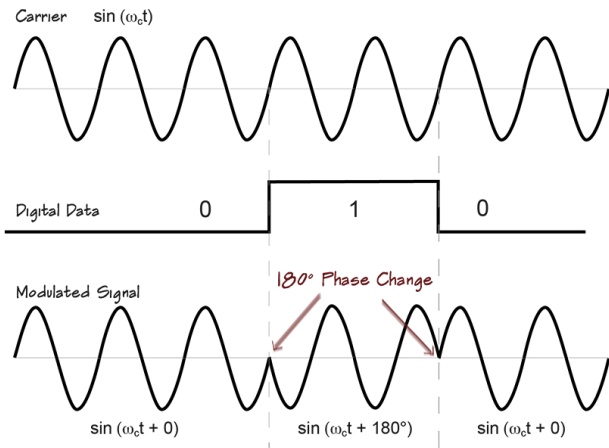


Figure 1.1: BPSK Data Stream

The data being transmitted in BPSK can only take on two values which makes it the most robust form of digital communications. However, one drawback is that only one bit can be transmitted at a time which limits the data throughput thus advocating slow data rates.

BPSK has been expanded on to create Quadrature Phase-Shift Keying, most commonly referred to as QPSK. QPSK takes advantage of the nature of quadrature signals like sine and cosine. Sine and cosine are said to be quadrature signals because they are 90° out of phase; this means that in the frequency domain the spectra of sine and cosine will not interfere with each other. In QPSK, one data stream (I-Channel) can be modulated with a sine wave and another data stream (Q-Channel) can be modulated with a cosine wave. Compared to BPSK, double the data can be transmitted at the same bandwidth. At the receiving end, the data can be decoded into a 4-point constellation diagram with each symbol having the binary value of '00', '01', '10', or '11'. Figure 1.2 shows the constellation diagram of QPSK modulation.

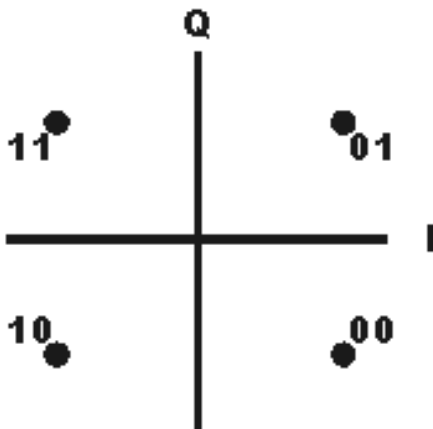


Figure 1.2: QPSK Constellation Diagram

Amplitude Modulation can be used in conjunction with QPSK to create Quadrature Amplitude Modulation, referred to as QAM. In QAM, the data streams in the I- and Q-Channels no longer only take on values of 1 and -1, but can now have multiple discrete values. Let's look at an example.

In a QAM system there are an I-Channel and a Q-Channel, each of which has 2 bits to represent the analog voltage of the digital waveform: '00' represents -1, '01' represents -0.33, '10' represents 0.33, and '11' represents 1. The I-Channel is then modulated with a sine wave and the Q-Channel is modulated with a cosine wave. The received symbols are represented with 4 bits (2 bits from each channel) to create a 16 point constellation diagram, seen in Figure 1.3. This type of modulation is called 16QAM because it yields a constellation diagram of 16 points.

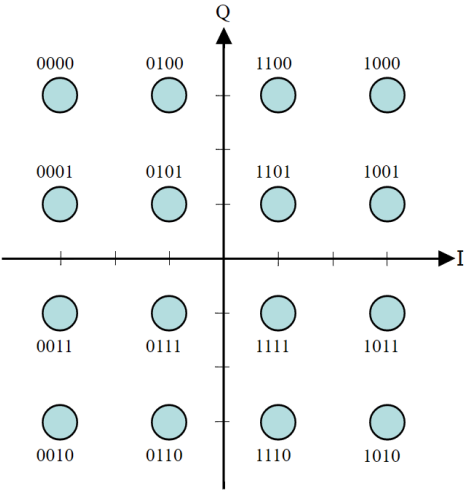


Figure 1.3: 16-Point Constellation Diagram

Larger constellation diagrams can be achieved by increasing the number of bits in the I- and Q-Channels: 64QAM, 256QAM, 1024QAM, etc. With a higher number of bits in the I- and Q-Channels comes a higher data transmission rate, however, the integrity of the correct symbol being decoded is at risk.

The constellation diagrams shown in Figures 1.2 and 1.3 are the ideal depiction of what the constellation diagram should look like. In practice, a decoded symbol may not fall directly on the referenced symbol location; this can be quite problematic in higher QAM systems. A measurement called Error Vector Magnitude, EVM, is used to represent this deviation from ideality. As seen in the Figure 1.4 below, the ideal symbol location is at '11', however, the transmitted symbol was decoded at a much different location.

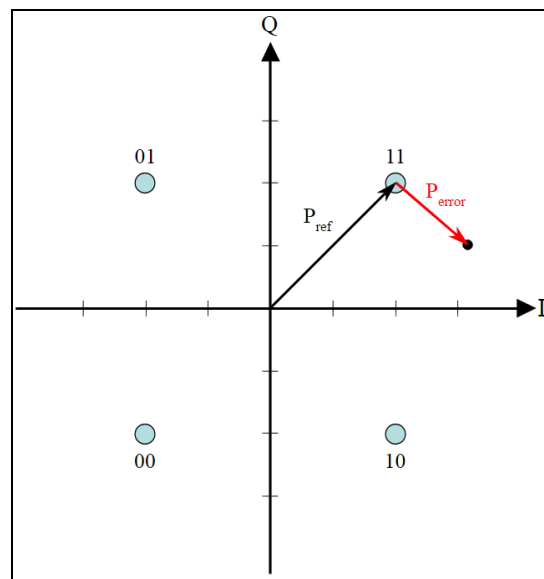


Figure 1.4: Graphical Interpretation of Error Vector Magnitude (EVM)

A magnitude vector labeled P_{ref} is used to represent the location of the ideal symbol, P_{error} denotes the actual location of the transmitted symbol. EVM is a calculated measurement that displays the ratio of P_{error} to P_{ref} . Often displayed in dB or a percentage, the two most common calculations for EVM are: $EVM(dB) = 10\log_{10}(P_{error}/P_{ref})$ and $EVM(\%) = (P_{error}/P_{ref})^{1/2} * 100$. One drawback of this measurement is that it only shows the deviation from the intended location. In higher QAM systems, the intended location on the constellation diagram may become quite ambiguous. This ambiguity implies that the EVM may not be the most reliable error measurement.

1.2 OFDM

Orthogonal Frequency Division Multiplexing (OFDM) is a digital data encoding method that allocates data to various different frequencies. This is done by splitting the data stream into multiple lower bit rate streams each of which is placed onto a predetermined frequency. Each of the split data streams occupy their own bandwidth such that there is no channel interference due to the orthogonality of the signals. In OFDM we call each of the carrier frequencies sub-carriers; for OFDM to work, it is important that each of these sub-carriers are orthogonal. Orthogonality allows for simultaneous data transmission on adjacent channels with minimal interference.

Let's go through an example to better understand how OFDM works. Say we have a binary data stream of 1, 1, 1, -1, 1, -1, 1, -1, -1 and an OFDM link with three sub carriers: c1, c2, and c3. The data stream first undergoes a serial-to-parallel conversion, each sub-carriers handles a third of the data. c1 will be transmitting bits 1, -1, and 1, c2 will be transmitting bits 1, 1, and -1, and c3 will be transmitting bits 1, -1, and -1. The data in c1, c2, and c3 all make up their own symbol, which is different from the 'symbol' we discussed in the previous section. The modulation frequencies are chosen such that it satisfies the Nyquist Criterion; in order to minimize distortion between symbols the frequency of c2 and c3 are harmonics of c1. Each symbol then undergoes an Inverse Fast Fourier Transform (IFFT). The equation for the FFT and IFFT can be seen below:

DFT(FFT):

$$X(k) = \sum_{n=0}^{N-1} x(n) \cdot e^{-j\left(\frac{2\pi}{N}\right)nk} \quad (k = 0, 1, \dots, N-1)$$

IDFT(IFFT):

$$x(n) = \frac{1}{N} \sum_{k=0}^{N-1} X(k) \cdot e^{j\left(\frac{2\pi}{N}\right)nk} \quad (n = 0, 1, \dots, N-1)$$

Equation 1.1: Fast Fourier Transform (FFT) and Inverse Fast Fourier Transform (IFFT)

Performing an IFFT here seems to be counter-intuitive. Usually when we think of an IFFT we imagine a function that converts a spectrum to a time domain signal, however, this is not always the case. In reality, this block can be either the FFT or IFFT, the latter is chosen simply because it produces a time domain signal. One must remember that the FFT and IFFT are linear functions, this means that it does not matter which is used on the transmit end as long as the other is used on the receive end. Figure 1.5 show the linear property of the FFT and IFFT.

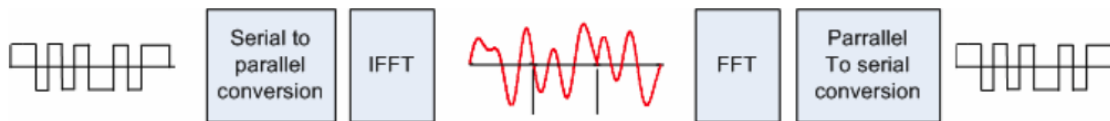


Figure 1.5: FFT/IFFT Linearity

The IFFT block quickly computes the time domain signal of the parallel inputs simultaneously rather than doing each carrier individually. The signals are then added together using a parallel to serial converter.

The final step before transmitting the data is called cyclic prefixing. Generally in OFDM signals, the last 10% to 25% of the data is copied and added to the beginning of the data stream. Ideally, we would want to do this for each of the carriers, but since the data is a linear combination of all the carriers we can only do it on the aggregation of the package. Adding a cyclic prefix is important because it reduces intersymbol interference (ISI), as well as mitigates the possibility of circular convolution (important for frequency domain data processing). We must remember that adding a cyclic prefix increases the length of the data we wish to transmit, this will increase the bandwidth of signals' spectrum. This increase in bandwidth must be accounted for such that our signal does not interfere with other signals operating at adjacent bands.

At the receiving end, the data is first brought back down to baseband using a demodulator. The cyclic prefix is then removed from the data stream. The data stream is then fed into a serial-to-parallel converter so that an FFT can be performed. The FFT is used to undo the effects of the IFFT in the transmitter side; this also removes carriers c_1 , c_2 and c_3 . Finally, the data goes through a parallel-to-serial converter to recreate the starting data stream. Figure 1.6 shows a basic block diagram of an OFDM link.

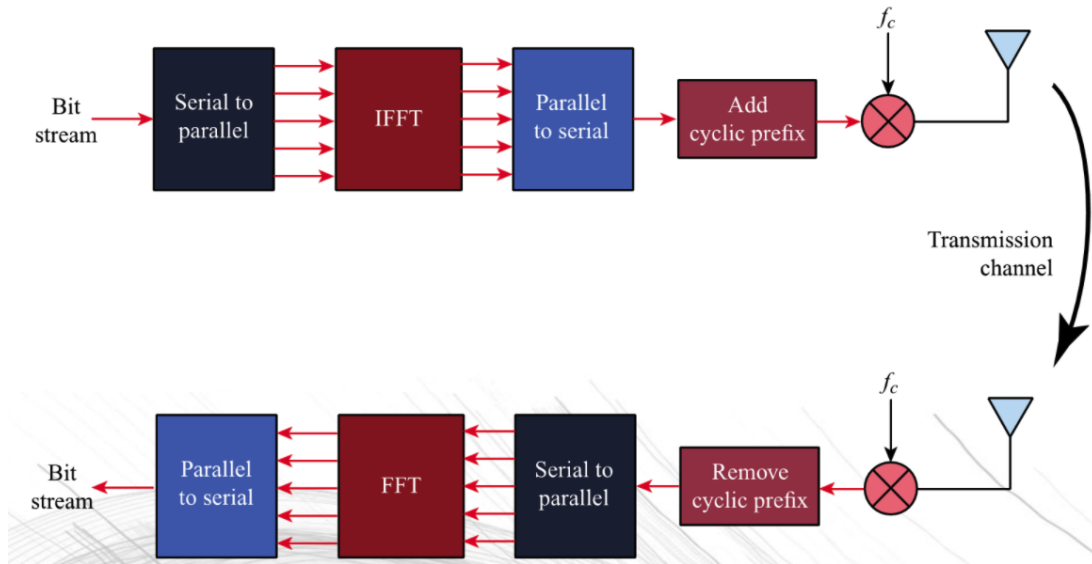
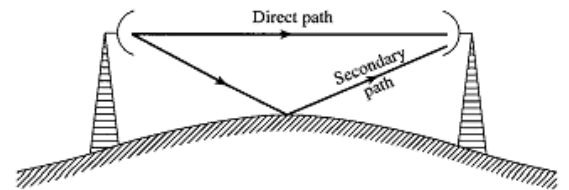


Figure 1.6: OFDM Communication Link

1.3 Multipath and Fading

Recently, MIMO systems have been designed to exploit the phenomena of multipath propagation, commonly referred to as just multipath; but what is multipath? Why is it problematic? And how can it be used to our

advantage? In simple terms, multipath is phenomena of wireless signals arriving at a receiver through various different paths. In the past, when using SISO links, this phenomena became very problematic because multipath propagation leads to multipath interference. Imagine that we are transmitting a signal and the signal that propagates along the secondary path arrives at the receiver with a 180° delay relative to the signal that propagates along the primary path. In this scenario, destructive interference would occur and our signal would be entirely wiped out; any chance of accurately decoding the signal would be lost! This destructive interference causes channel fading. The two most common forms of fading are Rayleigh fading and Rician



fading. Rayleigh fading occurs when signals from various paths arrive at the receiver with a Rayleigh distribution.

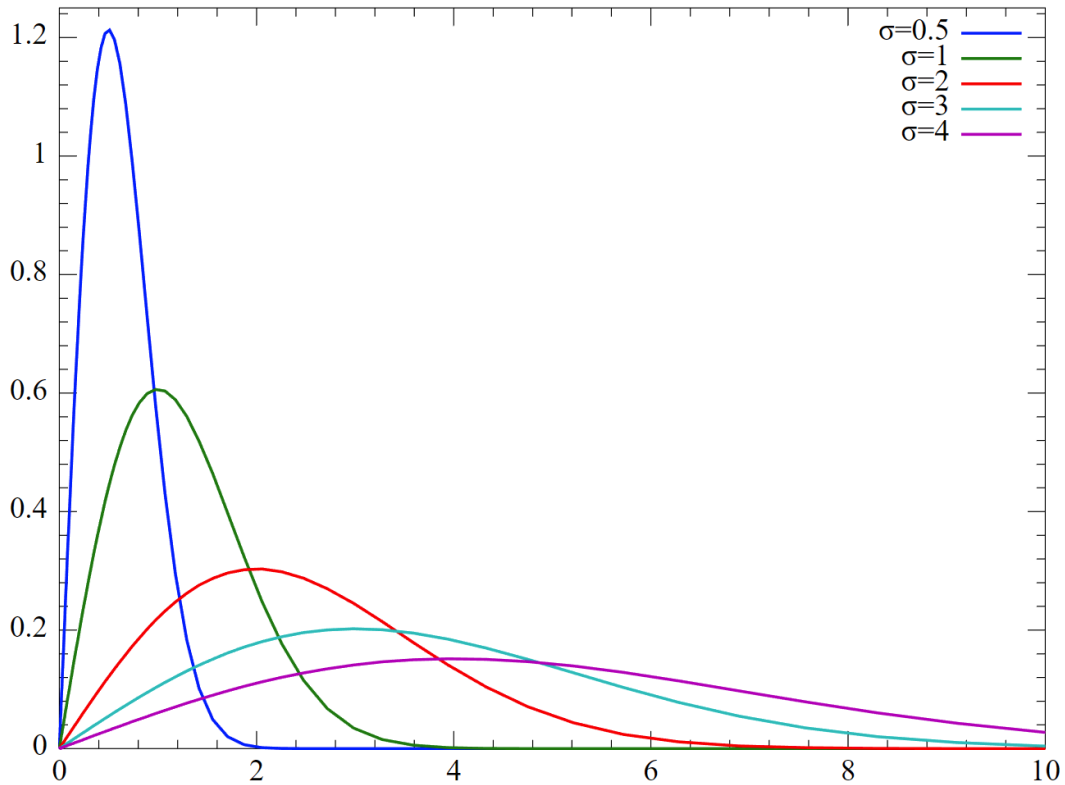
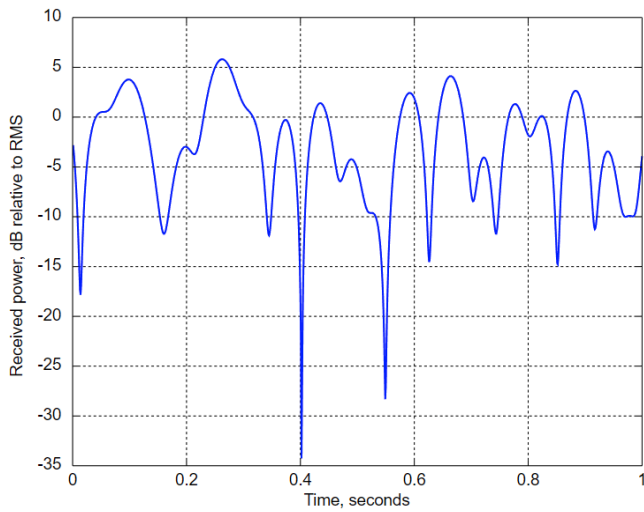
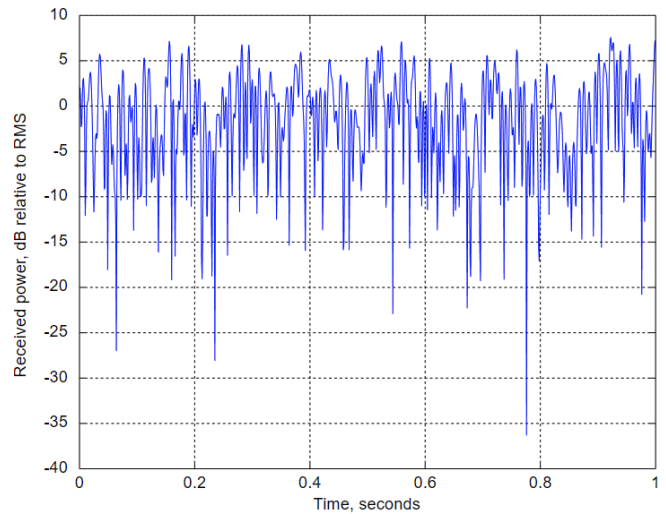


Figure 1.7: Probability Density Function of a Rayleigh Distribution

Figure 1.7 shows a probability density function for a Rayleigh distribution with multiple σ (standard deviation) values. In our case, the random variable is the incoming signals, the x-axis refers to time progression and the y-axis refers to signal magnitude; each secondary path would have a different standard deviation of attenuation. The fading is said to be Rayleigh if there is no apparent direct path; in other words, the arriving signals all appear to be propagating along secondary paths. Rayleigh fading is most common in densely packed cities where the signal can bounce off many objects such as buildings and cars. When the moving signal bounces off successive objects, doppler shifts occur. Figure 1.8 shows a time domain Rayleigh faded signal with a 10 Hz maximum doppler shift (left) and a 100 Hz maximum doppler shift (right).



10 Hz Maximum Doppler Shift



100 Hz Maximum Doppler Shift

Figure 1.8: Doppler Shift Effect on Rayleigh Faded Signal

As shown in Figure 1.8 as the doppler shift increases, the 'uglier' the arriving signal becomes. At higher doppler shifts, the signal can become almost impossible to decode.

On the receiving end, if there appears to be a signal that propagates along a direct primary path, Rician fading occurs (as opposed to Rayleigh fading where all signals appear to propagate along a secondary path). In Rician fading, the signals arriving at the receiver have a Rice distribution (often referred to as Rician or Ricean distribution), Figure 1.9 shows the probability density function of a Rice distribution.

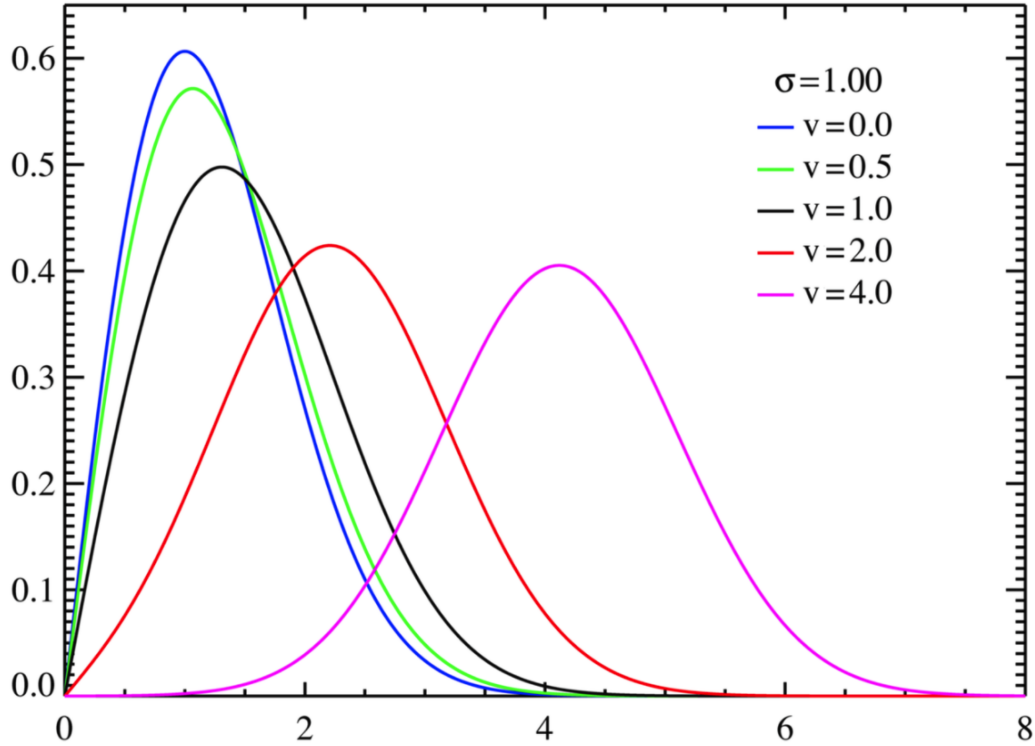


Figure 1.9: Probability Density Function of a Rice Distribution

In our case for the probability density function shown in Figure 1.9, the random variable is the incoming signals, the x-axis refers to time progression, and the y-axis refers to signal magnitude; each of the paths, primary and secondary, has its own σ , which refers to path attenuation. The received signal in a Rician faded channel can be described by the following equation:

$$f(x) = \frac{2(K+1)x}{\Omega} \exp\left(-K - \frac{(K+1)x^2}{\Omega}\right) I_0\left(2\sqrt{\frac{K(K+1)}{\Omega}}x\right)$$

Equation 1.2: Received signal in a Rician faded channel.

This function has two main parameters: K and Ω . K is the ratio of the power in the direct path to the cumulative power in the secondary paths. Ω is the power in all paths and can be defined by

$\Omega = v^2 + \sigma^2$, where $v = (K * \Omega)/(1 + K)$ and $\sigma = \Omega/2(1 + K)$. In the above function, I_0 refers to the 0th order modified Bessel function. Due to Rician fading having an apparent direct path, it can be less problematic than Rayleigh fading.

While fading is both important and problematic, it is not the only aspect of multipath we should be aware of. In digital communications, multipath can cause intersymbol interference (ISI), which refers to adjacent symbols interfering with each other in the channel; ISI is the main reason OFDM is often used with MIMO systems (see section 1.2). As will be discussed in further sections, channel capacity is increased when we use MIMO systems; we can exploit the new multiple paths to increase the capacity of our communication link. In the past multipath was a phenomena that was unable to be dealt with, however, with the use of MIMO each of the transmitters in a MIMO link have their own space-time code which ensures signal orthogonality. If the transmitter end of a MIMO link has knowledge of the channel, it can use the multiple paths in which the signal will propagate along by employing a certain amount of power to a particular transmitter.

1.4 MIMO Overview

Multiple-input multiple-output, commonly referred to as MIMO, is a data transmission technique which utilizes multiple antennas on the transmit and receive ends. MIMO was first introduced in the 1970s, however, it wasn't used until later to exploit multipath. MIMO relies on the theory of full channel state information (CSI), which means it is important to know the behavior of the channel. By having first-hand knowledge of the channel's behavior, the transmit power can be allocated in such a way as to utilize the multipath to an advantage. This was a revolutionary

concept as these factors that were detrimental to the loss of communication efficiency were now being used to beneficial purposes.

Crucial to the understanding of MIMO and why it's a more effective communication technique is a quick overview of the Shannon Capacity. Information theorists define information in bits as:

$$I = \log_2 P_i^{-1}$$

Equation: 1.3: Information in event with probability P_i

An event with probability P_i offers more information bits, the smaller its probability is or the more uncertain it is. The expected number of bits offered by an event with probability P_i is called its entropy and is denoted by $H(P_i)$. A communication channel is modeled by these two important equations:

$$y = x + n$$

Equation 1.4: Information transmission equation

$$I(x;y) = H(y) - H(y|x)$$

Equation 1.5: Mutual Information Function

'y' denotes the received information and 'x' is the sent information. Ideally, the two would be equal but noise 'n' is added by the channel. $H(y)$ is the entropy of the received symbol 'y' and $H(y|x)$ is the entropy of the received symbol 'y', knowing that symbol x was sent. This function is called the mutual information function and maximizing it means finding the Shannon capacity of the channel. Since we are aiming to maximize the mutual information function $I(x;y)$ and since entropy is proportional to uncertainty, the subtraction means finding the maximum reduction in uncertainty in the channel from sent random variable x and received random variable y. In other words, the received information y should tell one as much as possible about the sent information x. The Shannon capacity, therefore, represents a benchmark of the maximum amount of information that can be transmitted through a channel with zero errors by picking

intelligent coding techniques. It is not derived here, but $H(y)$ can be proven mathematically to max out when 'y' is a Gaussian distribution, while $H(y|x)$ becomes the entropy of the additive white Gaussian noise added by the channel, $H(n)$. Using in information theory what is called the Sterling approximation results in the well-known Shannon capacity for a single transmit and single receive communication link:

$$C_s = I_{\max}(x;y) = \frac{1}{2} \log_2(1+S/N) \text{ bits/sample}$$

Equation 1.6: Shannon Capacity

Assuming the sampling rate satisfies the Nyquist Criterion and normalizing by the bandwidth under design expresses the Shannon capacity in bits/sec/hz, referred to as just the capacity of the channel. Unfortunately, while the capacity of the channel does represent the maximum upper limit on communication performance it is not actually attainable in practice. The reason lies in the Sterling approximation, which implies that one must wait an infinite amount of time before the data can be transmitted to reach the capacity of the channel. However, even though the theoretical upper limit cannot be obtained, finite time delays still give excellent performance reaching to within 70% of the maximum capacity. This was the approach in single antenna communication.

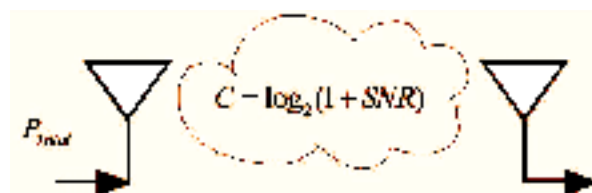


Figure 1.10: Channel Capacity of SISO

Up until the 1990's, the only method used for wireless data transmission has been one antenna at the transmit end and one antenna at the receive end; this is referred to as single input single output (SISO). As seen in Figure 1.10, the channel capacity of a generic SISO link can be modeled by the capacity equation discussed earlier $C = \log_2(1 + SNR)$; this implies that since

channel capacity is a function of SNR (signal to noise ratio) a higher capacity can be achieved simply by increasing the power of the transmitter. The channel capacity is represented as a logarithmic function which means that in order to achieve high capacities, the power of the transmitter must be extremely large. It became apparent that higher channel capacities could not be achieved with a SISO link. It was soon realized that higher channel capacities could be obtained by increasing the number of antennas on the transmit and receive ends of a wireless communication link. When the number of antennas on the transmit and receive ends are increased, more channels are created. This sounds quite intuitive, however, it's much more than a channel forming between a transmit antenna and its respective receive antenna. This is the topic of the following section.

1.6 How Adding Antennas Improves Data Transmission

As mentioned previously, the channel capacity of a wireless communication link increases when we add antennas. If we look at a SISO link, we can see that a single beam forms between the transmit and receive antennas; in other words, there is no diversity. In digital communications, diversity refers to the number of different paths that the same data has traveled to in order to get to the receiver. The transmit diversity increases as antennas are added to the receiver end of a SISO link. A SISO link is not only limited by channel diversity, but also limited by noise, interference, and channel fading. As discussed before, these limitations can be overcome simply by adding antennas.

To expand on this statement, let's take a look at a 2x1 MISO link, 2 transmit antennas and 1 receive antenna, shown in Figure 1.11.

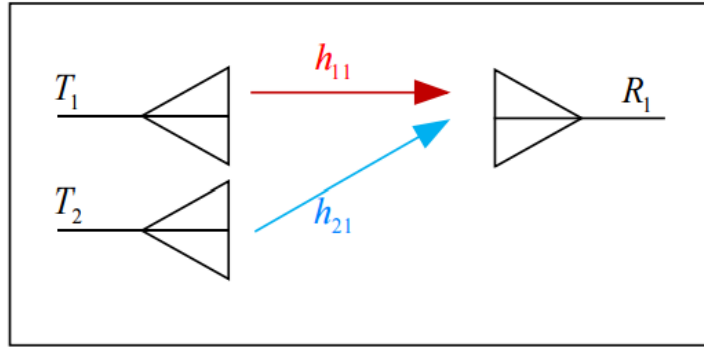


Figure 1.11: 2x1 MISO Link

If the path from T_1 to R_1 was to be lossy, we could always rely on T_2 to successfully transmit the data to R_1 . Imagine that two people are looking for a person, a person has a much higher probability of hearing their name being called by two people rather than just 1. The multiple channels can be represented by a matrix called the channel matrix. This matrix consists the sub channel elements. To better understand the concept of MISO, let's take a look at the channel capacity equation for an arbitrary link:

$$C_{MISO} = \log_2 \left(1 + \frac{\|\mathbf{h}\|^2 SNR}{N_T} \right) \text{ bits/s/Hz}$$

Equation 1.7: Channel Capacity of MISO

Where:

- N_T - number of transmit antennas
- $\|\mathbf{h}\|^2 = (h_1^2 + h_2^2 \dots + h_{N_T}^2)$ - average channel gain over all paths

Generally in MISO systems power is distributed equally amongst the all of the transmit antennas; this is why in the above equation, we divide SNR by N_T . As N_T increases the SNR at the receiving end decreases. The benefits of a MISO communication system can be compromised if we do not know the channel information (\mathbf{h} matrix). If the transmitter has no idea

what the channel looks like, we can make the assumption that $N_T = \|h\|^2$ which then yields the same capacity equation for a SISO system; thus making a MISO system obsolete.

Next, let's take a look at a SIMO link, shown in Figure 1.12.

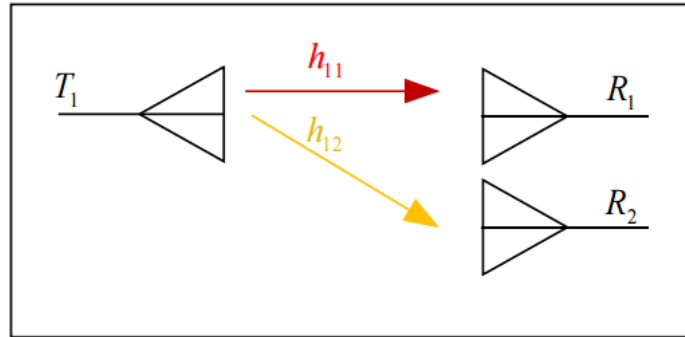


Figure 1.12: 1x2 SIMO Link

A SIMO link is defined by a communication link that has one transmit antenna, and multiple receive antennas. To conceptualize how a SIMO link can be better than a SISO link, imagine that a person are looking for their friends in a crowded area--the person has a much higher probability of finding them if that person shout all of their names instead of just shouting one.

The capacity equation for a SIMO link can be seen below:

$$C_{SIMO} = \log_2 \left(1 + \|h\|^2 SNR \right) \text{ bits/s/Hz}$$

Equation 1.8: Channel Capacity of SIMO

Since the channel only has as many paths as it does receivers, the value of $\|h\|^2$ is limited by the number of receive antennas (N_R). Knowing this, we can rewrite the above equation as:

$$C_{SIMO} = \log_2 \left(1 + N_R SNR \right) \text{ bits/s/Hz}$$

Equation 1.9: Channel Capacity of SIMO, adjusted

We can increase the channel capacity simply by increasing the number of receive antennas, however, this approach can become quite costly if we only manage to increase the capacity

logarithmically. Unlike a MISO link, the benefits of a SIMO link are not dependant on the transmit antenna having any knowledge of the channel; in other words, the transmitter is blindly throwing out data in hopes that at least one of the receiver antennas will pick it up. We can also observe the usefulness of a SIMO link from a statistical standpoint.

Let's say we have SISO link and a SIMO link. Each receiver antenna has 50% chance to decode the correct bit. We'll use the following conventions:

- $P[R] = 0.5$, probability that correct bit arrives at SISO receiver
- $P[R_1] = 0.5$, probability that correct bit arrives at SIMO receiver 1
- $P[R_2] = 0.5$, probability that correct bit arrives at SIMO receiver 2
- $P[R_{SIMO}]$ - probability that correct bit arrives at one of the 2 receive antennas in the SIMO link

$$P[R_{SIMO}] = P[R_1 \text{ or } R_2] = P[R_1] + P[R_2] - P[R_1 R_2]$$

$$\text{Where } P[R_1 R_2] = P[R_1] * P[R_2] = 0.25$$

$$P[R_{SIMO}] = 0.5 + 0.5 - 0.25$$

$$P[R_{SIMO}] = 0.75$$

From the above derivation we can see that a 1x2 SIMO link greatly increases the probability of the correct bit arriving at the receiver from a simple SISO link. The above example, while simple, is a surface level representation of the usefulness of a SIMO link. However, this seems like a lot of hardware to only achieve a logarithmic increase in channel capacity.

A MIMO link seeks to overcome the limited channel capacity of SISO, MISO, and SIMO by adding antennas to both the transmit and receive ends. MIMO is like a combination of MISO

and SIMO channels; it can reach higher capacities either with channel information (like MISO) or with no channel information (like SIMO). To expand on this claim, if there is no known channel information at the transmitter end of a MIMO link, the channel capacity equation can be simplified to:

$$C = \underline{\underline{M}} \log_2 \det \left(I_{N_R} + SNR \right)$$

Equation 1.10: Channel Capacity of MIMO

One thing to note from the above equation is that it is used for calculating the channel capacity limit. In this equation, 'M' is used to denote the minimum number of antennas, for example: if $N_T=3$ and $N_R=4$, then $M=3$. We can see that the channel capacity limit increases linearly as we add antennas while holding a constant SNR.

Now, let's look at a 2x2 MIMO link where the channel information is known, as seen in the following figure. We'll use 'T' to represent a transmit antenna, 'R' to represent a receive antenna, and 'h' to represent a subchannel. As seen in Figure 1.13, additional subchannels have formed between cross antennas. A 2x2 MIMO system has created a 4 channel link, similarly a 3x3 MIMO system has 9 channels, and a 4x4 MIMO system has 16 channels.

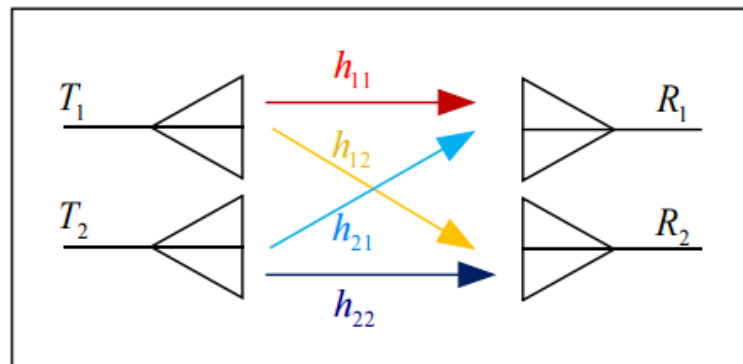


Figure 1.13: 2x2 MIMO Link

Furthermore, if the transmitting and receiving antennas are spaced very far apart with respect to the wavelength of the transmitting frequency, then MIMO reduces to N SISO links. Therefore, the worse MIMO can perform is as a multiple of SISO links. It might be beneficial to the reader to see mathematical description of the advantages of MIMO. This description centers on the assumption that the channel is deterministic and constant at all times.

For a deterministic channel that is constant at all times, the transmitted signal, received signal, the channel matrix and noise are denoted by the equation:

$$\mathbf{y} = \mathbf{H}\mathbf{x} + \mathbf{W}$$

Equation 1.11: Direct Transmission Model

Here, \mathbf{y} denotes the received signal matrix of $N_R \times 1$, \mathbf{H} is the channel matrix $N_R \times N_T$, \mathbf{x} is the transmitted signal matrix $N_T \times 1$ and \mathbf{W} is the additive white Gaussian noise with expected value of zero and variance in power of N_0 , $(0, N_0 \mathbf{I}_{N_R})$. From linear algebra, we recall that any matrix may be rewritten as the product of three matrices from the singular value decomposition (SVD) theorem. \mathbf{H} can be rewritten as

$$\mathbf{H} = \mathbf{U}\mathbf{\Sigma}\mathbf{V}^*,$$

Equation 1.12: Channel State Matrix

where \mathbf{U} and \mathbf{V}^* are orthogonal elementary square matrices of dimensions $N_R \times N_R$ and $N_T \times N_T$, respectively, and $\mathbf{\Sigma}$ is a diagonal matrix that has the same dimensions as \mathbf{H} . The importance of expressing \mathbf{H} as its SVD is $\mathbf{\Sigma}$ contains the singular values, λ , of \mathbf{H} in its diagonal entries. These singular values are important as they inform the designer how the power should be allocated among the multiple transmitters so that the crosstalk acts in a beneficial way to the transmission of information. Additionally, these singular values are important because they tell us the rank of the channel. The rank is the number of linearly independent columns in the channel matrix.

Ideally, the rank is equal to the minimum of (N_T, N_R) , the dimensions of the receive and transmit antennas. It is possible, though, to have a channel matrix \mathbf{H} with a rank less than the minimum of the (N_T, N_R) ; this occurs when one or more of the singular values evaluate to zero. Having a channel that is not full rank means the columns of the channel matrix may not be fully independent, rather they are linearly related. This highlights the fact that to fully take advantage of MIMO, we need channels that have diverse crosstalk. This affects diversity gain and the spatial multiplex gain, as discussed later. Substituting the SVD of \mathbf{H} into equation 1.11 and multiplying both sides by the conjugate transposed \mathbf{U}^* , it can be shown that the expanded result is:

$$y_i' = x_i' \lambda_i + w_i', \quad i = 1, 2, \dots, n_{\min}$$

Equation 1.13: Direct Transmission Model, substituted

The reason behind performing the SVD of \mathbf{H} is it performs two coordinate transformations by expressing the input \mathbf{x} with columns of \mathbf{V} and the output \mathbf{y} with columns of \mathbf{U} . This results in an easier relationship between the inputs and the outputs of the communication link, similar to a SISO relation. The SISO -like form allows substitution into the capacity equation of a SISO link. The capacity equation for a MIMO link results in:

$$C = \sum_{i=1}^{n_{\min}} \log_2 \left(1 + \frac{P \lambda_i^2}{N_o} \right) \text{ bits/s/Hz}$$

Equation 1.14: Channel Capacity of MIMO, simplified

The capacity equation reveals the singular values in the design of the MIMO communication link. Since the singular values are involved in the capacity equation, it reveals how the power should be distributed among the channels of the link. The subchannels with the larger singular values are favored for transmission power. Furthermore, we see that this capacity relation grows a lot easier for a certain combination of input power as opposed to the capacity of a SISO link.

For a SISO link, the capacity grew logarithmically with the input power. Here, we have extra terms being added to the capacity of a MIMO link. Also, because of the ability to allocate the power among the transmitters with the largest singular value, the designer can maximize the capacity of the link.

A graphical interpretation of this can be seen through the logarithmic curves shown below. As shown on the graph, all of the logarithmic curves have a larger slope initially, but as they grow they start rising much slower and slower. If one can imagine these curves representing the various log terms in the capacity of the MIMO link, the largest curve represents the subchannel with the highest singular value, the second largest curve is the 2nd largest singular value, and so on. By allocating the power to favor the subchannels with the bigger singular values, effectively, we are taking advantage of this brief, faster rise in the log curves. By allocating the power, just enough is given to the highest $\log(x)$ curve to utilize this higher slope region. Once the largest $\log(x)$ curve slows its growth, rather than keep feeding this subchannel power, the remaining power is allocated to the next subchannel $\log(x)$ curve while it's still in that fast transition region, and so on for the next subchannel $\log(x)$ curve. This is how MIMO can attain a much better capacity relation with power. In SISO, all of the transmit power was used on the single channel and it resulted in logarithmic increase in capacity. Here, with multiple capacity terms, the singular values tells us how to allocate the transmit power to utilize crosstalk in an effective manner. This process of allocating the power among the channels is called water filling.

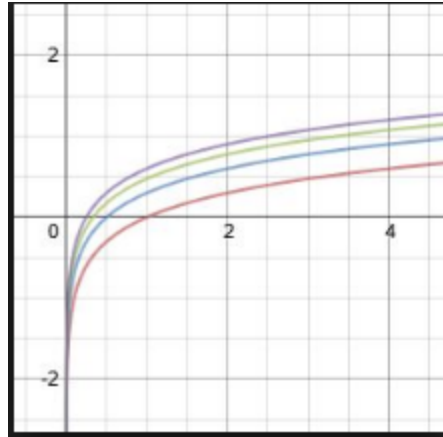


Figure 1.13: Example of Waterfilling

Now, being able to fit more bits of information onto a single channel is very important, but what does it matter if the bits arriving at the receiver are incorrect? Although capacity is very important to know about, it is not the only aspect of a wireless communication link we should be aware of. Capacity tells us how many bits can fit in a channel, it does not, however, tell us how well the link successfully and accurately transmits bits. A measurement called Bit Error Rate, BER, was created to determine how many errors there are in bits that have been transmitted across a channel. In order to calculate the BER the data received is compared to the data that was sent. Usually this is done in Matlab using a Monte Carlo simulation, which allows for the test to be run thousands of times; this ensures that the data measurement is reliable. The most common way to display the BER is through the use of a 'Waterfall' curve. A Waterfall curve is a graph that has BER as the dependent variable and E_b/N_o as the independent variable. E_b/N_o is the energy per bit, but is commonly referred to as SNR. To generate a Waterfall curve E_b/N_o is swept and BER is calculated and plotted. An example of Waterfall curve can be seen in Figure 1.14.

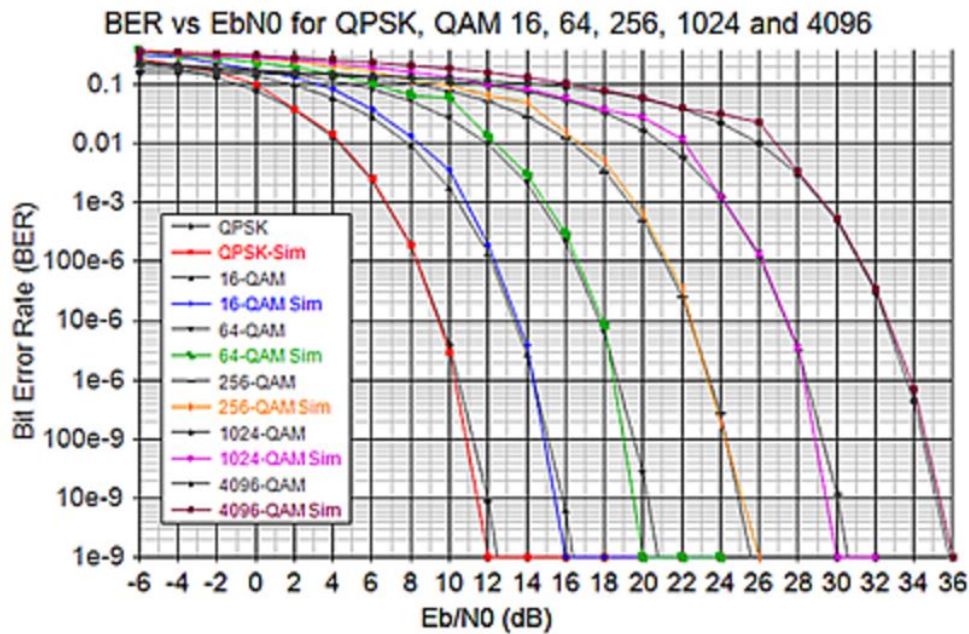


Figure 1.14: Waterfall Curve Example

Figure 1.14 shows the Waterfall Curve for QPSK and 16, 64, 256, 1024, and 4096 QAM (modulations explained earlier). We can see that QPSK has the lowest BER per E_b/N_0 input, which makes sense due QPSK being the simplest modulation form of the ones listed in the following section. Fortunately, Matlab created a MIMO channel diversity demo in which Waterfall Curves were constructed. Figure 1.15 shows the Waterfall curves for various channel diversities.

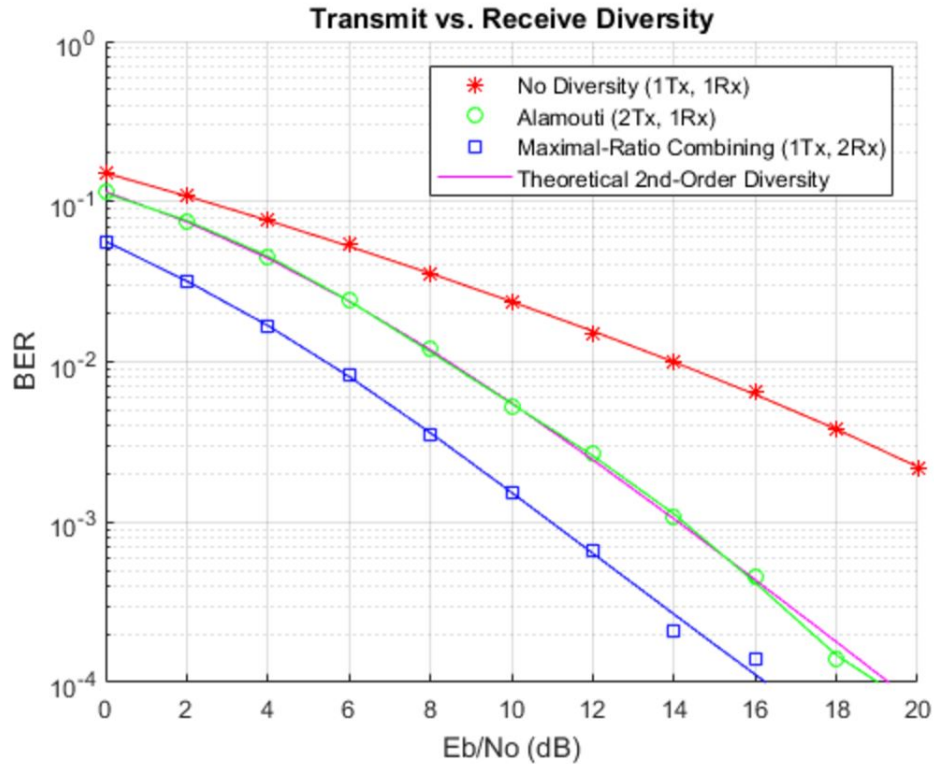


Figure 1.15: BER Performance for Different Diversities

The Waterfall curve in Figure 1.15 allows the viewer to compare the BER of a SISO link, a 2x1 MISO link, and a 1x2 SIMO link. It is not much of a surprise that the MISO and SIMO systems greatly out-performed the SISO system. Each of the systems were BPSK modulated and all have 2nd order diversity (except for the SISO link). These systems are said to have 2nd-order diversity because the same data travels across two different paths to the receiver. As discussed earlier in the chapter, for a MISO link to be advantageous, the transmit antennas must have knowledge of the channel and its frequency response. A SIMO link does not require that the antennas be aware of the channel behavior, this is why the SIMO simulation (blue plot) has the lowest BER of all the other systems. As we increase the number of receiver antennas, we also increase the likelihood that at least one of them will properly decode the incoming data, which is all we need for robust data transmission. We can see that for all three system that as we

increase the E_b/N_o , the BER decreases. However, increasing E_b/N_o can become quite costly especially if we are transmitting a lot of data, let's see what happens when we increase the channel diversity.

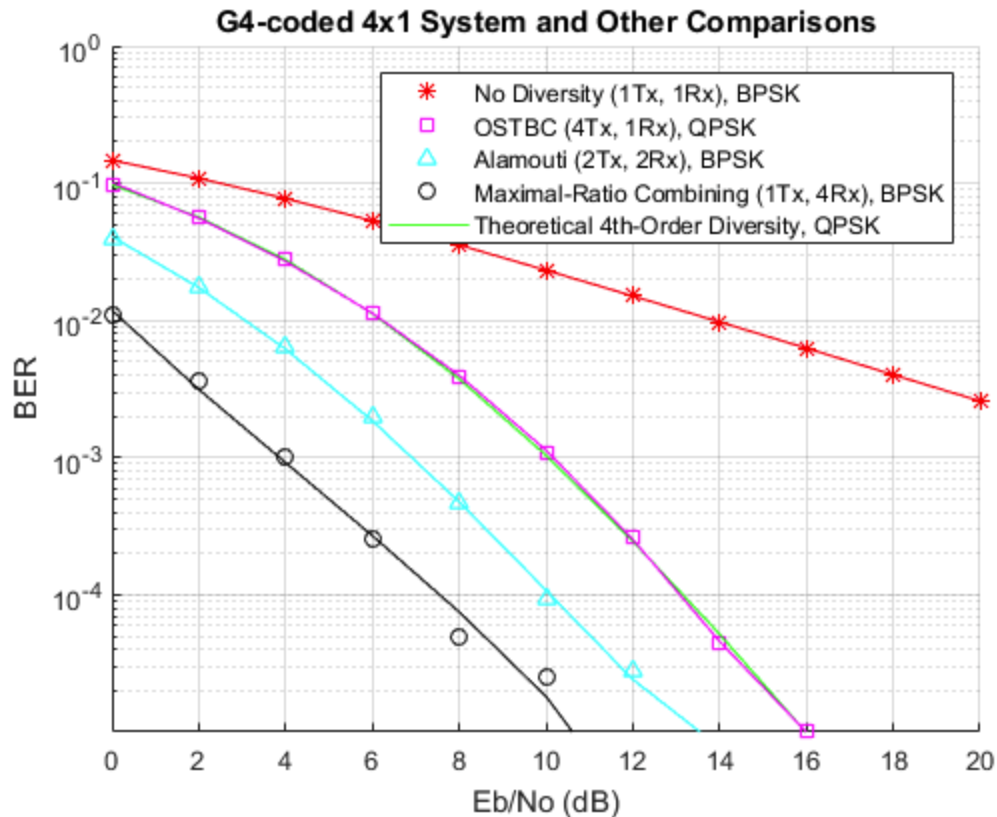


Figure 1.16: Increased Channel Diversity From Figure 1.15

Figure 1.16 shows the waterfall curve for multiple 4th-order diversity systems; the same SISO plot from Figure 1.15 has been added to the plot for reference. We can immediately notice that increasing diversity decreases the BER. If we compare the 4th-order diversity SIMO system with the 2nd-order diversity SIMO system we can see that the former achieves a BER of 10^{-4} when $E_b/N_o=10.5$ dB while the latter achieves a 10^{-4} BER when $E_b/N_o=16$ dB. What may be a surprise to us is that the 1x4 SIMO system outperforms the 2x2 MIMO system. Having discussed the

basic concepts of MIMO, it is beneficial to provide an overview of beamforming and the different flavors of MIMO: Precoding, Diversity Coding, and Spatial Multiplexing (SM).

1.7 Beamforming

In beamforming the phase and amplitude of a signal can be adjusted at the transmitting end such that certain interferences can be achieved at the receiving ends. It is utilized when one has more than one antenna at either end or both ends of the communication link due to the extra subchannels created by the multiple antennas.

The concept of beamforming is possible based on the spatial diversity or extra possible paths created by the multiple antennas discussed in section 1.6. Spatial diversity is analogous to the magnitude of a vector. If one can imagine a 2D vector with x and y components, the magnitude of the vector is the root sum square of the components x and y . Ideally, x and y should be such that they maximize the magnitude of the vector but also stay as diversely distributed as possible. The reason for this is, if x , in the extreme case that it dominates the magnitude of the vector such that y approaches zero, then the combination of x and y starts becoming more like a single direction. Similarly, in beamforming the diversity is proportional to the norm of the subchannels vectors. The diversity gain should be as large as possible so that crosstalk becomes advantageous for beamforming. Once the antennas are placed closer and closer together, though, they start experiencing the same channel and this diversity gain is lost and no beamforming can be performed. A diversity gain is preferred as one channel may be lossy and then all the transmit power would be forced through this lossy channel. If there are multiple subchannels, then if one channel looks worse in terms of performance than power can instead be transmitted through the better channel. These are the concepts of transmit and receive

beamforming with the norm $\|h\|$ factor in the capacities of SIMO and MISO discussed in sections 1.2.

Let's look at an example to better conceptualize what is happening: take a 2x2 MIMO link, if we are aware that channel h_{11} is quite lossy, we can adjust the phase and relative power of the signal coming from T_2 such that it constructively interferes with the signal coming from T_1 , thus allowing R_1 to receive a clean and readable/decodable signal. Again, this is possible only through the spatial diversity created by adding multiple antennas.

Beamforming should not be confused with the water filling method using the singular values of the subchannels. The difference between waterfilling and beamforming is hardware. For example, if beamforming is desired, the antennas could be oriented in a certain configuration such that the radiation pattern points in a preferred direction. This would create a channel matrix which could then be analyzed using the SVD method to find the singular values and perform water filling. In other words, beamforming would form your channel matrix based on the orientations of the antennas and water filling would then be used to determine how to appropriately ratio the power. Beamforming is not limited to MIMO applications, in fact, it is actually quite hard to implement and has many other uses: radar, sonar, seismology, radio astronomy, acoustics, and biomedicine. In order for beamforming to be successful in digital communications the channel information must remain constant, which is an incredibly rare occurrence.

One of the most common applications for beamforming found today is beamforming routers. In the past, Wi-Fi routers would transmit data equally in all directions, similar to the way a lightbulb

emanates light. A beamforming Wi-Fi router aims the data transmission beams at points of interest such as computers, laptops, and other devices with Wi-Fi access. However, for beamforming routers to work, the devices at the receiving end of the data must have the hardware to accommodate this. Think of a beamforming router as a lightbulb with a shade over it such that the light only goes to the directed locations.

1.8 Precoding

Precoding uses beamforming for successful transmission of data of wireless communication systems. The idea behind precoding is that the transmit end can anticipate the loss in the channel. Let's say that the received signal is 'r', the sent signal is 's'. Ideally, $r=s$, however, in wireless communications, this would be impossible due to loss in the channel as well as channel noise. We'll use 'h' to represent the transfer function of the channel and 'n' to represent the random white gaussian noise. Without precoding, the equation for the received signal is $r = s*h + n$. To apply precoding, the sent signal 's' is divided by the anticipated transfer function of the channel ' h_{pre} '; the new transmitted signal is ' s/h_{pre} '. The equation for the received signal is now $r = (h/h_{pre})*s + n$. If ' h_{pre} ' is properly chosen ($h = h_{pre}$), we get $r = s + n$. This implies that the only effect on the transmitted signal is the noise of the channel which can be easily mitigated by increasing signal power on the transmit end. Precoding can be done linearly and nonlinearly.

1.9 Diversity Coding

Diversity Coding is a flavor of MIMO that is primarily used when the transmitter has no knowledge of the channel. Diversity coding takes advantage of independent fading as well as signal orthogonality to transmit data. The same signal is emitted from each of the transmit

antennas. However, before the signal is transmitted it undergoes a coding technique called Space-Time Coding (STC). STCs transmitted multiple copies of the same data in hopes that at least one of the data streams arrive at the receiver with minimal amounts of interference such that the receiver can accurately decode the data, much like a SIMO link. This coding method can be subdivided into two main types: Space-Time Trellis Codes (STTCs) and Space-Time Block Codes (STBCs).

STTCs apply multiple Trellis/Convolutional codes to the data and send the coded data to each of the transmit antennas, with each antenna receiving a different copy of the encoded data. Arriving at the receiver are multiple packets of diverse data; while this data may seem diverse, the content is all the same. An example of a simplified Convolutional encoder can be seen in Figure 1.17:

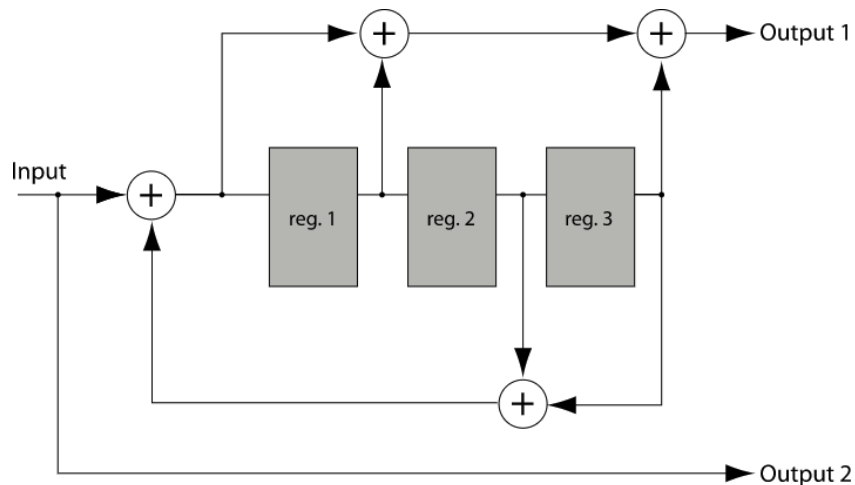


Figure 1.17: Simplified Convolutional Encoder

A convolutional encoder uses a finite state machine to encode an incoming data stream. Conventionally, it consists of shift registers, adders, and XOR gates. The shift registers continue to shift until each has no remaining bits; once this happens, the data has been successfully encoded. As seen in figure 1.17, 'Output 1' is the encoded data stream and 'Output 2' is the

data before it was encoded. Output 1 is the aggregation of multiple shift registers and adders applied to the input data. If the data at Output 1 were compared with the data at Output 2, they would appear to be very different. A convolutional encoder can be recursive or nonrecursive; Figure 1.17 is an example of a recursive encoder. An encodement sequence for a convolutional encoder can be represented using a trellis diagram which explains why this method is often called Trellis coding. On the receiver end, Convolutional encoded data is most often decoded using the Viterbi Algorithm, however, when the encoded data appears to be long, the Fano Algorithm is most often used.

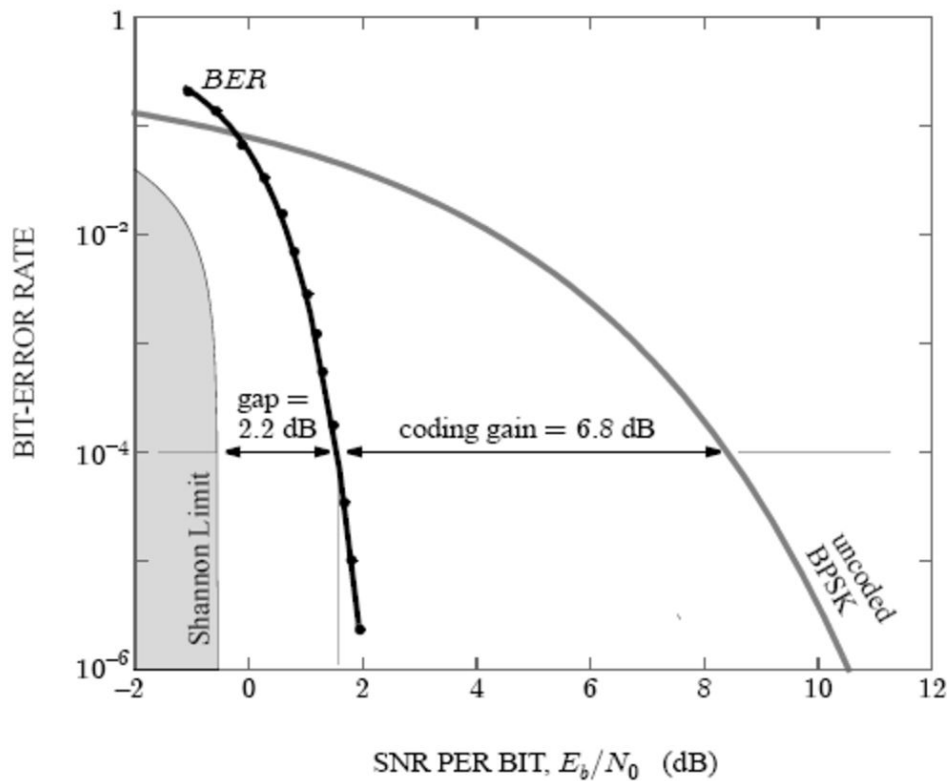


Figure 1.18: Convolutional Encoded BPSK vs. Uncoded BPSK

The plot in Figure 1.18 shows the BER waterfall curve for a convolutional encoded BPSK data stream and an uncoded BPSK data stream. We can see that the data with forward error

correction, FER, has very few errors; we can see that as the energy per bit is slightly increase the BER falls drastically. Compared to STBCs, STTCs have better coding gain as well as diversity gain. STTCs are also far superior at achieving lower BER per E_b/N_o . One of the main drawbacks of STTCs is that they require convolutional codes which can make the hardware quite complex and intricate; this issue also carries over to the receiver end in that the viterbi decoder must be just as complex. STBCs are easy to implement and can also be processed linearly.

As stated earlier, diversity coding does not rely on any channel knowledge at the transmitter, this implies that useful aspects of MIMO like beamforming and array gain are unusable in diversity coding systems. However, if there is slight knowledge of the channel at the transmitter, diversity coding can be used in conjunction with spatial multiplexing.

1.10 Spatial Multiplexing

Another flavor of a MIMO system is a spatial multiplex system. Because MIMO consists of multiple antennas on the transmit side and the receive side, this opens up a spatial degree of freedom in which data streams can be divided in the MIMO channel. This is the concept of Spatial Multiplexing. Spatial Multiplexing focuses on enhancing the data rate by allocating data among the multiple transmit antennas of the channel. By using the various transmitters available in the MIMO system, segments of the signal information essentially travel in parallel and recombine at the receiver. This is analogous to a backed up highway in which a second lane opens up allowing space for other cars to travel in parallel. A contrast to this example is a SISO link which sends data serially.

A measure of this enhancement in data rate is called the spatial multiplexing gain (SMG). Intuitively, the SMG is dependent on the minimum of the number of antennas on either the transmitter or the receiver end of the MIMO link. For example, if there are three antennas on the transmit side and four on the receive side, the SMG will equal the minimum of both numbers, three as discussed in previous sections. This is due to the fact that even though the receiving end has a greater number of antennas, the signal can only be split up three ways on the transmitting end. A similar argument follows for when the transmitting side has a greater number of antennas than the receiving side. A second relationship for the diversity gain comes through knowledge of the data rate and the SNR of the channel. This relationship is expressed as:

$$SMG = \lim_{SNR \rightarrow \infty} \frac{r}{\log(SNR)}$$

Equation 1.15: Spatial Multiplexing Gain

A real benefit of MIMO communication comes when both a diversity gain and SMG are introduced into the design of the MIMO link. Since a diversity gain and a multiplex gain are both benefits available to us through the multiple number of antennas on both sides of the communication link, it makes sense that both, together, should and enhance the communication link. In this case, however, one must decide on which gain is more important since both gains, fully, cannot be applied to the system. The intuition behind this limitation can be explained as follows. If diversity gain works by allocating the same dataflow on each transmitting antenna while spatial multiplexing works by splitting up sections of that dataflow and then sending them through the different multiple transmitting antennas, then it makes sense that one cannot fully apply both. In other words, one must decide whether one's transmitting antennas are each sending the same data or if they are each sending a different section of a cumulative dataflow.

For example, let's say one have a MIMO communication link consisting of 2 antennas on the transmit side ($N_T = 2$) and 3 antennas on the receive side ($N_R = 3$). The diversity gain is calculated as the product of both $N_T \times N_R$ which comes out to 6 for this case. The SMG is the minimum of the two, so the SMG equals 2. This MIMO link cannot be designed to have both a diversity gain of 6 and also an SMG of 2 due to the limitations described earlier. However, depending on the system goal, often the MIMO link can be designed on an optimal tradeoff of both diversity gain and SMG. In this example, a trade-off is a diversity gain of 3 and an SMG of 3.

1.11 MIMO In Wi-Fi

MIMO is commonly used in wireless local area networks (WLAN). In 2009, IEEE developed the WLAN 802.11n protocol which gave rise to MIMO, however, it wasn't until 2013 when IEEE developed WLAN 802.11n that MIMO came into use. The introduction of MIMO in 802.11n increased the data rates from 20 Mbps to around 200 Mbps and the range of reception over the standards of old 802.11a/g from ~25m to ~50m. The concepts discussed thus far crucial to the operation of 802.11n are transmitter beamforming, spatial division multiplexing and spatial diversity. To apply the theory of spatial diversity and spatial division multiplexing, 802.11n utilizes the space-time block coding (STBC) discussed earlier. The 802.11n protocol utilizes OFDM to transmit data across wireless channels, operates at the 5 GHz band, and can obtain bandwidths of 20, 40, 80, or 160 MHz.

Chapter 2: Keysight VSA/VSG Overview

2.1 VSG Overview

The purpose of the vector signal generator (VSG) is to generate radio, wireless, or cellular signals to test a system. The generated signals usually have digital modulation since radio, wireless, and cellular signals require modulation when being transmitted. The VSG allows for OFDM signals to be transmitted which are essential to testing digital communication systems.

The reason the VSG is integral to testing the communication methods is because it allows for a known reference signal to be sent through a channel. Since the signal is a known reference it allows for comparison between the propagated and the received signal to determine if the communication system is performing to specifications. This project specifically uses the Keysight PXIe M9381A VSG because it can send a reference 802.11n signal through the channel. As discussed previously in section 1.5 one of the current applications using MIMO is WiFi, which uses the 802.11n signal, so the M9381A VSG utilized is compatible with the current application of MIMO analyzed.

2.2 VSA Overview

A vector network analyzer displays the magnitude and phase of the received input signal at a single specified frequency. The purpose of the vector signal analyzer is to make in-channel measurements of error vector magnitude which is used to derive the SNR. The SNR rate is the

parameter which is being used in this project to evaluate a test antenna's configuration performance.

The purpose of the vector signal analyzer (VSA) is to see what distortions occur in the desired signal after sending it through some sort of path. A VSA displays the magnitude and phase of the received signal so an engineer can see if the distortion is acceptable or not and how to design to account for the distortion. Some vector signal analyzers can also perform measurements like error vector magnitude (EVM) of the received signal to known signals.

The evaluation of communication systems relies heavily on the SNR. Since SNR describes the communication system's sensitivity to noise, the higher the SNR rate the less sensitive the channel is to noise. To be less sensitive to noise means that it is easier for the receiver to discern the desired signal from the noise in the channel. The SNR rate can be found from the EVM using the equation $EVM (\%) = \sqrt{1/10^{(SNR_{dB}/10)}} \times 100$ and solving for SNR. The reason the Keysight M9391A VSA is used for the testing portion of the project is because the VSA has software that can display the EVM, constellation diagram, and frequency response of the 802.11n signal. Since the VSA has these measurements calculating the SNR and observing the performance of the digital communication system is far easier.

2.3 Testing Hardware

To test the performance of the digital communication systems the following Keysight hardware was used: M9381A VSG, M9391A VSA, and the M9018A PXIe Chassis. The hardware generates a reference signal and evaluates it after propagation through each of the antenna configurations. The chassis acts as a mount for the VSG and VSA, and it includes a module that

allows for computer interface to be established. This allows the user to interact with the VSG and VSA hardware and software.

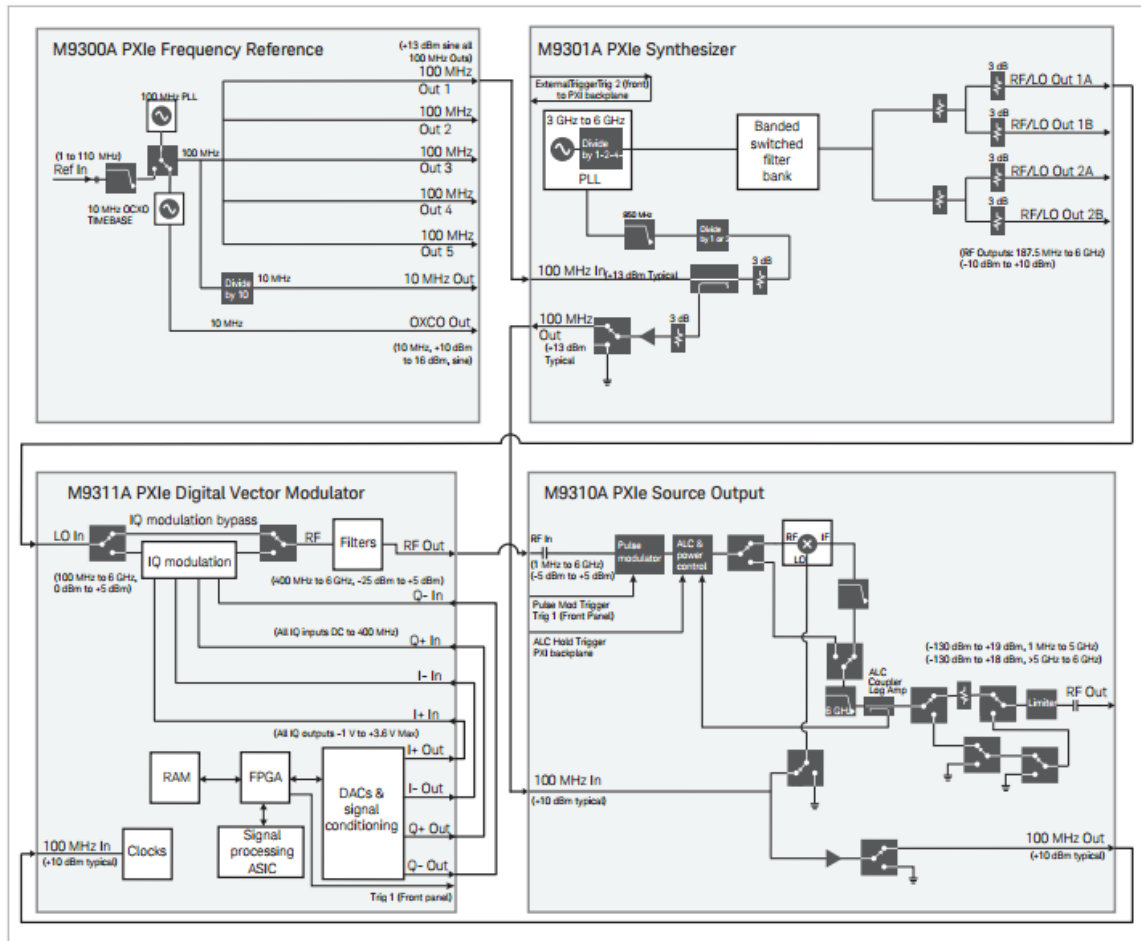


Figure 2.1: Block Diagram of the M9381A VSG module from Keysight M9381A datasheet

The M9381A PXIe VSG (shown in Figure 2.1) consists of the M9300A frequency reference, M9301A synthesizer, M9311A digital vector modulator, and M9310A source output to generate the reference signal. An important aspect of the M9300A frequency reference is only one is required per chassis because the frequency reference is used to provide a 100 MHz signal to each of the synthesizers. Since the same signal is used to drive both the VSA and VSG synthesizers, there should be no variance in the signal because the other components use the 100 MHz signal and the local oscillator signal (LO) from the synthesizer to perform their tasks.

The M9301A synthesizer uses 100 MHz signal to transmit a signal at a frequency given by the user to the source output. The M9311A digital vector modulator receives the LO signal from the synthesizer at the LO input and at the 100 MHz input accepts the 100 MHz signal from the M9310A source output. The digital vector modulator modulates the LO signal and uses the 100 MHz from the source output to run its internal clock. The modulated signal is then sent to the source output through the RF output to RF input. The M9310A source output adds power and sends it out to the environment through the RF out port using the 100 MHz signal from the M9301A synthesizer and the RF signal from the M9311A digital vector modulator.

The M9391A PXIe VSA comprises of the M9300A frequency reference, M9301A synthesizer, M9350A RF downconverter, and M9214A IF digitizer (shown in Figure 2.2). The VSA is used to evaluate the reference signal after it has propagated through the selected antenna test configuration. The M9300A is the same as the one used in the M9381A PXIe VSG and performs the same function. The M9301A synthesizer uses the 100 MHz signal to transmit a desired LO signal and the original 100 MHz signal to the downconverter. The downconverter receives the LO signal from the synthesizer at the LO input and at the 100 MHz input accepts the 100 MHz signal from the synthesizer. The purpose of the down converter is to bring the received signal down to the intermediate frequency (IF), which is significantly lower than the signal received at the input of the downconverter. The reason the IF is used is because the low frequency allows for circuitry to perform well without the use of waveguides, less hardware needs to be used to process the received signal, and it improves frequency selectivity. The downconverter passes the IF signal to the IF digitizer along with the 100MHz signal. The IF digitizer takes the 100MHz signal and uses it as an internal clock to perform signal processing on the receive IF signal. For the purposes of this project, the IF signal is converted by the

onboard signal processing to I/Q diagram data that is observed using the 89600 VSA program.

The data can also be processed and displayed in other ways such as a frequency response and as a time domain signal.

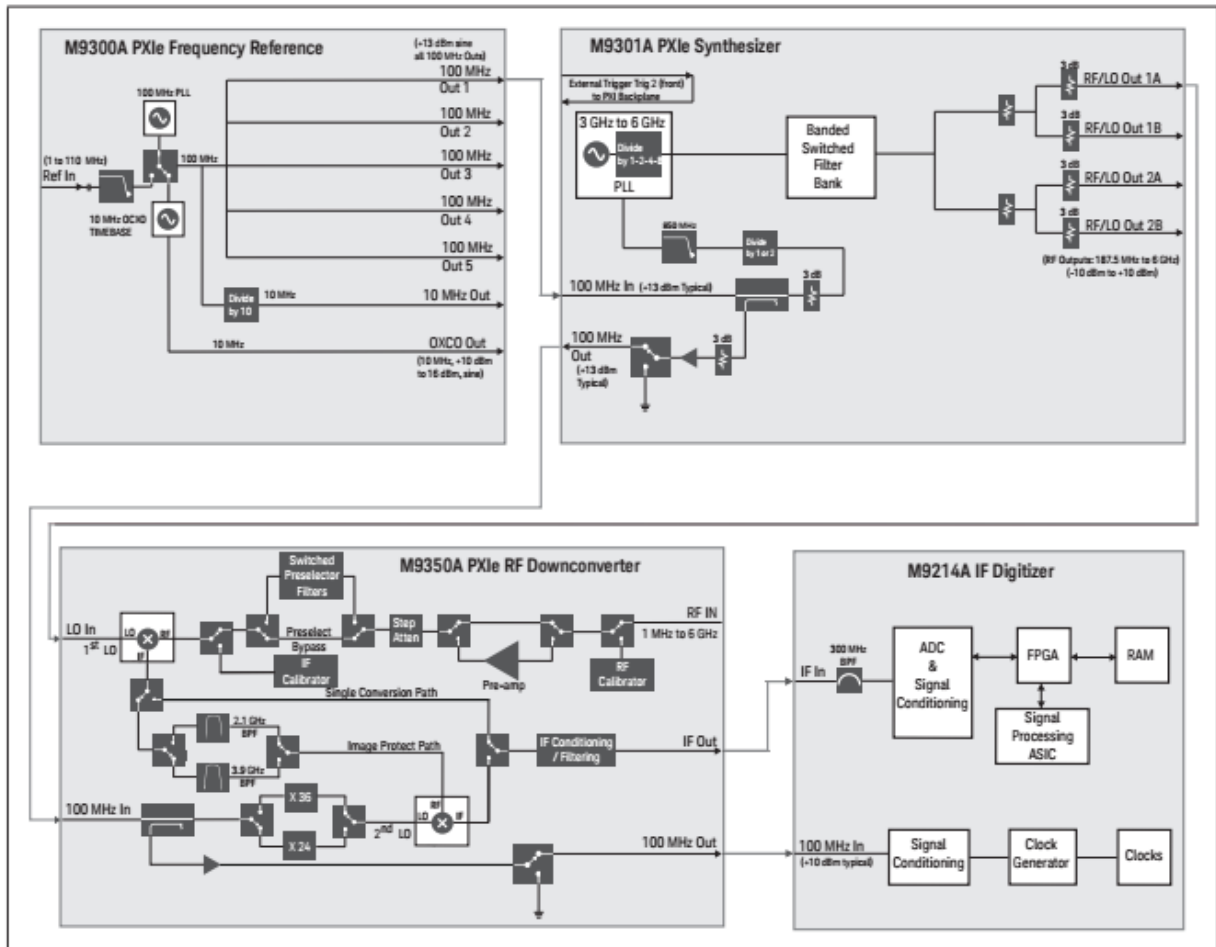


Figure 2.2: Block Diagram of M9391A PXle VSA module from Keysight M9381A datasheet

2.4 Testing Software

Multi-Channel PXle Config Utility

The Multi-Channel PXle Config Utility is used to generate the internal connections between desired VSGs and VSAs. Once the configuration is generated the user can decide to save the

configuration and develop a 89600 VSA configuration. Also, after a successful configuration a file called Persisted.xml should appear in the same directory as the Multi-Channel PXIe Config Utility. The Persisted.xml is used by the Multi-channel Demo Tool to configure the back panel connections in the Multi-Channel PXIe Config Utility created at the end of the configuration generation.

Multi-Channel Demo Tool

The Multi-Channel Demo Tool allows for a user to select MIMO signals and send them into the system. The user can also control the power and phase of the signal sent through each channel.

89600 VSA




The 89600 VSA is a program where the received signals can be viewed and analyzed. Useful tools include I/Q diagram, H-matrix, frequency response, impulse response, and EVM measurements. These measurements, especially the EVM and I/Q diagrams, help determine the overall performance of the data transmission method. Accurate measurements require the user to specify what waveform the M9391A VSA is expected to receive, so the program knows what the desired results are. Configuration of the 89600 VSA program is discussed in more detail in Section 2.6.

Waveform Creator

Waveform creator is an application which allows the user to create their own signals using different types of modulation, added noise, input power, among other settings. The waveform then can be sent to the M9381A VSG and transmitted to the M9391A VSA and analyzed.

2.5 Configuration Generation Walkthrough

To focus on the beam-forming techniques of MIMO the Keysight VSA and VSG modules had to be wired in shared-LO configuration to ensure the references are in phase. The shared LO configuration requires the two VSGs to share a single synthesizer and the two VSAs to share a single synthesizer. The reason for sharing the synthesizer between common components is to preserve phase coherence, meaning there is no phase difference between the two components. So the only phase shifting that could occur would be if the user or the propagation method introduced a phase shift. Originally, the modules were not in the proper places, which did not allow for a proper configuration. The modules were removed and placed in the proper configuration as shown in the Keysight LTE/LTE-A Multi-Channel Reference Solution Startup guide.

-  Semi-rigids
-  LO distribution connections (E6630-60004, SMA-SMA)
-  Unused M9301A modules

Primary 100 MHz - 8121-2175 Secondary 100 MHz & IF - 8120-5091 Semi-rigid - various Shared LO - E6630-60004 Unused M9301A

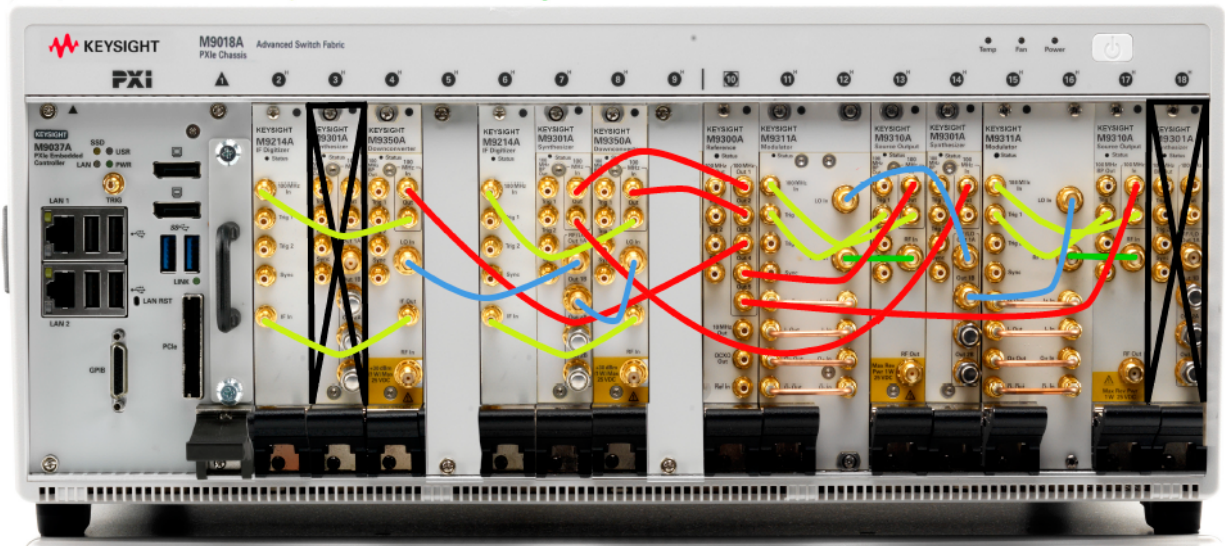


Figure 2.3: Shared LO wiring and module locations

To remove the modules safely, the chassis was turned off and unplugged and a wrist strap was used to prevent electrostatic discharge (ESD). Next, all the wire and semi rigid connections were removed. To move the modules around, the screws were removed and the black extension was pushed down until the module popped out of the chassis. Once a module popped out it was removed and placed next to the other components that made up the individual VSAs and VSGs. Some important things to remember when removing the modules are to keep the individual components that make up a VSA or a VSG module together; to remove and place the blanks in correct places; and to always put the reference module in slot 10.

Once all the slots were placed in the slots as shown in Figure 2.3 the focused turned to wiring the modules together. During the process we realized we did not have enough wires and some of the semi-rigid cables did not fit the connections, so new semi-rigid cables were crafted and SMA-SMA cables were ordered. Once all the wires were connected the next step is to generate a configuration using the Multi-Channel Demo Tool software provided by Keysight.

To figure out how to use the Multi-Channel Demo Tool the Keysight LTE/LTE-A Multi-Channel Reference Solution User's guide was consulted. The first thing required when the Multi-Channel PXIe Config Utility is used for the first time or the modules are moved is to verify the slots and the components in the slots. The program will display a list of detected modules and their corresponding slot locations and the user must verify by visual inspection of the unit that the locations and module list are correct. The user verifies the list by clicking yes and then the Multi-Channel PXIe Config Utility opens and the user can generate a configuration.

To generate a shared LO configuration first open up the Multi-Channel PXIe Config Utility and open up the properties tab. Once the properties tab is open select the following settings: Shared VSG LO, Shared VSA LO, and Apply User Configuration on User Login. The shared VSG LO and shared VSA LO tell the Multi-Channel PXIe Config Utility that the system is to be configured in the shared LO configuration with a reference module located in the chassis. Even though the location and connections between modules usually stay consistent across power cycles, the multi-channel configuration does not. To avoid having to use Multi-Channel PXIe Config Utility every time the system is turned on, the 'apply user' configuration on user login can be selected. Once it is selected and the user logs onto the computer, the configuration will automatically generate and apply the desired configuration.

Once the settings are selected click the generate configuration button. When pressed, the program will ask for devices that are part of the multi-channel configuration. For the 2x2 shared LO configuration all the devices are selected. Next, the Config Utility will ask for which synthesizer to use for the VSA and VSG. Select the synthesizer located in slot 7 for the VSA and slot 14 for the VSG. Once the slots are selected the Config Utility should have a green circle next to generate configuration. Click the apply button and the Config Utility to connect the chassis to the reference module and to make changes to connect the other devices in the desired configuration. Once the configuration is applied successfully, a green dot will appear to the left. If there is a red dot, go back to the previous step and make sure everything is selected properly. Next select run alignments and follow the instructions given and make any additional connections necessary to do the tests. If errors occur, consult the Keysight manuals for assistance. When the alignments are passed a green circle will appear on the left of the run alignments button. The final step in the configuration is to run a self test. If any errors result consult either Keysight or the manual.

The Multi-Channel PXIe Config Utility also allows the user to run a sample waveform through the configuration. To run the sample waveform first the 89600 VSA software must be configured, which can be done by selecting the configure 89600 button. When the button is clicked a name needs to be specified and auto calibrate should be selected. The Config Utility will then open and configure the 89600 VSA software. When the software opens, connect a BNC-BNC cable from each VSG to VSA and click the “Play Sample Waveform” button. After the button is pressed, a square waveform should appear on both the channels of the 89600 VSA software. If

these do not appear, make sure all the cables connecting the VSA and VSG modules are connected correctly.

Some issues that were encountered when running the self test was the firmware for the chassis needed to be updated, but once it was updated the MIMO Demo Tool would not connect to the chassis. After communicating to Keysight about the connection issue, it was determined to be a hardware problem. The exact hardware problem could not be found and remains a mystery. So the focus turned to using coding to control the VSAs and VSGs instead of the programs.

2.6 Using C# to Generate Testing Environment

While the chassis containing the VSA and VSG modules were being configured for the MIMO Demo Tool, another approach was used to run MIMO tests: through the use of Visual Studio and C#, the components that make up the VSA and VSG modules can be manipulated on a much lower level.

To start a new project: 'File' → 'New' → 'New Project'. After selecting new project a large list of various different project types will appear, be sure to select 'Console Application'. This will start a new project and an open text editor will appear. One will immediately see at the top of the page several 'using' statements. In order to allow this source code to communicate with the hardware, references must be added. To add a reference right-click the 'Reference' tab at the far right end of Visual Studio and select 'Add References'. Next, select the tab labeled 'COM' and type in *IVI AgM9018 1.3 Type Library*, *IVI AgM9300 2.1 Type Library*, and *IVI AgM938x 2.1 Type Library*, select the box next to each and then click 'OK'. The required references have now been added!

The code written has several regions: *Create Driver Instances*, *Initialize Driver Instances* and *Check for Errors*, *Route Backplane Triggers from M9300A to VSGs*, *Setting Up the M9381A PXIe VSGs for WLAN Rx Testing*, *Start Waveform Playback on the M9381A PXIe VSGs*, and *Close Driver Instances*.

In many cases when writing code, we begin by creating variables such as ints, doubles, chars, etc. Figure 2.4 shows how instances of the VSGs, Reference, and the Chassis are created; one may notice 'IAgM938xEx', 'IAgM9300Ex', and 'IAgM9018'; these data types allow us to communicate with and drive the VSGs, Reference, and Chassis. This portion of the code simply creates empty instances of the modules, objects, that will be used for later tests and measurements. Note that if this program were to drive the VSA modules, it would need to create empty instances of the 'IAgM9391Ex' data type.

```
#region Create Driver Instances
IAgM938xEx M9381A_VSG1 = new AgM938x(); // Create VSG 1
IAgM938xEx M9381A_VSG2 = new AgM938x(); // Create VSG 2, Used by 2x2 MIMO
IAgM9300Ex M9300A_REF1 = new AgM9300(); // Create the Reference
IAgM9018 M9018A_CHASSIS1 = new AgM9018(); // Create Chassis
#endregion
```

Figure 2.4: Creating Driver Instances

The next region of the code initializes the driver instances and checks for errors. The code starts out by declaring the the resource names of all the drivers. Figure 2.5 shows how the resource names for VSG 1 and VSG 2 are declared. The resource name indicates which modules belong to each driver instance. For example, the components that make up the M9381A VSG are the M9311A Modulator, M9310A Source Output, and M9301A Synthesizer, which are located in slots 3 through 6 (for VSG 1). The resource name tells the program which

slots these components are placed in such that commands are sent to the correct modules. Notice that the resource name for VSG 1 is longer than that of VSG 2, this is because only one of the VSGs resource names must include the M9300A Reference located in slot 10. The resource names can be obtained using the M9381 SFP software by selecting which slots contain the required components.

```
string M9381A_VSG1_ResourceName = "PXI7::0::0::INSTR;PXI12::0::0::INSTR;PXI13::0::0::INSTR;PXI20::0::0::INSTR";  
string M9381A_VSG2_ResourceName = "PXI27::0::0::INSTR;PXI26::0::0::INSTR;PXI21::0::0::INSTR";
```

Figure 2.5: VSG 1 and 2 Resource Names

C# is an object oriented programming language; back in the first region, objects were created. Objects can be manipulated/acted upon using methods. In Figure 2.6, the Initialize() method is used on the M9381A_VSG1 object. This method initializes VSG 1 and checks for errors; if any errors are present the initialization process will fail. However, if the initialization passes “M9381A PXIe VSG Channel 1 - Driver Initialized” will be written to the console.

```
//Initialize M9381A Channel 1 and clear startup messages & warnings, if any.  
M9381A_VSG1.Initialize(M9381A_VSG1_ResourceName, IdQuery, Reset, M9381A_VSGx_OptionString);  
do  
{  
    M9381A_VSG1.Utility.ErrorQuery(ref errorcode, ref message);  
    if (errorcode != 0)  
        Console.WriteLine(message);  
} while (errorcode != 0);  
Console.WriteLine("M9381A PXIe VSG Channel 1 - Driver Initialized");
```

Figure 2.6: Initialization

The next region of the code routes the back panel trigger busses of the M9018A PXIe Chassis. Each chassis has 3 back panel trigger busses: bus segment 1 which extends from slot 1 to 6, bus segment 2 which extends from slot 7 to 12, and bus segment 3 which extends from slot 13

to 18. Each bus segment has 8 trigger lines. In order for the system to be configured for MIMO, the bus triggers must satisfy three conditions: there must be a PXI trigger from M9301A (Synthesizer) to M9311A (Modulator), there must be a PXI trigger from M9311A to M9310A (Source Output), and none of the triggers can conflict with each other. The last condition refers to if there are multiple M9381A VSGs in a single chassis; if there are two M9381A VSGs present, then they cannot both use the default trigger lines.

After the back panel trigger busses have been properly routed, the program then proceeds to ready the M9381A VSGs for outputting a signal. Figure 2.6.4 shows the sequence of methods used on the M9381A_VSG1 object to configure the external triggers; the same sequence of methods are used on the M9381A_VSG2 object. The methods used are '.Triggers', '.ExternalTrigger', and '.Configure()'. This allows for VSG 1 and 2 to be synchronized with the reference and enable waveform playback.

```
M9381A_VSG1.Triggers.ExternalTrigger.Configure(true, 0.01, 0.5, AgM938xTriggerSlopeEnum.AgM938xTriggerSlopePositive,
AgM938xTriggerEnum.AgM938xTriggerPXITrigger0, AgM938xTriggerTerminationEnum.AgM938xTriggerTermination500hm, 10000,
AgM938xTimeoutModeEnum.AgM938xTimeoutModeTimeoutAbort);
```

Figure 2.7: Configuring external triggers

The code in Figure 2.8 prompts the user for his/her desired modulation frequency. The user must enter the frequency in the console in units of Hertz. The frequency is read in as a string using the 'Console.ReadLine()' method, and then converted to a double using the 'Convert.ToDouble()' method. Using the 'RF' and 'Frequency' methods, the modulation frequency of M9381A_VSG1 and M9381A_VSG2 are set.

```

// Sets RF Frequency
Console.WriteLine("\n\nWhat is the desired Modulation Frequency in Hz?");
double Frequency = Convert.ToDouble(Console.ReadLine());
double FreqGHz = Frequency / 1e9;
Console.WriteLine("\n\nDesired Modulation Frequency: {0} GHz", FreqGHz);

Console.WriteLine("\n\tSet RF Frequency:");
M9381A_VSG1.RF.Frequency = Frequency;
Console.WriteLine("\t... on VSG 1 to {0}", Frequency);
M9381A_VSG2.RF.Frequency = Frequency;
Console.WriteLine("\t... on VSG 2 to {0}", Frequency);

```

Figure 2.8: Setting the Modulation Frequency

Following the user input frequency, the program then prompts the user to input the desired power level for both VSG 1 and 2, the code for which looks quite similar to that shown in Figure 2.8. Adjusting the power of VSG 1 and VSG 2 will allow for the user to run various different types of tests such as beamforming. Modulation and RF Output for objects M9381A_VSG1 and M9381A_VSG2 and enabled using the following commands:

M9381A_VSG1.Modulation.Enabled = true; and *M9381A_VSG1.RF.OutputEnabled = true;*. The system is now ready to play a signal!

Now that both VSG drivers have been initialized, the next step is to upload a waveform for the them to play. Unfortunately, the 'Ctrl+V' paste command does not work in the C# command window. The user has two choices: type out the name of the waveform or paste the waveform name using an alternative method. To paste the name of the desired waveform the user must right-click the top of the command window, click 'Edit', and then select 'Paste'. The figure below shows what this sequence of events looks like:

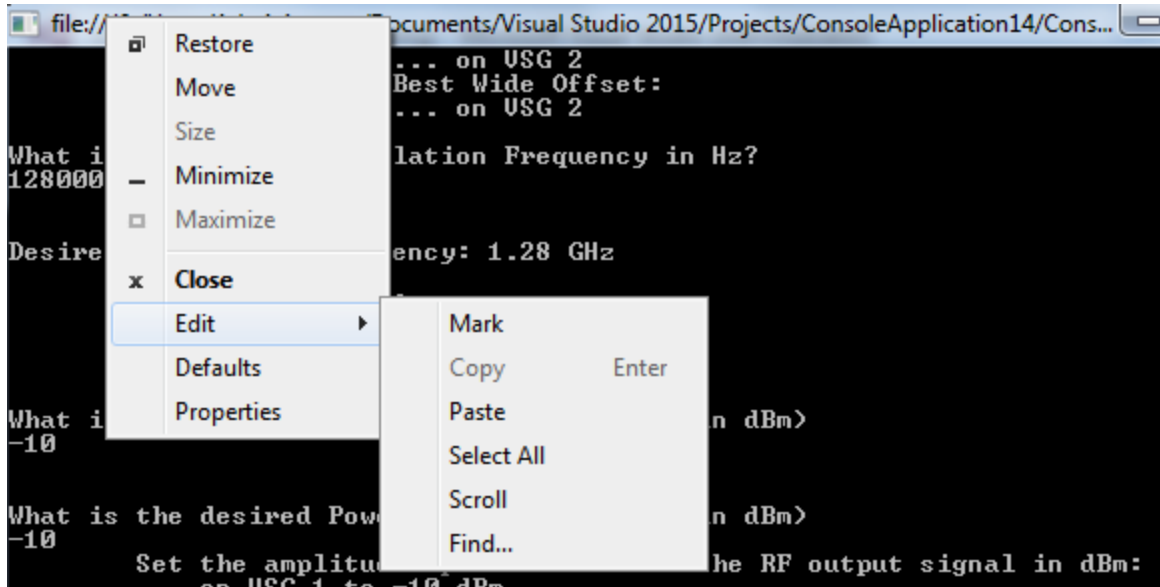


Figure 2.9: Uploading an Arbitrary Waveform

```

What is the desired Modulation Frequency in Hz?
1280000000

Desired Modulation Frequency: 1.28 GHz

Set RF Frequency:
... on USG 1 to 1280000000
... on USG 2 to 1280000000

What is the desired Power Level of USG 1? <in dBm>
-10

What is the desired Power Level of USG 2? <in dBm>
-10

Set the amplitude <power/level> of the RF output signal in dBm:
... on USG 1 to -10 dBm
... on USG 2 to -10 dBm
Enable Modulation:
... on USG 1      ... on USG 2      Enable RF Output:
... on USG 1      ... on USG 2

Please specify the desired waveform
Must come from C:\Program Files (x86)\Agilent\M938x\Example Waveforms\
Waveform:
WLAN_11n_64QAM_40MHz.wfm

```

Figure 2.10: User Prompts

Figure 2.10 shows what the command window will look like once the user has responded to all the prompts. As seen above, the user is first asked to specify his/her desired

modulation frequency in 'Hz'; for this example we chose 1.28 GHz. The next two prompts ask for the user to specify the desired output power level for VSG1 and VSG2 in dBm. The output power level of both VSGs do not need to be the same, however for this example they were both chosen to be -10 dBm. The final user input required is the desired arbitrary waveform. It is important that the waveform comes from 'C:\Program Files (x86)\Agilent\M938x\Example Waveforms', otherwise the code will not run. For this example we chose to upload 'WLAN_11n_64QAM_40MHz.wfm'. Once the user presses enter after uploading the waveform the VSGs will begin to continuously play the signal until stopped.

Now that the VSGs are playing a waveform let's go over how to configure the VSAs to read the generated signals. To read these generated signals, we used the 'Keysight 89600 VSA 21.0' software. Before we could use it to read our waveforms, we first needed to have it drive two VSAs simultaneously, this software is defaulted to only drive VSA1. To do this, first open Keysight 89600 VSA 21.0, then click on 'Utilities' → 'Hardware' → 'Configurations...' as seen in Figure 2.11.

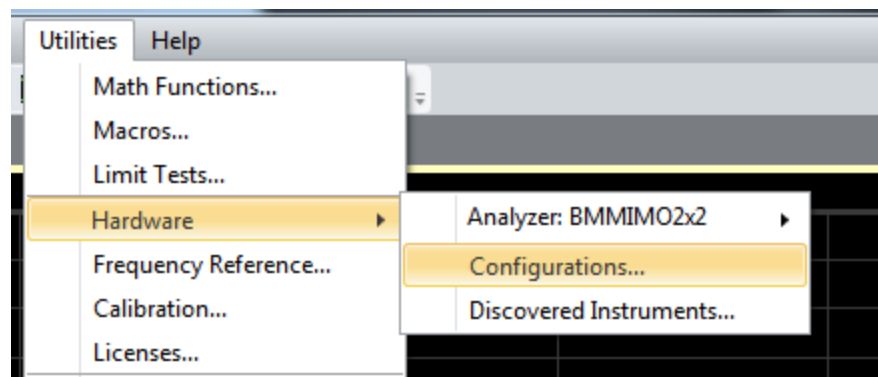


Figure 2.11: How to open Configurations

Selecting 'Configurations...' will bring the user to a new window that allows for him/her to select which components are used for each VSA. This window can be seen in Figure 2.12.

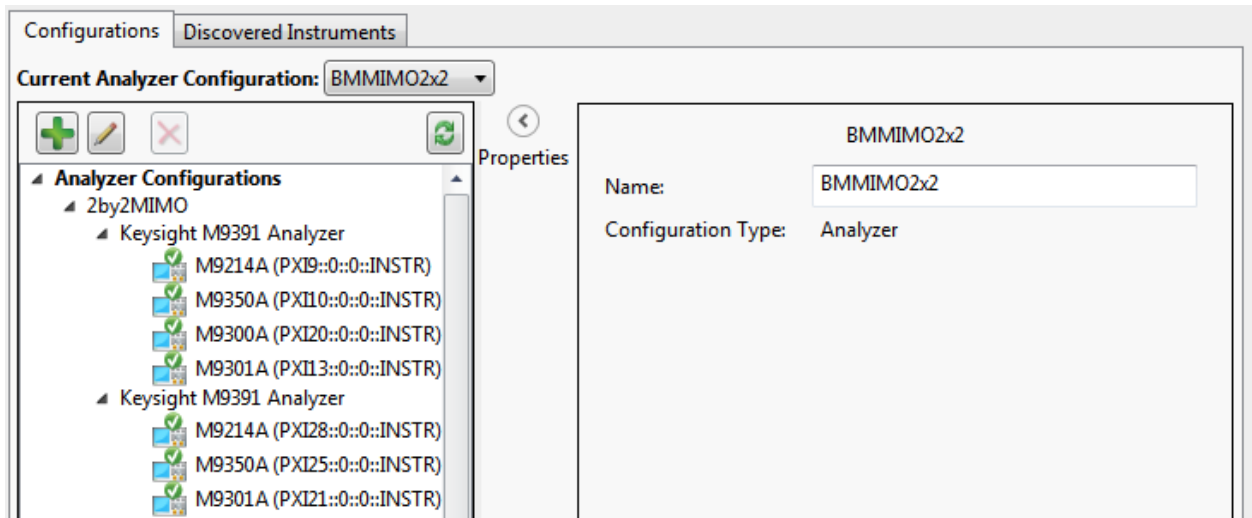


Figure 2.12: Configuration Window

To add a new configuration, click the green plus sign near the top left part of the window. This will bring one to the window named 'New Hardware Configuration'. Under 'Possible Logical Instruments' click and drag 'Keysight M9391 Analyzer' over to the tab labeled 'Configuration': do this twice. Under the 'Configuration' tab click on either of the analyzers and select which instruments belong to it, do this for each of the VSAs. Just like with the VSGs only one may have the reference included as a component. Be sure that no individual component is used for both of the VSAs. Figure 2.13 shows what the above steps look like when implemented.

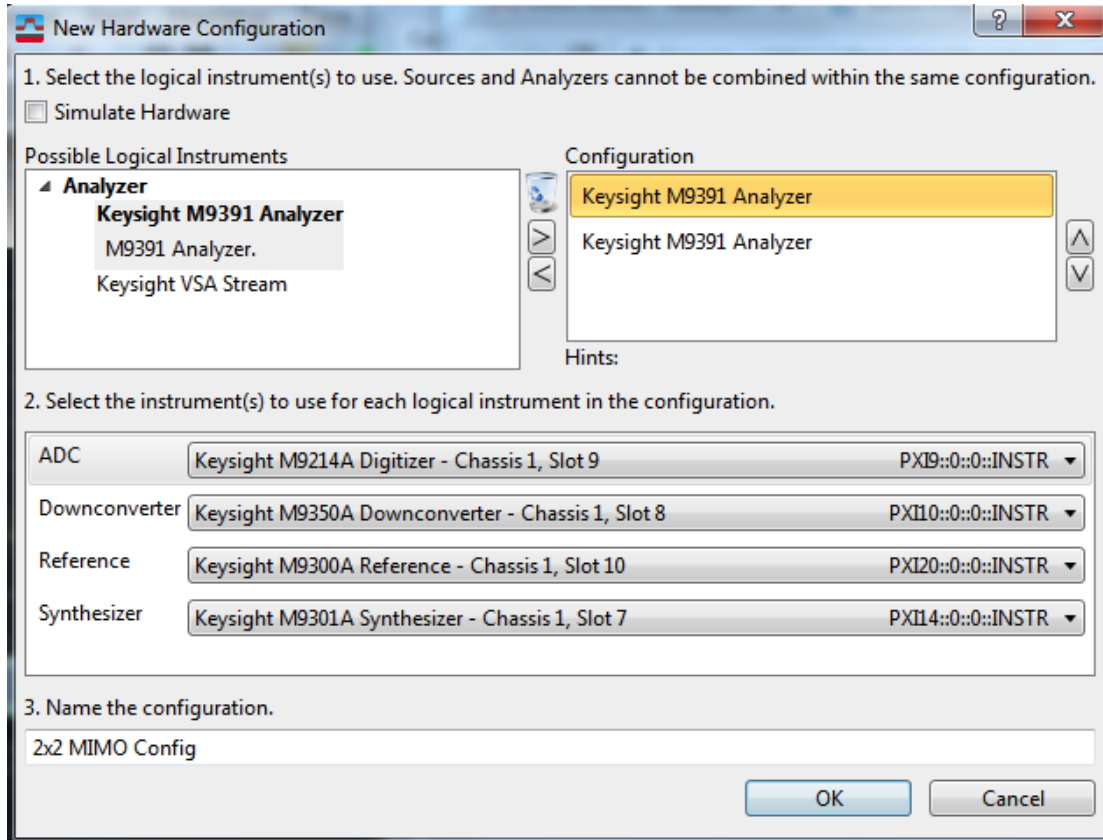


Figure 2.13: VSA Instrument Selection

For our tests, we chose VSA1 to be the master and VSA2 to be the slave, all this means is that VSA1 will have the reference as one of its components while VSA2 will not. As discussed above, the instruments in slots 3, 4, 5, 6, 14, 15, 16, and 17 are used for VSG1 and VSG2, we must be sure to not select the M9301A Synthesizer from slots 6 or 17 to be a components in either of our VSAs (this is the only instrument that is used in both VSA and VSG). For our experiments we chose VSA1 to consist of M9301A Synthesizer in slot 7, M9350A Downconverter in slot 8, M9214A IF Digitizer in slot 9, and M9300A Reference in slot 10; we chose for VSG2 to consist of M9301A Synthesizer in slot 11, M9350A Downconverter in slot 12, and M9214A IF Digitizer in slot 13. After selecting the instruments, give the configuration a name and then finally select 'OK'. After creating one's own configuration, implement it by selecting 'Utilities' → 'Hardware' and select the new configuration.

Now that the proper hardware configurations have been made, we must now change the inputs. To do this select 'Input' → 'Channel' → 'Custom', this will cause a window named 'Channel Configuration' to open. Change the connections in this window to look like they do in Figure 2.14.

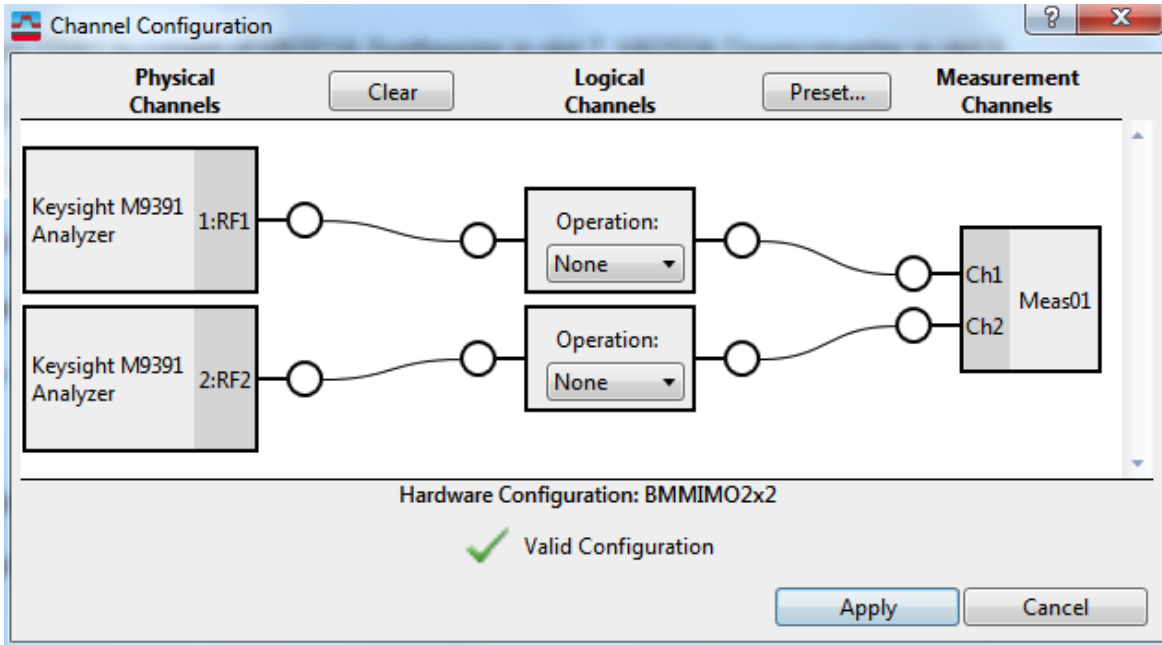


Figure 2.14: Channel Configuration

Click 'Apply' and confirm that it is a valid configuration. The connection shown above tells the Keysight 89600 VSA software to expect data streams arriving at both VSA1 and VSA2; this allows for both VSAs to be active simultaneously.

The final configuration step is to choose a setup. This is done by clicking 'File' → 'Recall' → 'Recall Setup...'. The user will be prompted to choose a setup for his/her test. Navigate to the same folder in which the waveform file was taken from and choose the setup that corresponds to the waveform that was specified in the command window. For example: if we chose

WLAN_11ac_256QAM_80MHz.wfm to be our arbitrary waveform, the setup file would be WLAN_11ac_256QAM_80MHz.setx, which can be seen in Figure 2.15.

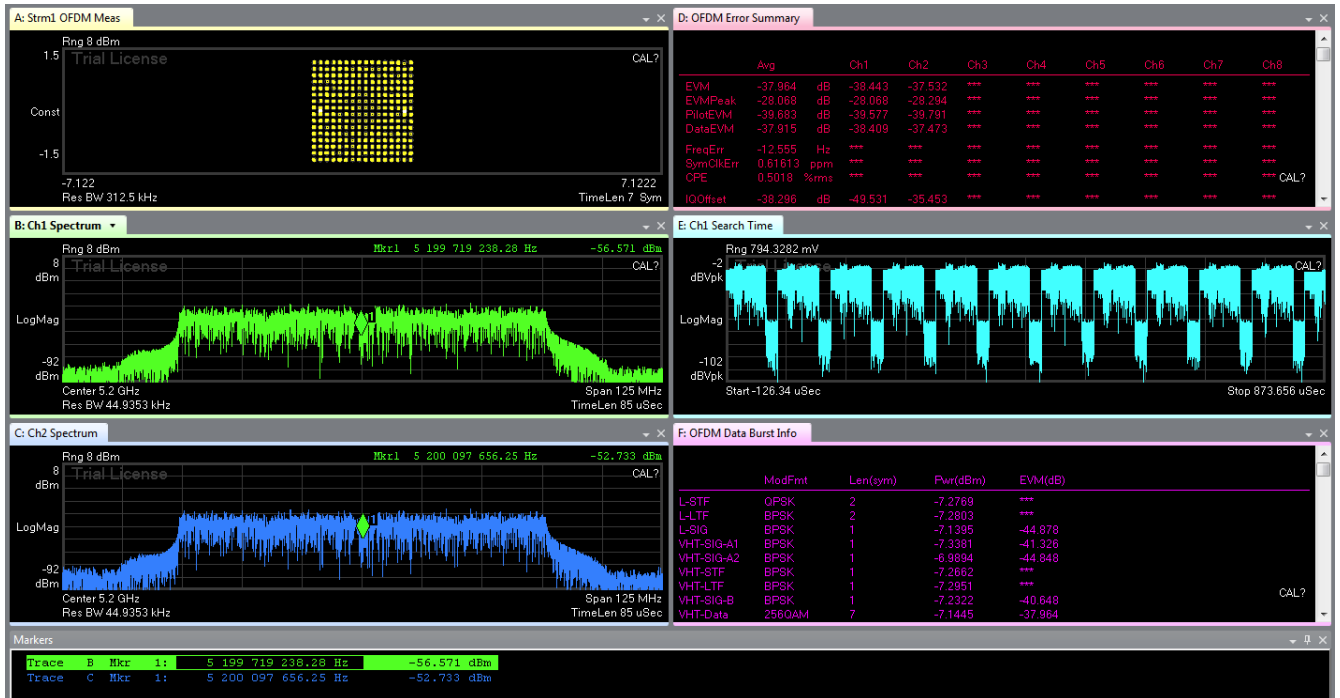


Figure 2.15: WLAN_11ac_256QAM_80MHz.setx

The user must change the 'Center' on the channel spectrum such that it matches the modulation frequency chosen; this will cause the 8960 software to start displaying data. The user can also change the measurement types by selecting the window tab and specifying his/her desired measurement, as shown in Figure 2.16.

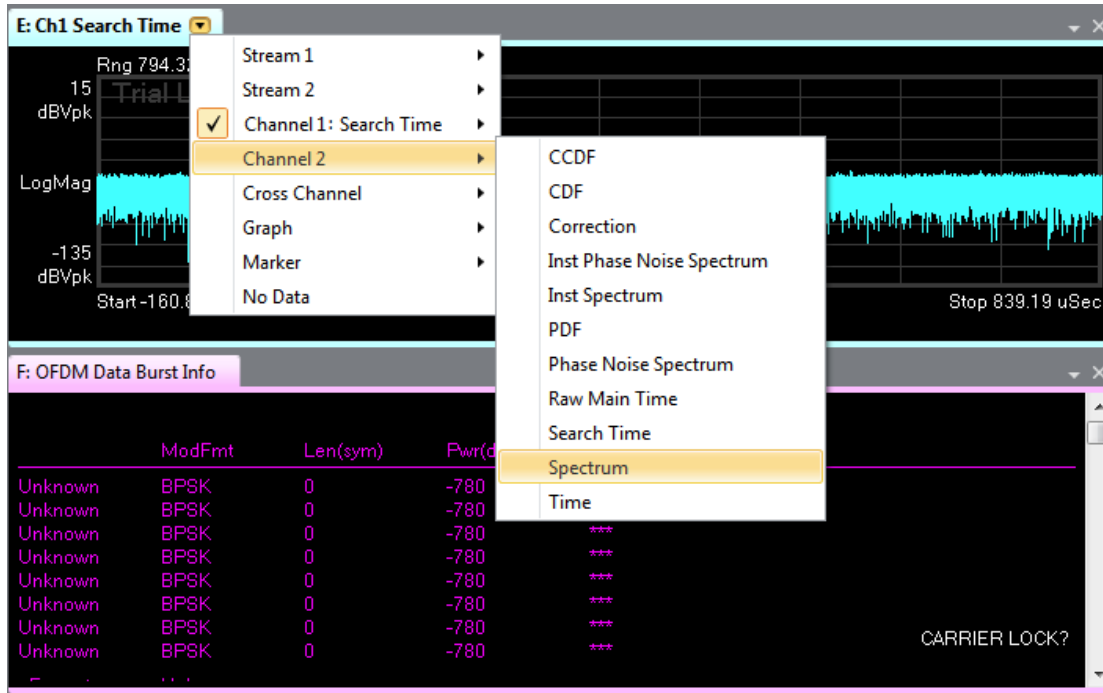


Figure 2.16: Change Measurement Type

Chapter 3: Antennas and Pre-Amplifiers

Since antennas are crucial to the study of the various communication links, the team also spent some time developing and creating various antennas to use for the implementation of this project. The following chapter emphasizes some of the important concepts of antennas necessary to their construction. In this MIMO project, antennas and other hardware will be created at 1.3 GHz due to ease of design and cheaper available hardware at lower frequencies.

3.1 Antennas Overview

Antennas are the primary means of transferring information wirelessly. An antenna is defined as an electrical conductor for radiating electromagnetic energy or receiving electromagnetic energy.

Upon transmission of a signal, radio frequency current is converted into electromagnetic energy by the antenna and radiated out into the environment. Upon reception, an electromagnetic signal is converted back into a radio-frequency current and fed into the receiving circuitry. There are a few concepts that will help you understand antennas. Antennas can be characterized by multitudes of properties: frequency, radiation pattern, field regions, directivity, efficiency, gain, beamwidth, bandwidth, polarization, effective aperture, and temperature.

Frequency

Antennas operate by transmitting or receiving electromagnetic waves in the radiowave to mmwave region. However, antennas do not work over a large range of frequencies typically, just as human vision can only detect red to violet on the electromagnetic spectrum. In the design of an antenna, it is important to know the frequency of operation--otherwise information may not be correctly received. For example, for AT&T cellular devices, AT&T uses their licensed 1.9 GHz band, along with the WiFi bands of 2.4 GHz and 5.8 GHz. The designer of those cellular devices must create an antenna that is able to receive energy at those select frequencies. Figure 3.1 shows how frequency bands have been allocated in industry.

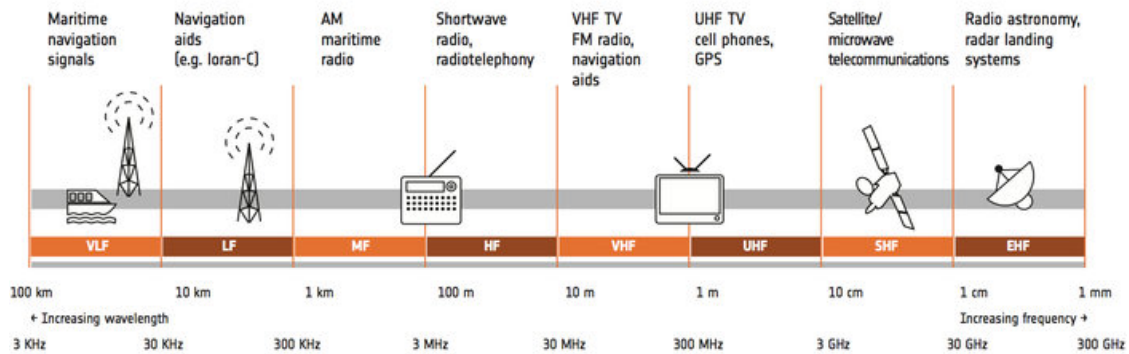


Figure 3.1: Frequency bands, taken from

http://www.esa.int/spaceinimages/Images/2013/11/Satellite_frequency_bands

Radiation Pattern

Radiation pattern describes a plot that visualizes where an antenna transmits or receives power. The plots are usually 3-dimensional and sometimes 2-dimensional, where the 2-dimensional plots are slices of the 3-dimensional plot. This kind of plot uses standard spherical coordinates where the angle Θ is measured off the z-axis and the angle ϕ is measured counterclockwise off the x-axis. An example radiation pattern is displayed in Figure 3.2.

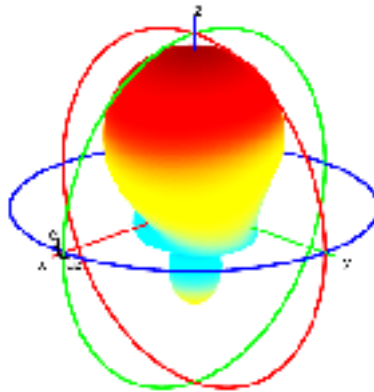


Figure 3.2: Radiation pattern example, taken from

https://www.mathworks.com/help/antenna/ref/patterncustom_3dpolar.png

There are a certain radiation patterns denoted: isotropic, omnidirectional, and directional.

Isotropic refers to a radiation pattern that is uniform in all directions--imagine a spherical radiation pattern. In practice this does not exist, but it is useful to compare the gain of different antennas. Omnidirectional refers to an antenna that is isotropic in a single plane, such as x-y or y-z. Some examples include dipole, helical, and umbrella antennas. Directional refers to an antenna typically has a single peak direction in the pattern of radiation. Some examples include patch, Yagi-Uda, phased-array, and cantennas. Directional antennas are the most common types of antennas. Examples of all types are shown in Figure 3.3

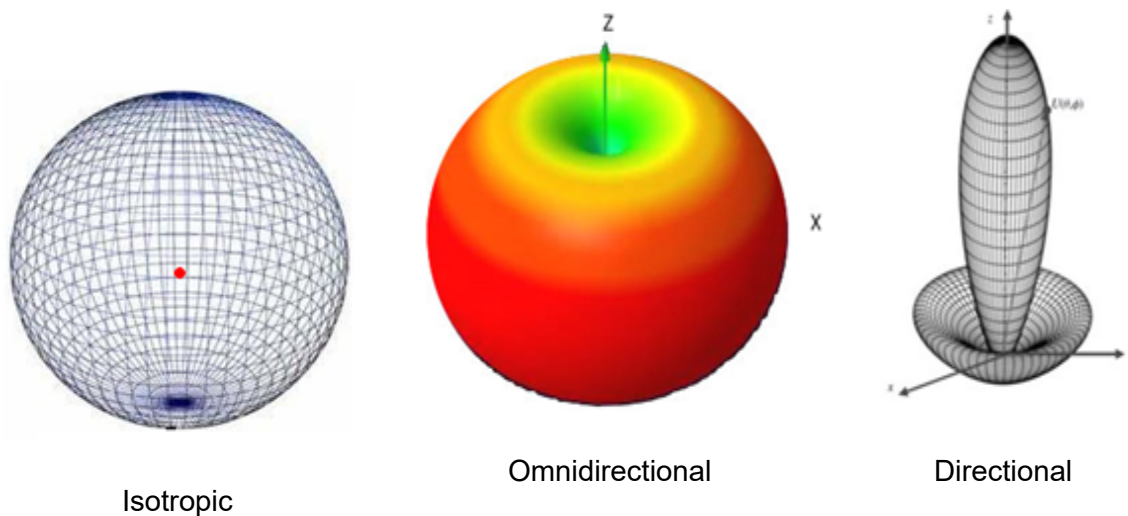


Figure 3.3: Types of radiation patterns, taken from

<https://wisense.files.wordpress.com/2014/12/isotropic-12.png?w=418&h=428>

<http://bpastudio.csudh.edu/FAC/LPRESS/471/hout/wireless/omni1.jpg>

<http://www.mtiwe.com/uploads/imagesgallery/antennafundamentals5.jpg>

Field Regions

There are three field regions: reactive near field, radiating near field, and far field. The far field is the most important region, since antennas are used to communicate wireless from lengthy distances.

The reactive near field is where the electric field and magnetic field may not be in phase, and angular field distribution is dependent upon the distance from the antenna. Determining these patterns at such a close range involves heavy calculus and mathematical techniques. The radiating near field, or Fresnel region is better, but angular field distribution is still dependent upon the distance from the antenna. In the far field region, the phase difference between electric and magnetic field is almost constant, and angular field distribution is independent upon the distance from the antenna. The far field region is the region of which anechoic chambers measure antenna patterns. Figure 3.4 visualizes the three different field regions.

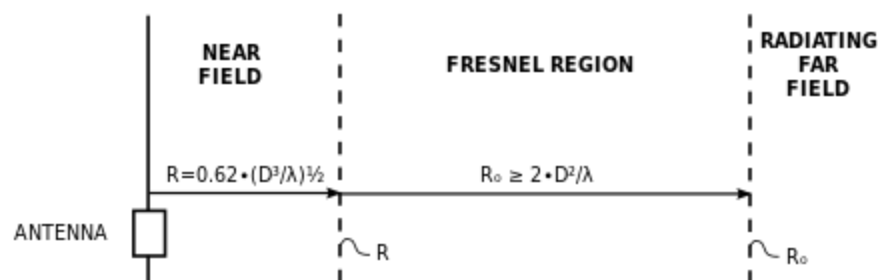


Figure 3.4: Visualizing Field Regions. R is distance, D is largest feature of antenna, and λ is wavelength. Taken from

<https://www.everythingrf.com/rf-calculators/antenna-near-field-distance-calculator>

Directivity

Directivity is the measure of the peak value of radiated power divided by the average. Peak directivity is most often used to describe directivity; note that directivity is a function of angle. Unlike antenna gain, directivity does not take into account actual losses that may occur. High directivity is wanted to maximize transmit power. Examples include remote sensing applications, beamforming, and radar. However, low directivity may also be desired for cases such as cell phones, radio, and WiFi. In the context of MIMO, cellular base stations may want to have highly directive antennas. Receivers, such as cell phones may want to have low directivity in order to receive the signal from varying angles. However, something such as WiFi may require low directivity as well, since the target device's location may not be in one direction.

Efficiency

Efficiency is a measure of how well input power is transferred over to an antenna. This is the same in concept compared to transmission lines. One would want all the input power to be transmitted, and none to be reflected for highest efficiency. This implies to well-match the impedance of the antenna (the load) to the impedance of the source. On a network analyzer, this can be measured as S11, the return loss. The closer an antenna's input impedance at the target frequency is to the characteristic impedance of a system (ex. $50\ \Omega$ or $75\ \Omega$), the higher the efficiency.

Gain

Antenna gain denotes the power transmitted in the peak radiation direction relative to an isotropic source. Essentially, gain is the concept of directivity combined with efficiency. This is

often denoted in the units of “dBi” or “decibels relative to an isotropic antenna.” For example, a directional antenna with a gain of 10 dBi has 10 dB more gain than an isotropic antenna. Directional antennas may have a gain higher than 0 dBi typically. Omnidirectional antennas may not necessarily have a gain higher than 0 dBi.

Beamwidth

Beamwidth is an angular measurement for an antenna radiation pattern. The beamwidth measurement is usually with respect to the mainlobe at $E = 1$. Two typical beamwidth measurements are the half power beamwidth (HPBW) and the beamwidth between first nulls (FNBW). The HPBW is an angular measurement from the main lobe to the half-power $E = (-3\text{dB})$ level on the main lobe. The beamwidth between first nulls is the angular measurement between the main lobe and the nulls between the main lobe and the first side.

Beamwidth is measured in angles, unlike the typical bandwidth. For example, beam width of antenna arrays maybe small, but provide the largest gain within that angle range. If a receiver is not within the beamwidth, a much smaller or even no signal may be detected.

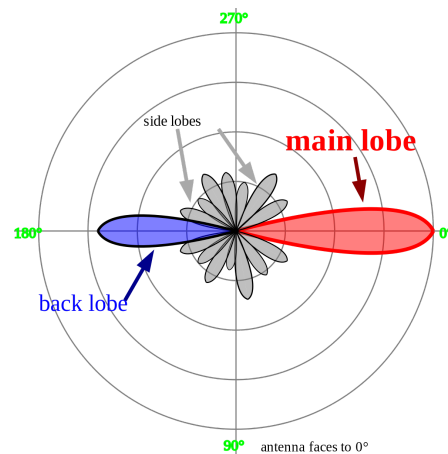


Figure 3.5: Lobes visualized, taken from

<https://upload.wikimedia.org/wikipedia/commons/thumb/7/74>

/Sidelobes_en.svg/1200px-Sidelobes_en.svg.png

Another measurement of beamwidth is null-to-null beamwidth. This is where the radiation pattern decreases to 0, or negative infinity dBi.

Sidelobes are smaller beams that occur besides the main beam. These side lobe may not be completely eliminated; in the context of directivity, this is wasted power. Side lobe level (SLL) is another measurement to characterize side lobes. It measures the maximum gain of a side lobe relative to the main lobe's maximum.

Bandwidth

In the frequency domain, this is where the antenna is 3 dB (half the power) lower than its maximum gain. If the bandwidth is not large enough for the information signal, some information will be lost. Another specification in design of an antenna is not to make the bandwidth too large; this may pick up undesired signals. However, a filter following the receiver may be used to remedy this problem.

Bandwidth and antenna efficiency usually have an inverse relationship. Highly efficient antennas have low bandwidth. High bandwidth antennas have low efficiency. This design consideration is a tradeoff important to consider when creating specifications for an antenna.

Polarization

Depending on the type of application, antennas can be designed to contain a specific polarization ideal for the transmission desired. Three types of polarizations common in communications systems are vertical, horizontal and circular. The polarization and orientation of the radio wave radiated by the antenna is determined by the electric field plane. If the antenna's electric field plane is perpendicular to the surface of the earth, the antenna possesses vertical polarization. Similarly, if the electric field plane is parallel to the surface of the Earth, the antenna

contains a horizontal polarization. Lastly, circular polarization rotates through all the planes including the horizontal and vertical planes. Its bias in radiation towards a certain plane determines what is called the axial ratio measured in dB. An axial ratio 1-2dB indicates that radiation is tilted more towards a certain plain creating an elliptical-like polarization, while an axial ratio of 0dB indicates that the radiation is equal in all planes, forming a circular polarization.

Temperature

Antenna noise temperature is a characterization of the antenna with regards to the amount of noise it introduces at the input of a receiver. Usually, this is modeled in a system diagram by replacing the antenna with a resistor that produces the equivalent noise power. The higher the temperature, the more noise there is. The equations below model this noise; note that these are the thermal noise equations.

$$v_n = \sqrt{v_n^2} \sqrt{\Delta f} = \sqrt{4k_B T R \Delta f}$$

$$P = v_n^2 / R = 4k_B T \Delta f.$$

Where P = noise power, v_n = RMS noise voltage, k_B = Boltzmann's constant, T = temperature

Δf = bandwidth, and R = antenna impedance

Equation 3.1: Thermal Noise Equation

Note that the antenna noise temperature models thermal noise. The two other prominent noise sources typical in circuits are flicker noise (dependent on active components) and shot noise (more relevant in circuits with small current).

<http://ieeexplore.ieee.org/stamp/stamp.jsp?arnumber=7485875>

Friis Transmission Equation & the Wireless Domain

The equation, one of the fundamentals of antenna theory, models loss due to wireless transmission:

$$P_R = \frac{P_T G_T G_R \lambda^2}{(4\pi R)^2}$$

Where P_R = power received, P_T = power transmitted, G_r = receiver gain, G_T = transmitter gain,

λ = wavelength, and R = distance between antennas

Equation 3.2: Friis Transmission Equation

This can be rearranged in a logarithmic scale for easier computation:

$$[P_R]_{dB} = [P_T]_{dB} + [G_T]_{dB} + [G_R]_{dB} + \left[\left(\frac{\lambda}{4\pi R} \right)^2 \right]_{dB}$$

Equation 3.3: Friis Transmission Equation, logarithmic form

The lower the frequency, the lower the loss due to distance. This indicates that smaller frequencies (ex 1 GHz versus 10 GHz) can travel a lot farther before reaching the same power level. At high frequencies, there are high losses incurring, so the usage may not necessarily be for long-range communication, but rather short range. However, keep in mind that while a low frequency operation may have lower losses, antennas are usually a lot larger. Note that antennas may be the size of its quarter wavelength or half wavelength to create resonance.

Another factor is loss due to polarization mismatch:

$$P_R = (PLF) \cdot \frac{P_T G_T G_R c^2}{(4\pi R f)^2}$$

Equation 3.4: Friis Transmission Equation, polarization factor

There are more loss factors such as those due to effective aperture and cross-section of an antenna; even atmospheric conditions may be a factor. Other factors that may occur include a doppler shift or frequency change, as well as multipath (signals bouncing around).

In Figure 3.6 to the right, resonance with the molecular oxygen structure creates heavy attenuation at radio frequency bands such as around 60 and 120 GHz. The Friis equation does not account for this. A general trend to note is that the higher the frequency, the more

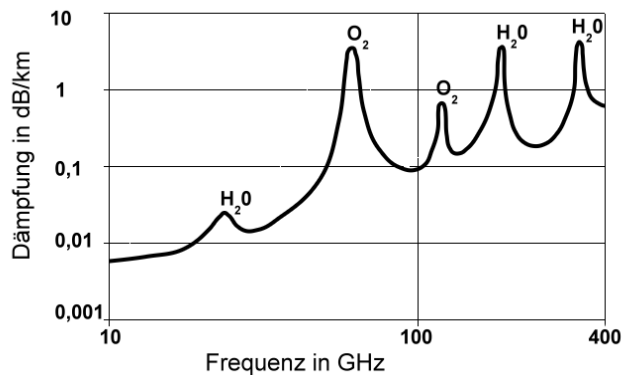


Figure 3.6: Atmospheric attenuation, based on frequency

attenuation per km. Certain frequencies have resonance with the water and oxygen in the atmosphere, proving difficult to transmit signals at those frequencies without higher transmission power.

3.2 Anechoic Chamber Overview

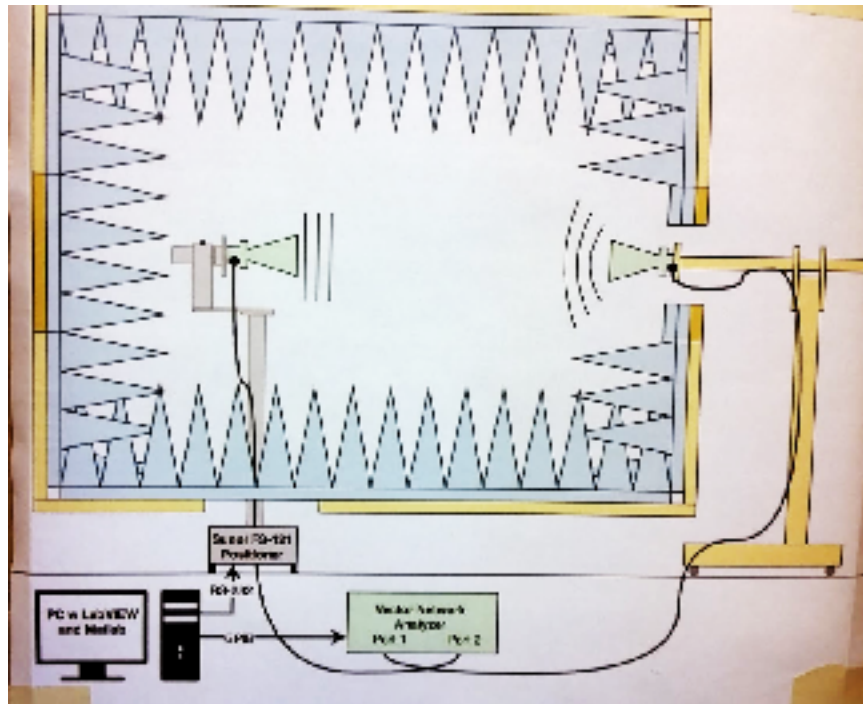


Figure 3.7: Block diagram of anechoic chamber in room 20-113 located in Cal Poly San Luis Obispo.

An anechoic chamber measures an antenna radiation pattern using a vector network analyzer. This is done by measuring the loss at a single-point frequency, and taking measurements every few degrees, until a full rotation of the positioner is completed. Given the distance of separation, gain of the transmit antenna, loss of both wires, the system can be de-embedded to be normalized to the gain of the antenna-under test. Using Friis' transmission equation will assist in determining the loss of air. The gain of the transmit antenna is typically given. Wire loss can be determined using a vector network analyzer. Assuming all components are well-matched, one does not need to de-embed the system by undoing scattering parameter systems. Rather, the S21 data will tell the overall loss of the setup. The only unknown is the gain of the antenna-under-test, which can be determined by simple arithmetic (in the logarithmic

scale) of subtracting cable and air losses, and adding antenna gain. In the anechoic chamber used, there is a program that will automate the process. The full block diagram is seen in Figure 3.7.



Figure 3.8: Anechoic chamber in room 20-113 located in Cal Poly San Luis Obispo.

The overall chamber is shown in Figure 3.8. To prevent unwanted interference, put covers on the viewing windows when the device is under test. Otherwise, it is acceptable to leave these covers open when loading antennas or tests are not running.

Ensure that the antennas are directly facing one another. If misaligned, the radiation pattern will not be centered correctly. The transmit side (side with the known antenna gain) has a wooden frame that assists in getting as close to a perpendicular fit as possible. Figure 3.10 shows this fit. Unfortunately, one will have to eyeball the receive antenna (antenna-under-test). This is where removing the hatches for better viewing will help, as seen in Figure 3.9.

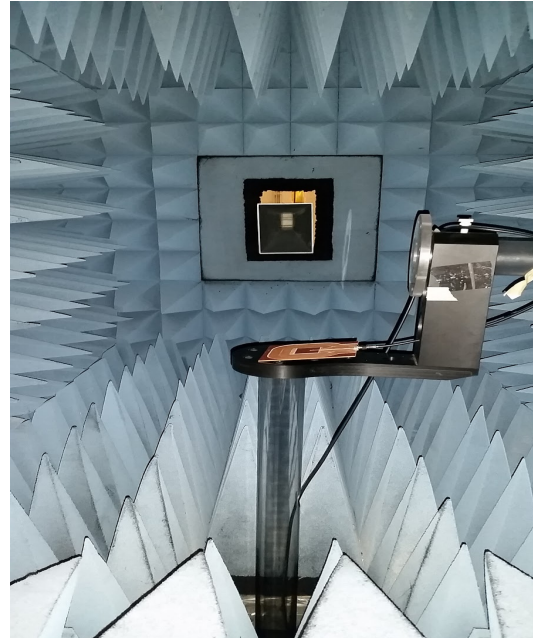


Figure 3.9: Inside of anechoic chamber

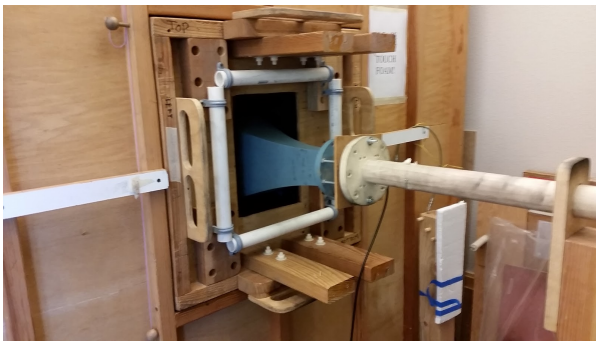


Figure 3.10: Transmit antenna for anechoic chamber.

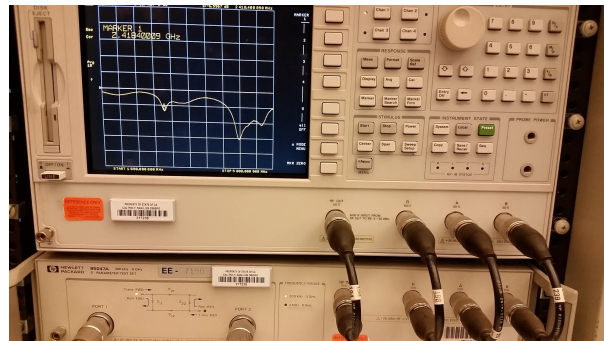


Figure 3.11: The vector network analyzer used for antenna pattern measurements

Ensure that this vector network analyzer and the positioner power are on. Figure 3.11 shows the the specific VNA. Also, ensure the cables are plugged into Port 1 and Port 2. The program on the computer will control the VNA and positioner using LabView to take data. The instructions

to use the program are on the wall panel of the anechoic chamber and will not be discussed in this report. Contact Dr. Arakaki for more assistance in using the anechoic chamber.

3.3 Antenna Hardware

Antenna Overview

The antenna is designed with the purpose of being a jammer, due to its high directivity. The antenna is based on a circular waveguide design. This is a directional antenna with circular polarization. The frequency of operation is directly related to the dimensions of the can. Most antenna designs recommend that the feed length and location be determined experimentally.

Furthermore, the feed's location determines the propagating mode. TE₁₁ is the desired propagating mode, as it is the lowest propagating mode. The waveguide must be able to pass frequencies above TE₁₁'s cutoff limit. Also, the waveguide must be designed such that higher-order modes do not propagate. The waveguide propagating modes are visualized in Figure 3.12. The target frequency of operation is 1.3 GHz. The metal can selected has a radius of 7.75 centimeters. From this, the lower and upper frequencies of operation can be determined, using circular waveguide cutoff frequency formulas.

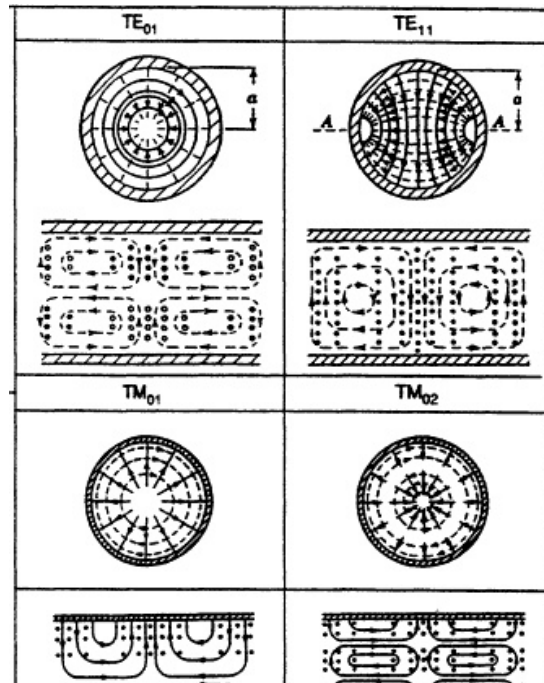


Figure 3.12: Waveguide propagating modes visualized, taken from <https://www.nap.edu/openbook/0309050278/xhtml/images/img00056.jpg>

Cantenna Implementation

Tables 3.1, 3.2: Transverse magnetic and transverse electric field mode constants

TM Modes			
n	Pn1	Pn2	Pn3
0	2.405	5.52	8.654
1	3.832	7.016	10.174
2	5.135	8.417	11.62

TE Modes			
n	Pn1	Pn2	Pn3
0	3.832	7.016	10.174
1	1.841	5.331	8.536
2	3.054	6.706	9.97

$$\lambda_{c, nm} = \frac{2\pi a}{p'_{nm}}$$

Radius , $a = 7.75 \text{ cm}$

Free space wavenumber, $k = 2\pi/\lambda = 50.2655 \text{ (1/m)}$

Circumference, $c = 0.48695 \text{ m}$

Equation 3.5: Circular waveguide cutoff wavelength

Tables 3.3, 3.4: Computing cutoff wavelengths for transverse magnetic and transverse electric modes after applying equations

TM Modes- cutoff frequencies (Hz)			
TMnm	0	1	2
0	2.36E+09	4.32E+09	6.27E+09
1	1.13E+09	3.28E+09	5.26E+09
2	1.88E+09	2.07E+09	3.07E+09

TE Modes - cutoff frequencies (Hz)			
TEnm	0	1	2
0	1.48E+09	3.4E+09	5.33E+09
1	2.36E+09	4.32E+09	6.27E+09
2	3.16E+09	2.59E+09	3.58E+09

The lower and upper frequencies from the selected can are computed to be 1.13 GHz to 1.48 GHz, seen in Table 3.3 and 3.4 using the provided circular waveguide formula and the mode order constants seen in Tables 3.1 and 3.2. This fits our frequency of operation. The next step is to experimentally determine a working feed. TE modes will require the feed to be

perpendicular to the side of the can. TM modes will require a feed perpendicular to the bottom of the can. Some typical suggestions is to install the feed a quarter-wavelength from the end of the can. The quarter wavelength for 1.3 GHz is 5.77 cm. In Figure 3.13, a hole is drilled where a feed is applied at this location. The length of the exposed feed is determined by trial and error. A semi-rigid coax's outer conductor is removed, along with the PTFE material to expose the feed, seen in Figure 3.14. This is akin to a quarter-wavelength monopole, radiating inside a circular waveguide. Simulation in an antenna simulation program such as High Frequency Structure Simulator (HFSS) by ANSYS may provide better results, but may require additional time.

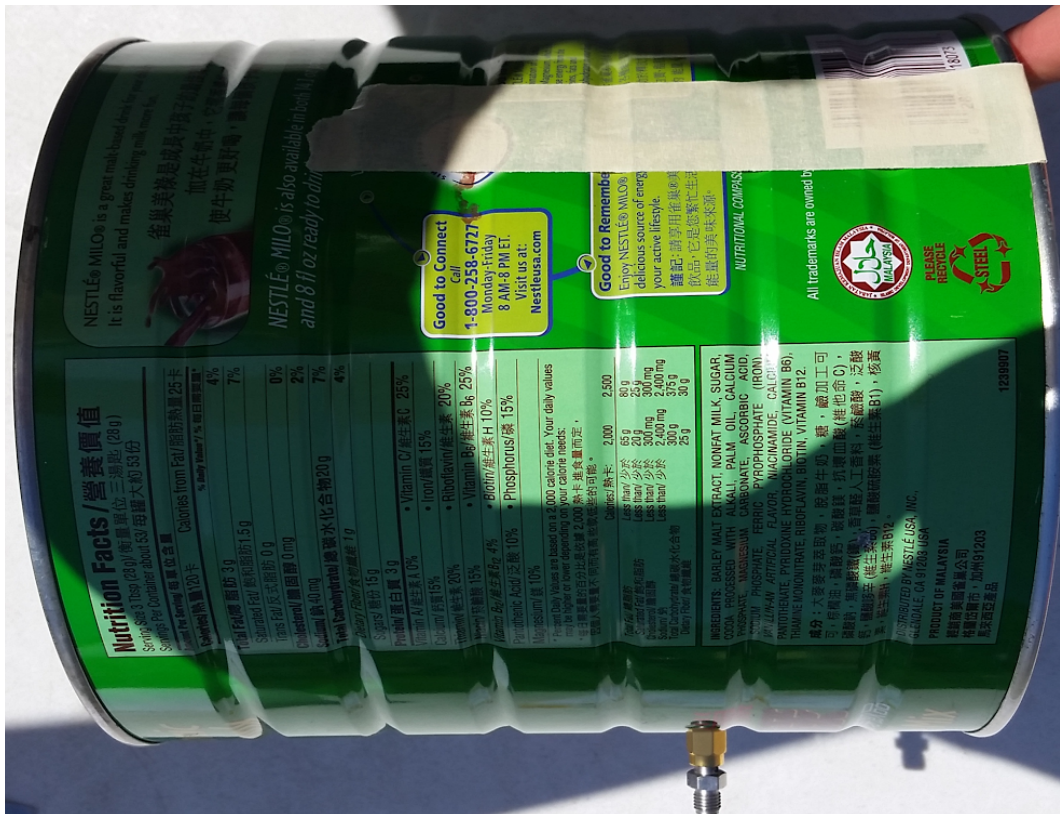


Figure 3.13: Cantenna with SMA feed installed



Figure 3.14 displays the initial feed, uncalibrated. Measuring return loss, or S11 to check efficiency shows that this antenna is not well matched to 50 ohms, as seen in Figure 3.15. Tuning is the next step to perform.

Figure 3.14: Feed length, untuned

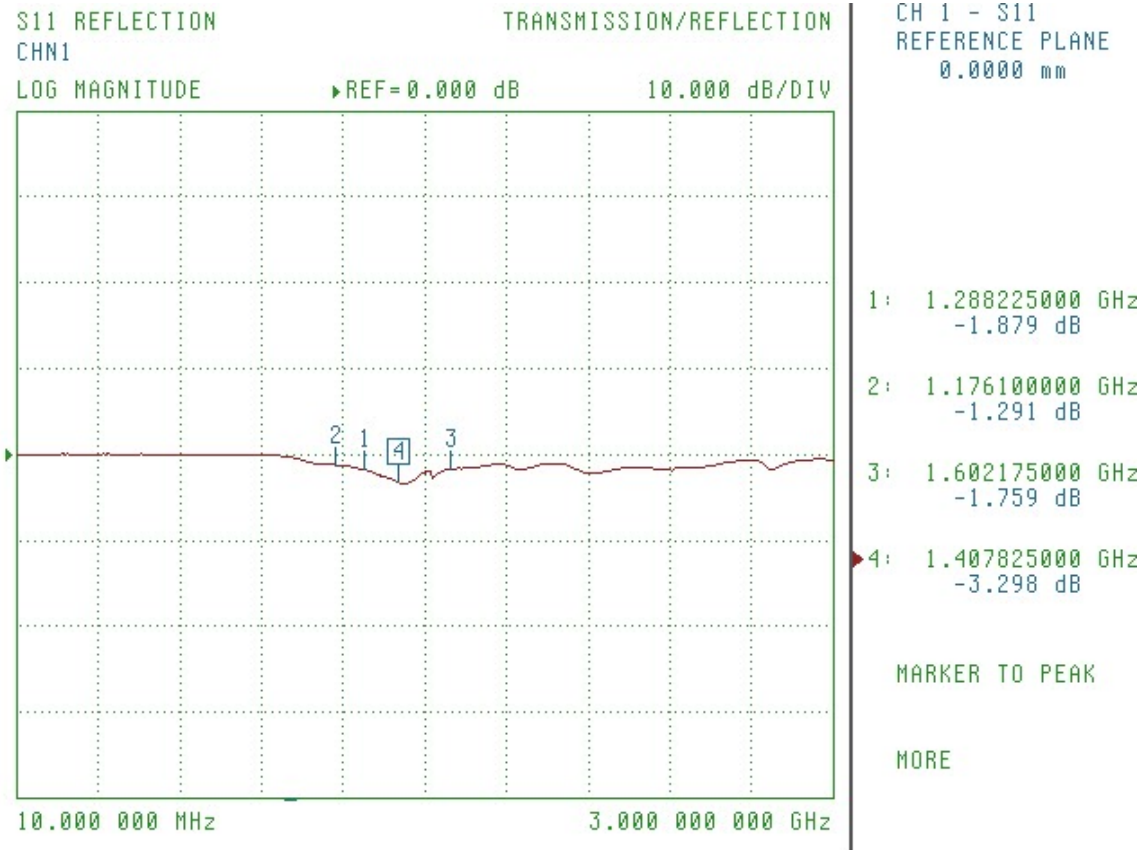


Figure 3.15: Uncalibrated feed, poor return loss and efficiency

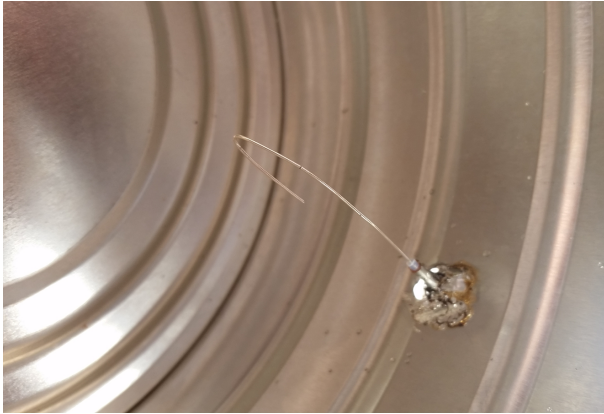


Figure 3.16 displays the feed, tuned. Measuring return loss, or S11 to check efficiency shows that this antenna is better-matched to 50 ohms, as seen in Figure 3.17. To better match this, simulations using a program may yield better results.

Figure 3.16: Feed length, tuned

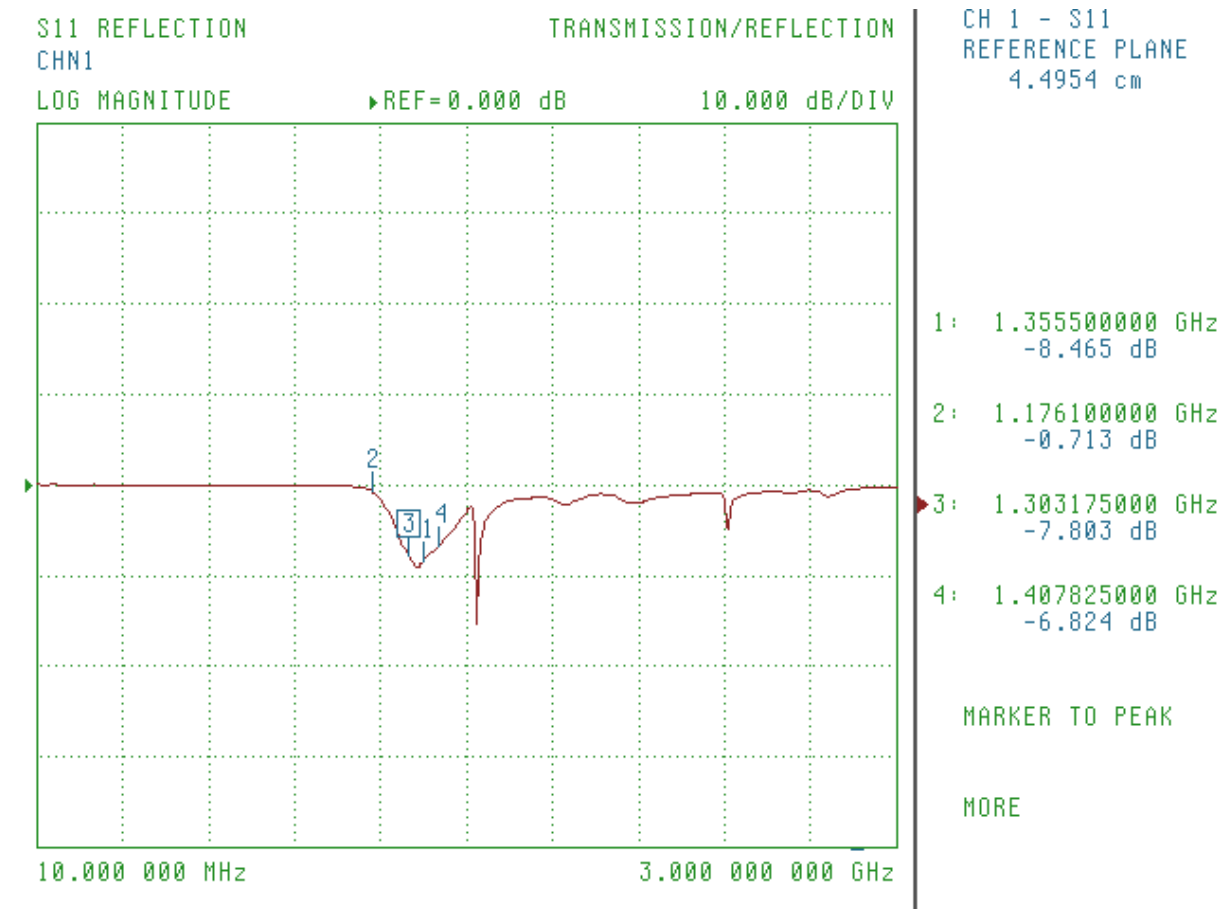


Figure 3.17: Calibrated feed, better return loss and efficiency

Here calibrating the feed has resulted in better power delivery at the select frequency of 1.3 GHz, as seen in a comparison between Figures 3.15 and 3.17. S11 reached -7.8 dB in the tuned antenna, whereas the untuned antenna did not reach even -4 dB. Bending the feed yielded in a better return loss. The result of bending the feed is “shortening” the feed. Cutting the bent portion may be beneficial for a final design; however, this is acceptable for a prototype structure. Note that high directivity is useless if efficiency is not sufficient; the overall antenna gain will suffer if efficiency is low.

With an acceptable efficiency achieved, where more power is delivered to the antenna, the radiation pattern is taken, seen in Figure 3.18 and 3.19. The separation between the antenna and transmit (patch) antenna is 57 inches. Using Friis transmission equation will determine the air transmission loss. The rest, such as cable loss and gain of the patch antenna are known. The anechoic chamber has a program that allows these losses and gains to be inputted, simplifying the data to the gain of the receive antenna. Note that some radiation setups have a higher gain than others.

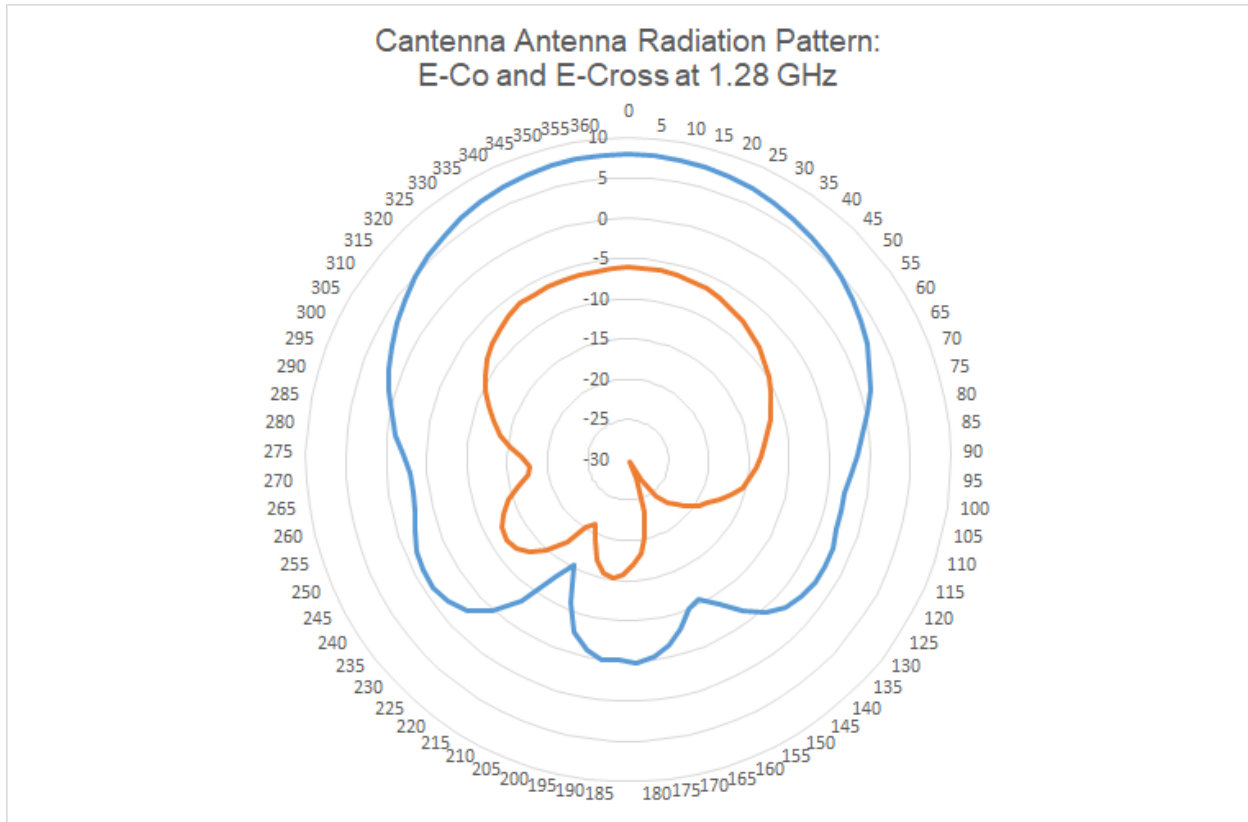


Figure 3.18: Antenna Radiation Patterns, E-co and E-cross

The max estimated gain is 8 dBi for E-coplanar, and -6.1 dBi for E-cross, assuming the transmitter patch antenna is accurately measured to be 5.2 dBi. E-coplanar is blue, E-cross is orange. The 3-dB beamwidth of E-co is 100 degrees.

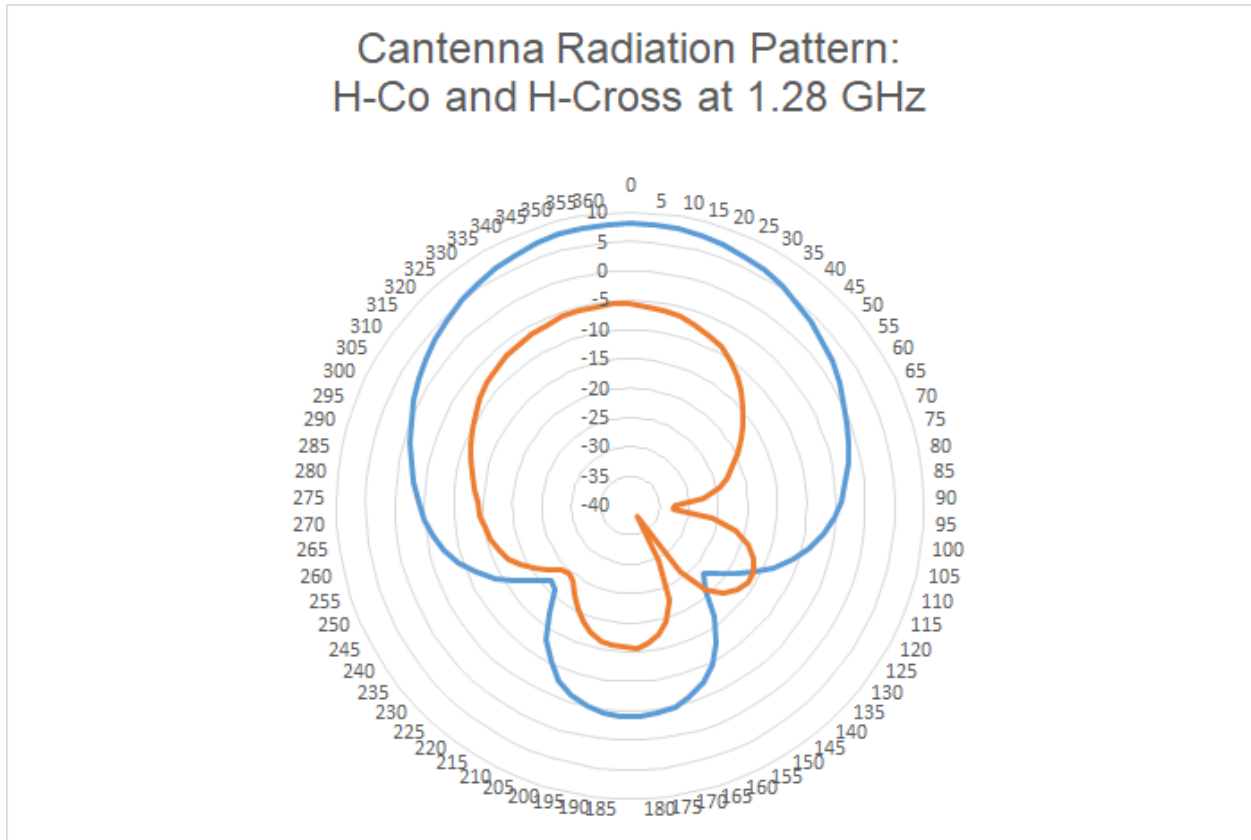


Figure 3.19: Antenna Radiation Patterns, H-Co and H-Cross

The max estimated gain 8.1 dBi for H-coplanar and -5.7 dBi for H-cross, assuming the transmitter patch antenna is accurately measured to be 5.2 dBi. H-coplanar is blue, H-cross is orange. The 3-dB beamwidth of H-co is 75 degrees.

The antenna is finally finished to be used as a jammer. Note that in later experiments, Chapter 4, the antenna is not used. This is primarily because the licenses for the other VSA/VSGs (non-MIMO VSA/VSGs) expired after fall quarter, only providing the demo license. The demo license did not permit frequencies at 1.3 GHz to be generated, only allowing lower MHz frequency signals to be created.

Patch Antenna Overview

Patch antennas, also known microstrip antennas, are antennas known for convenience of design, due to its low cost of printing onto circuit boards. Other advantages include its low profile, being mechanically sturdy, and flexible in relation to antenna characteristics, such as polarization, frequency, pattern, and impedance. The disadvantages include narrow bandwidth, low efficiency, low power, and spurious feed radiation. There are many different shapes and sizes used to create the patch antenna, as seen in Figure 3.20.

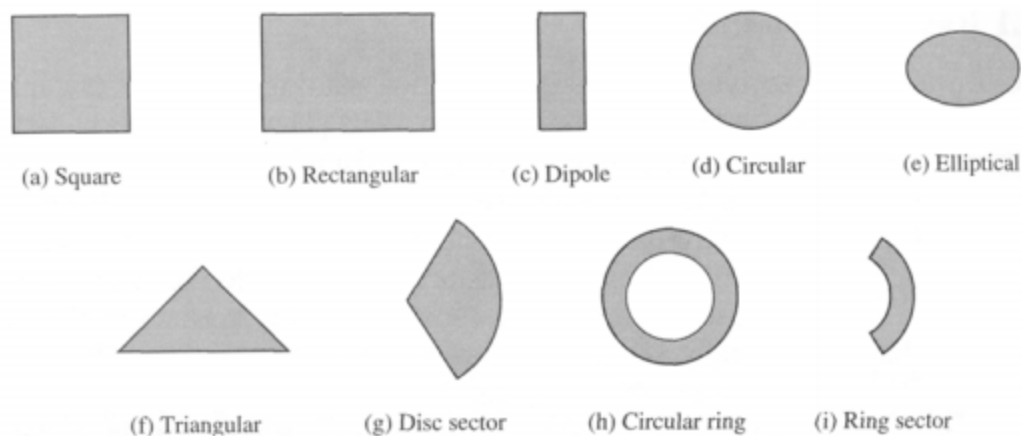


Figure 3.20: Differing microstrip patch elements, taken from Balanis, *Antenna Theory, Analysis and Design (Second Edition)*.

There are four common feed methods to radiate the signal onto the antenna. They are the microstrip transmission line, coaxial probe, aperture coupling, and proximity coupling, as seen in Figure 3.21. Each feed method has its benefits and disadvantages. For instance, a microstrip transmission line feed and a coaxial probe are easy to make and match. Aperture coupling and proximity coupling are harder to make and match. The microstrip transmission line feed, coaxial probe, and aperture coupling have lower bandwidths, ranging from 2% to 5%, whereas

proximity coupling can reach 13%. Microstrip transmission lines and coaxial probes may suffer from asymmetric feeds, resulting in cross-polarization problems. Microstrip transmission lines have the highest spurious radiation, whereas probe feed has less, and the other two even less.

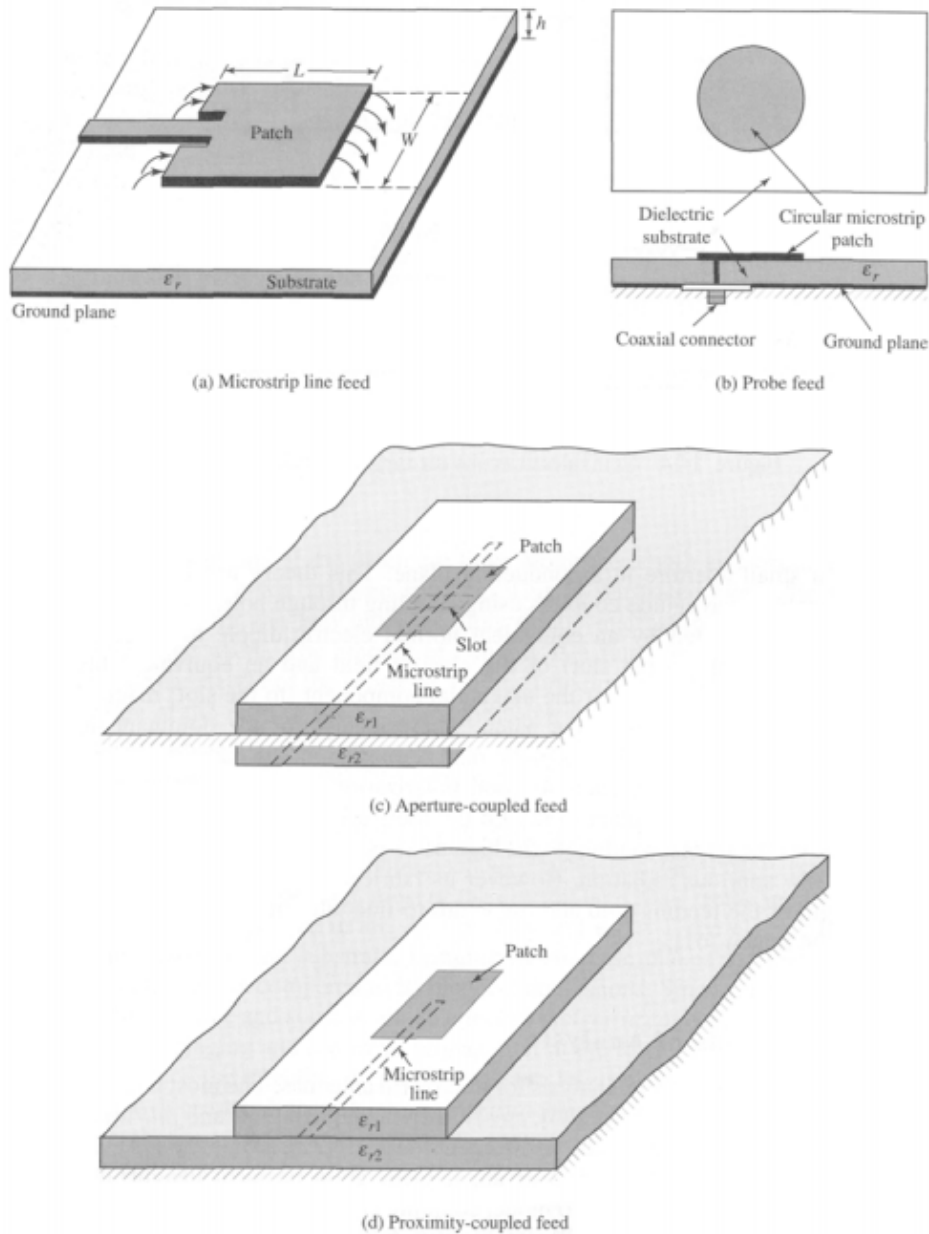


Figure 3.21: Differing feed methods, taken from Balanis, *Antenna Theory, Analysis and Design (Second Edition)*.

There are general guidelines for analyzing microstrip antennas, with three primary models. Transmission line modeling is the easiest to model, but may not be accurate due to inaccuracies in the lack of modeling coupling. The second model is cavity modeling, which is more accurate, but like the transmission line model, is hard to analyze coupling. The third and best model is the full-wave. This may be seen in 3-D simulators such as Advance Design System's Momentum.

$$W=L=\frac{c}{(2f\sqrt{\epsilon_r})}$$

Equation 3.6: Relative permittivity adjusted half wavelength

In general, the antenna's designed dimensions are related to a half-wavelength or quarter-wavelength of the desired frequency. This is dependent on the design chosen. Also taken into the dielectric material. This is modeled in the equation above, where the width and length are of a rectangular microstrip antenna is half the wavelength of the design frequency.

Patch Antenna Implementation

A patch antenna is designed using the formulas as initial starting points. The transmission line feed is chosen due to easy fabrication, seen in Figure 3.22. Design verification is performed using Advanced Design Simulation's Momentum simulator. In this simulator, different cases are simulated until the desired width and length are reached, as well as feed length, feed width, and slot width.

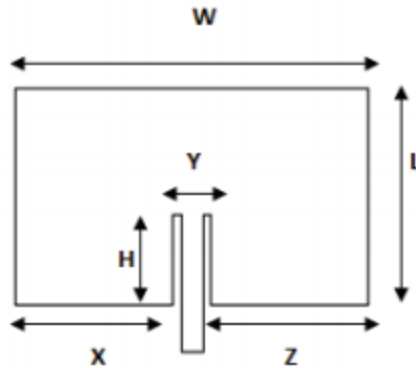


Figure 3.22: Design dimensions of patch antenna. A transmission line feed is chosen.

The target frequency of the patch antenna design is 1.3 GHz . The relative permittivity of the available material is $\epsilon_r = 2.55$. The conductor is 1 ounce copper, and the dielectric height is not important, as long as it is less than 5% of the wavelength. The antenna is matched to 50 ohms. The table below, Table 3.5, shows the final dimensions of the patch antenna. The simulations are shown in Figures 3.23 through 3.28.

Table 3.5: Physical dimensions of simulation-tuned patch antenna

Patch Antenna Dimensions		
Specifications		
ϵ_r	2.55	
f	1.3	GHz
Dimensions		
W	2882.8	mil
L	2882.8	mil
X	1153.1	mil
Z	1153.1	mil
H	800	mil
Y	576.6	mil
Feed width	228.5	mil

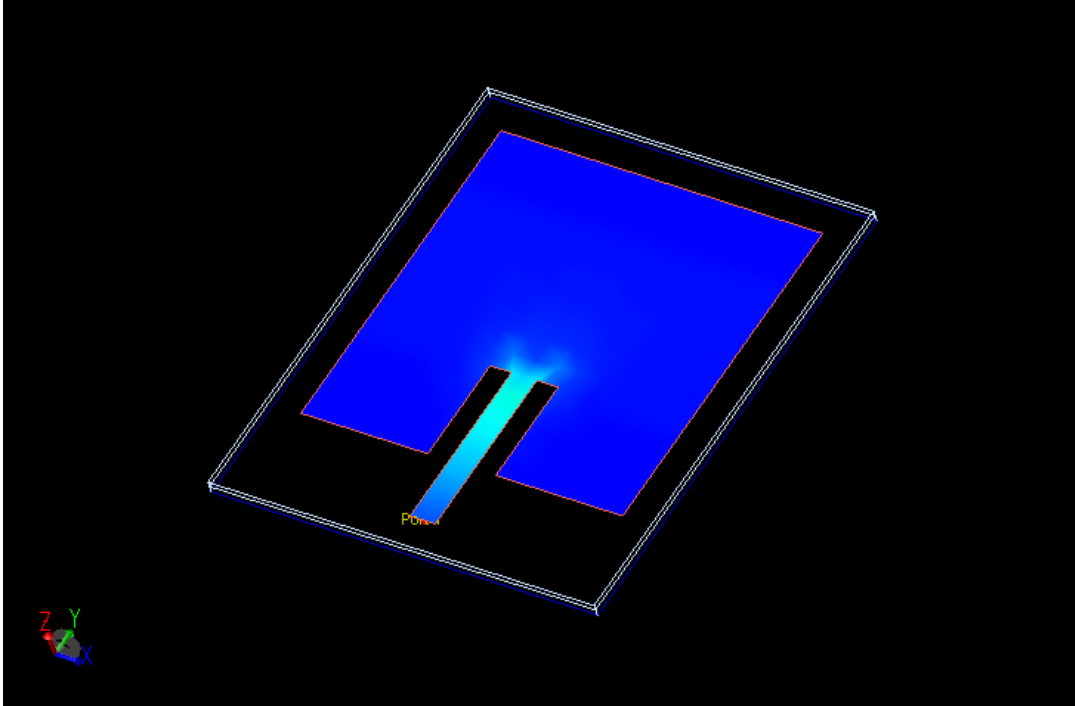


Figure 3.23: 3-D view of patch antenna.

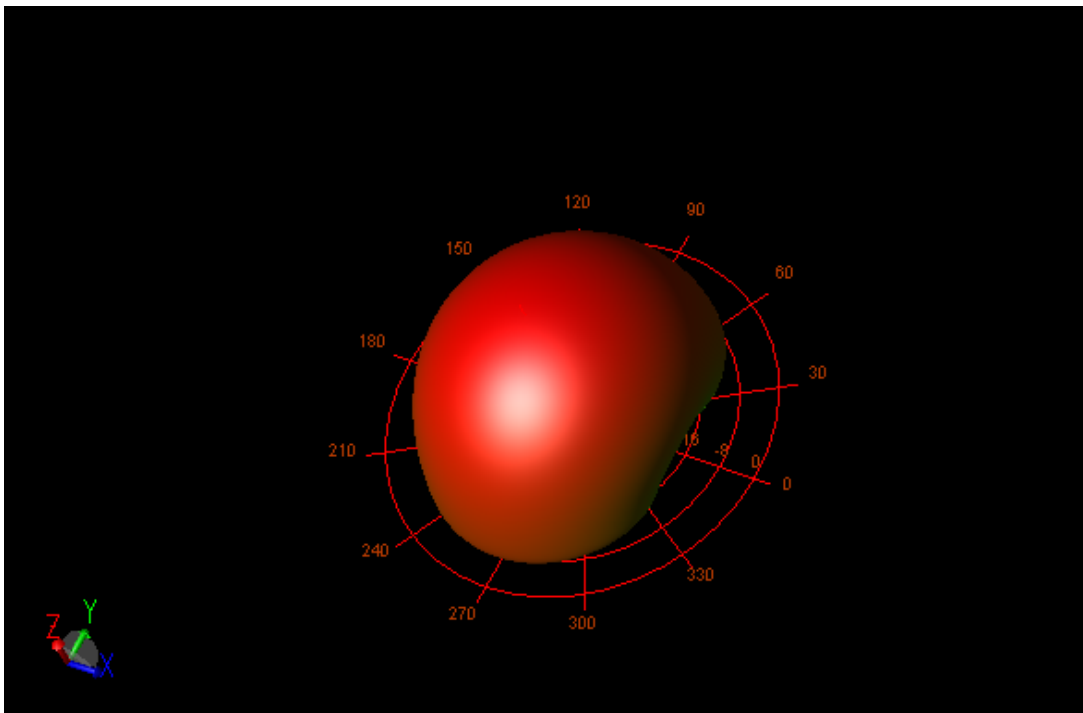


Figure 3.24: 3-D Radiation pattern of patch antenna.

Discrete Frequencies vs. Fitted (AFS or Linear)

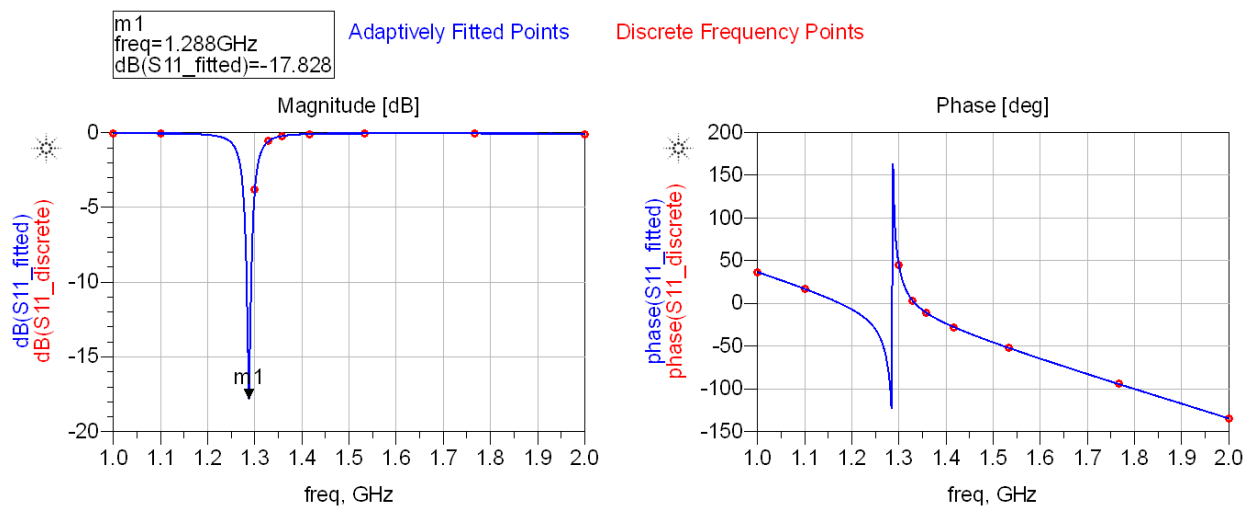


Figure 3.25: Return loss of patch antenna.

The return loss of -17.8 dB corresponds to a 7% loss. Note that at 1.3 GHz the return loss is about -5.8 dB corresponds to a 27% loss.

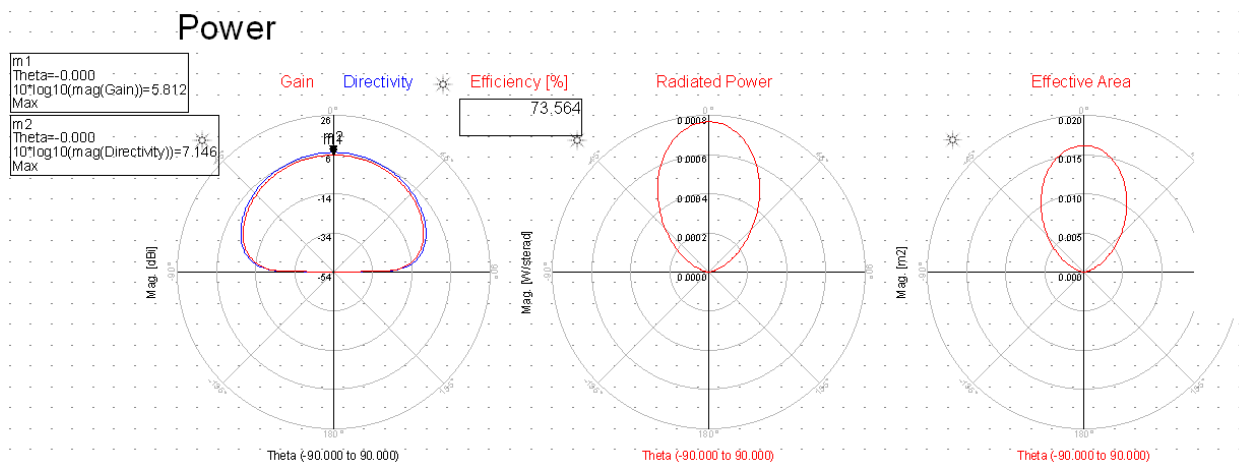


Figure 3.26: Power characteristics of patch antenna.

Here, the gain is 5.8 dBi at its maximum. Note that the efficiency of 73% is largely dependent on the return loss. This is tested at 1.3 GHz.

Absolute Fields

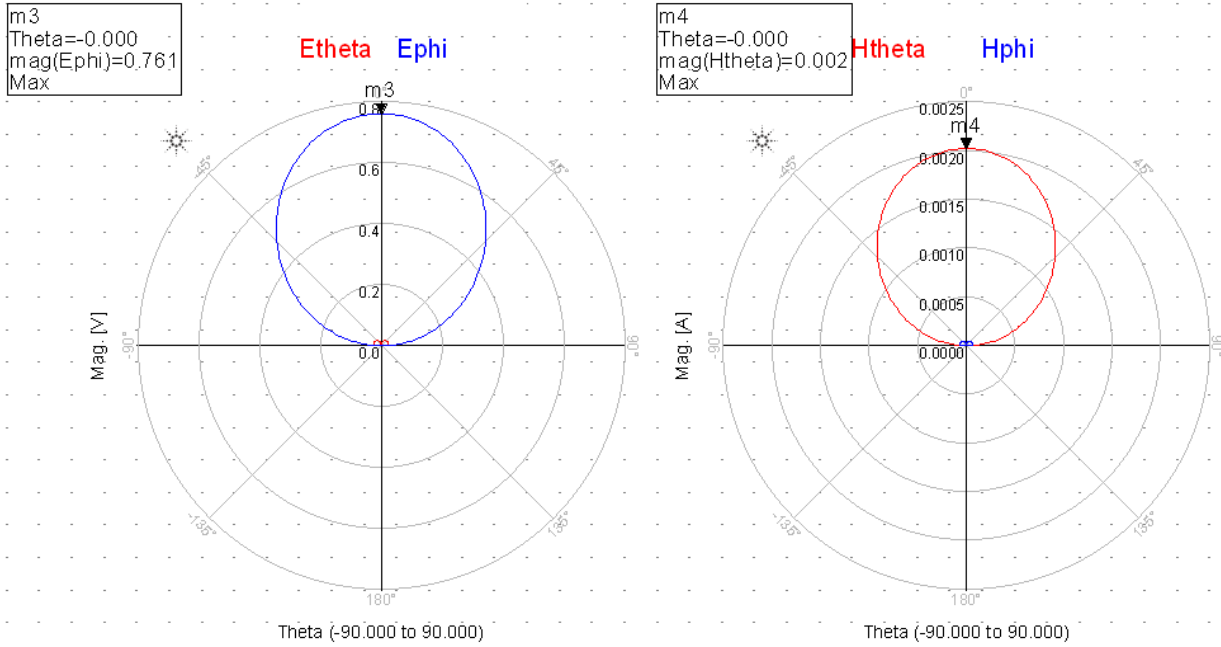
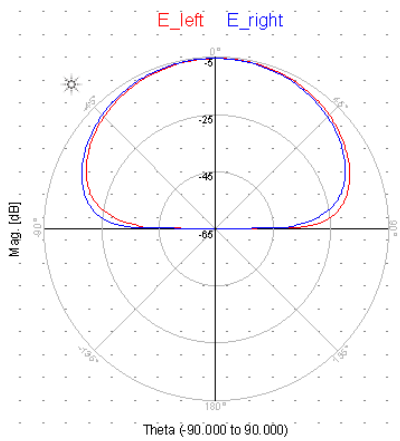


Figure 3.27: Field characteristics of patch antenna.

These fields are harder to directly measure; a simulation can better accomplish this than physically.

Circular Polarization



Linear Polarization

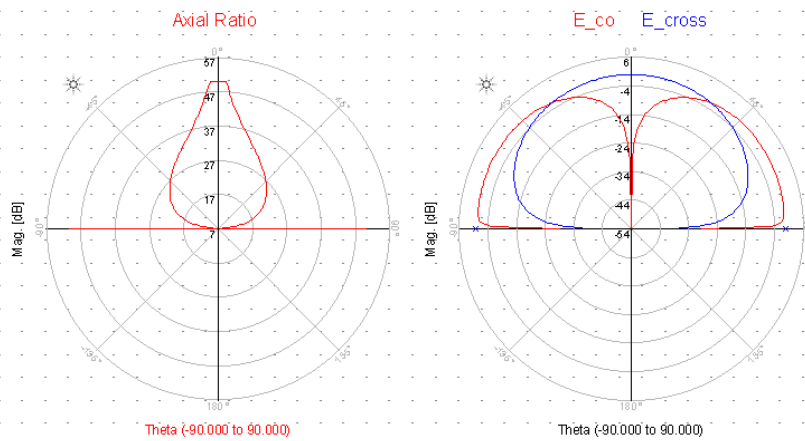
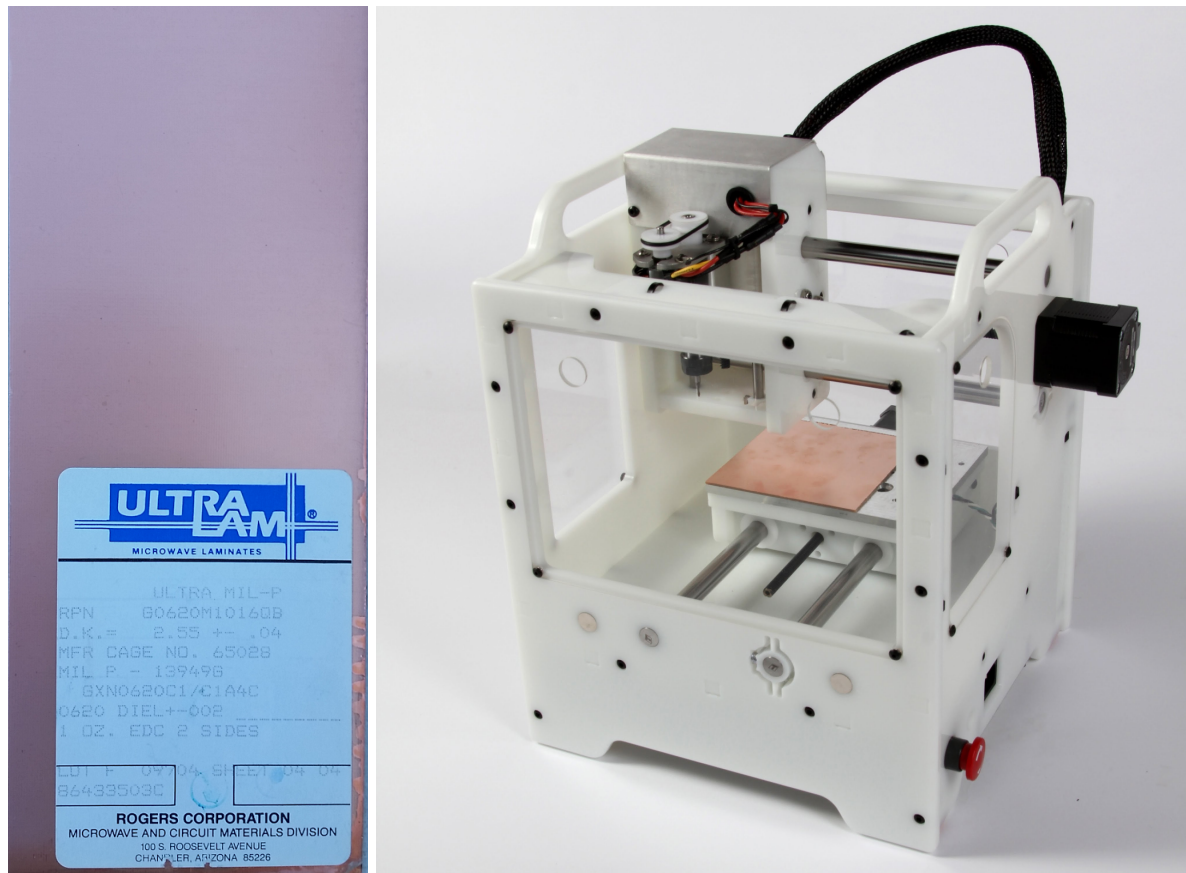


Figure 3.28: Polarization characteristics of patch antenna.

The physically-milled antenna uses a double sided copper-clad board, shown below in Figure 3.29. The duroid material has low loss. The height is 60 mils, and as mentioned earlier has a relative permittivity of 2.55 and has 1 ounce copper.



Figures 3.29, 3.30: Circuit board utilized (left) and Othermill Pro milling machine (right) to produce antenna.

The Othermill Pro has a limit of 1 mil and ability to creating 6 mil slots with its smallest drill, seen in Figure 3.30. The maximum size of a board that will fit in the machine is 5.5" x 4.5".

Understanding the limitations of manufacturing is important for a designer. The antenna design needs to be dimensionally sound to be produced--otherwise special processes must be used to

create the prototype. In practice, almost all circuit boards must pass design-for-manufacturing before being mass-produced. This milling machine, great for quick prototypes, is available in the Cal Poly IEEE room, and costs money per time used. Visit calpolyieee.org or room 20-115 on campus for more information.

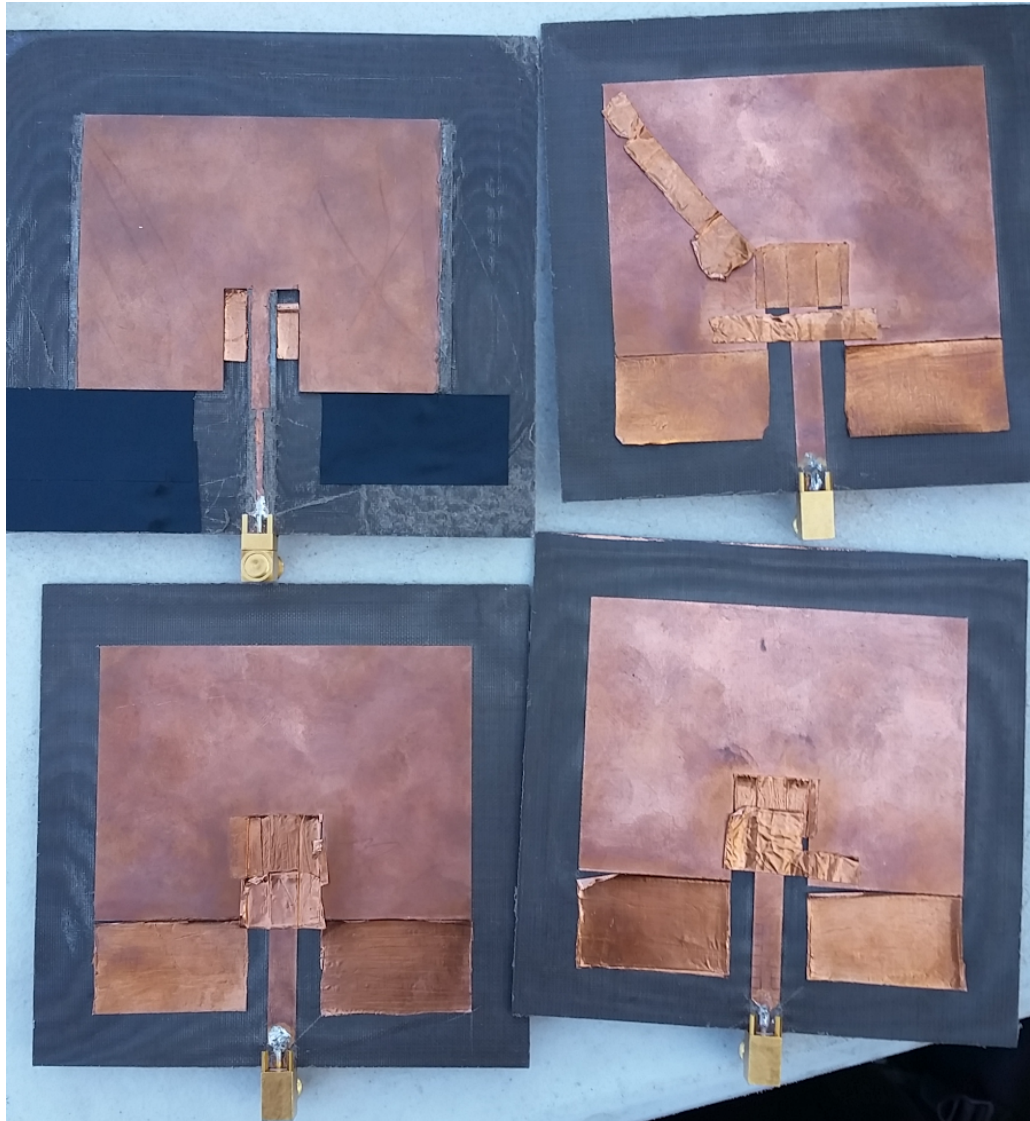


Figure 3.31: First prototype of the designed patch antennas. Copper tape is used to tune the antenna. The layout dimensions were drawn incorrectly.

The first batch of antennas, seen in Figure 3.31, were incorrectly produced, due to the layout producer not checking the specified dimensions carefully. The result is tuning by copper tape; however, the tape would sometimes come loose, demonstrating that the “fixed” antennas were not structurally sound. Visually on a vector network analyzer, the return loss would be acceptable, such as -11 dB, but as soon as the antenna is slightly budged, the return loss turns to -3 dB. Figure 3.32 demonstrates the return loss measurement. The resonance at 1.36 GHz might be due to the length L dimension being shorter; higher frequencies correspond to shorter wavelengths. Also note that if the board bends during the milling process, some parts of the dielectric might be lower than others, seen in Figure 3.31. Photo-chemical etching, a common circuit board design method, would not encounter this mechanical problem.

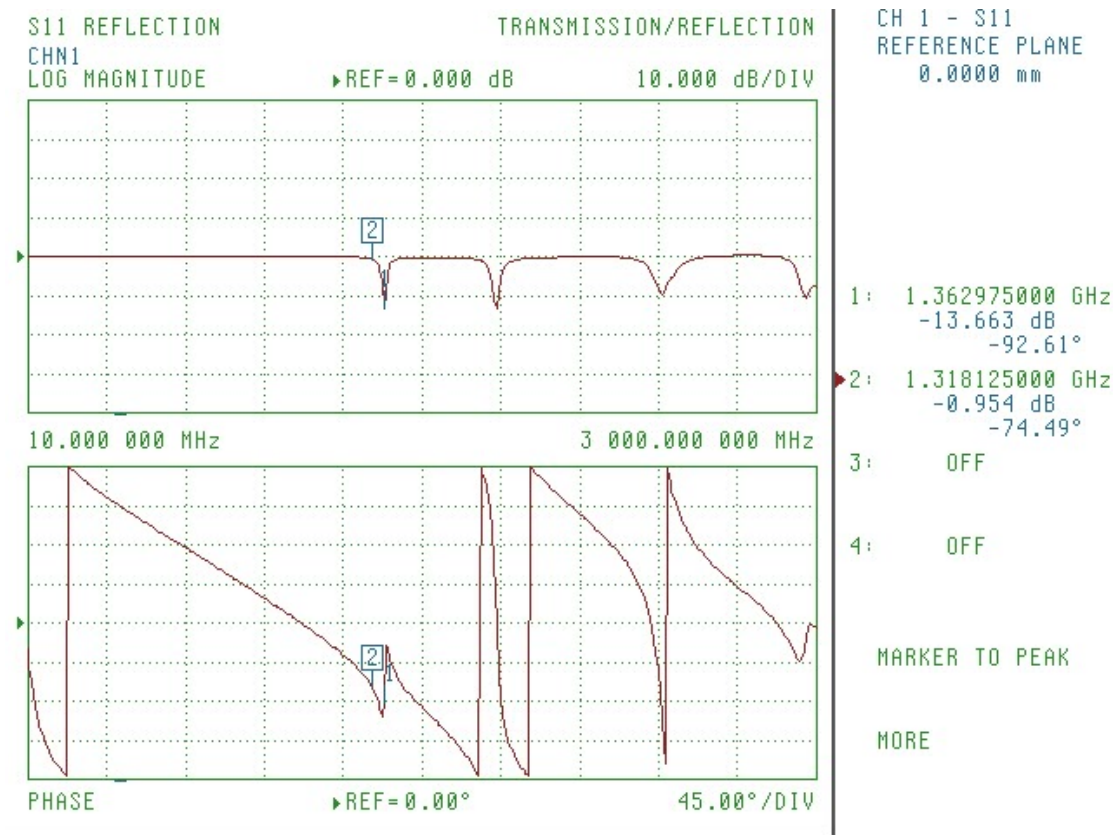


Figure 3.32: First prototype return loss. Note that it does not resonate at 1.30 GHz as intended.

After some tape it did resonate, but was not mechanically sturdy.

The boards were remilled for a second prototype after troubles with consistent return loss. Be sure to double-check dimensions; errors could cost a lot of money and time of the layout is more complex. The resulting look is shown in Figure 3.33 and the improved return loss is seen in Figure 3.34.

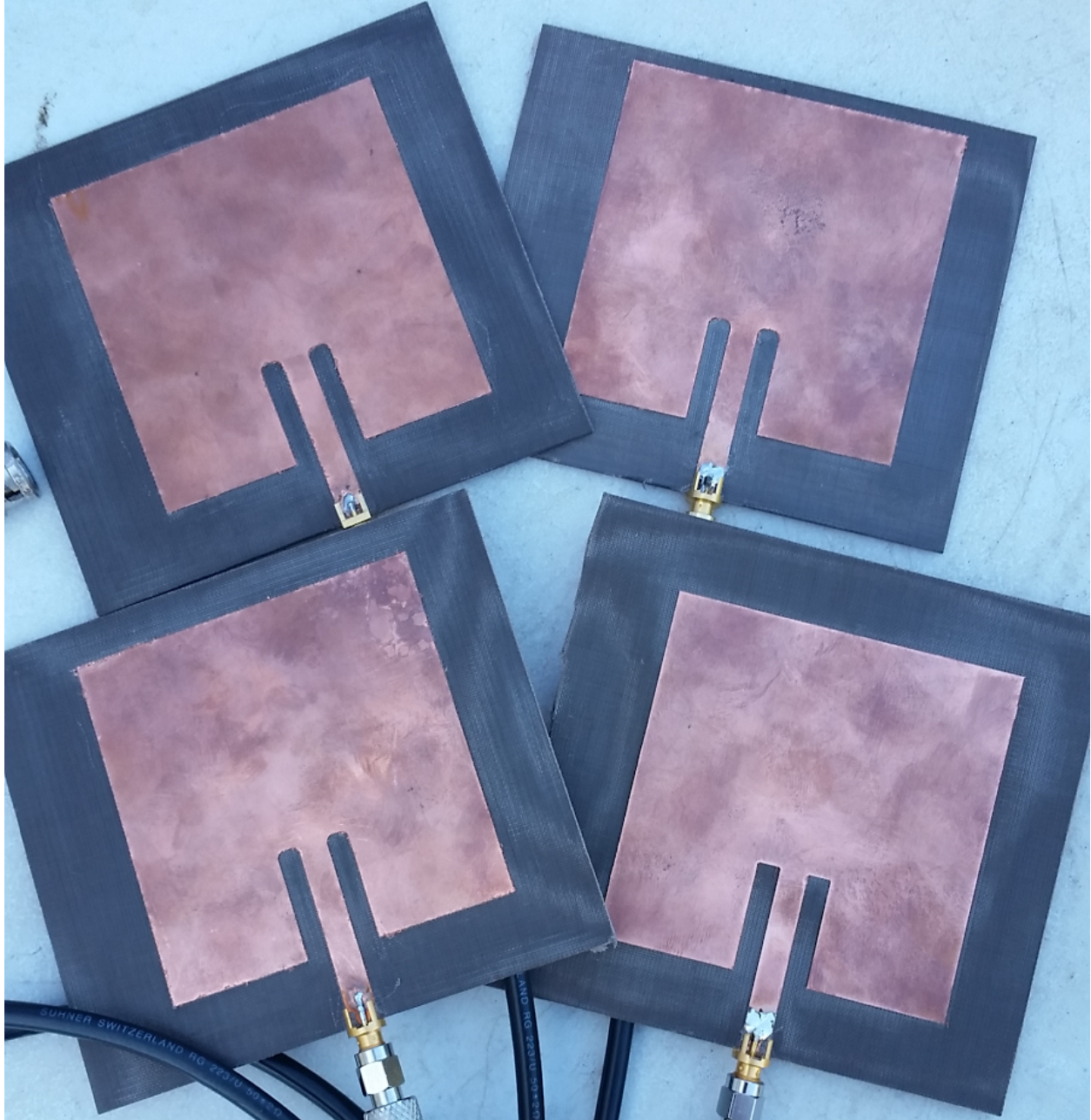


Figure 3.33: Second prototype of patch antennas.

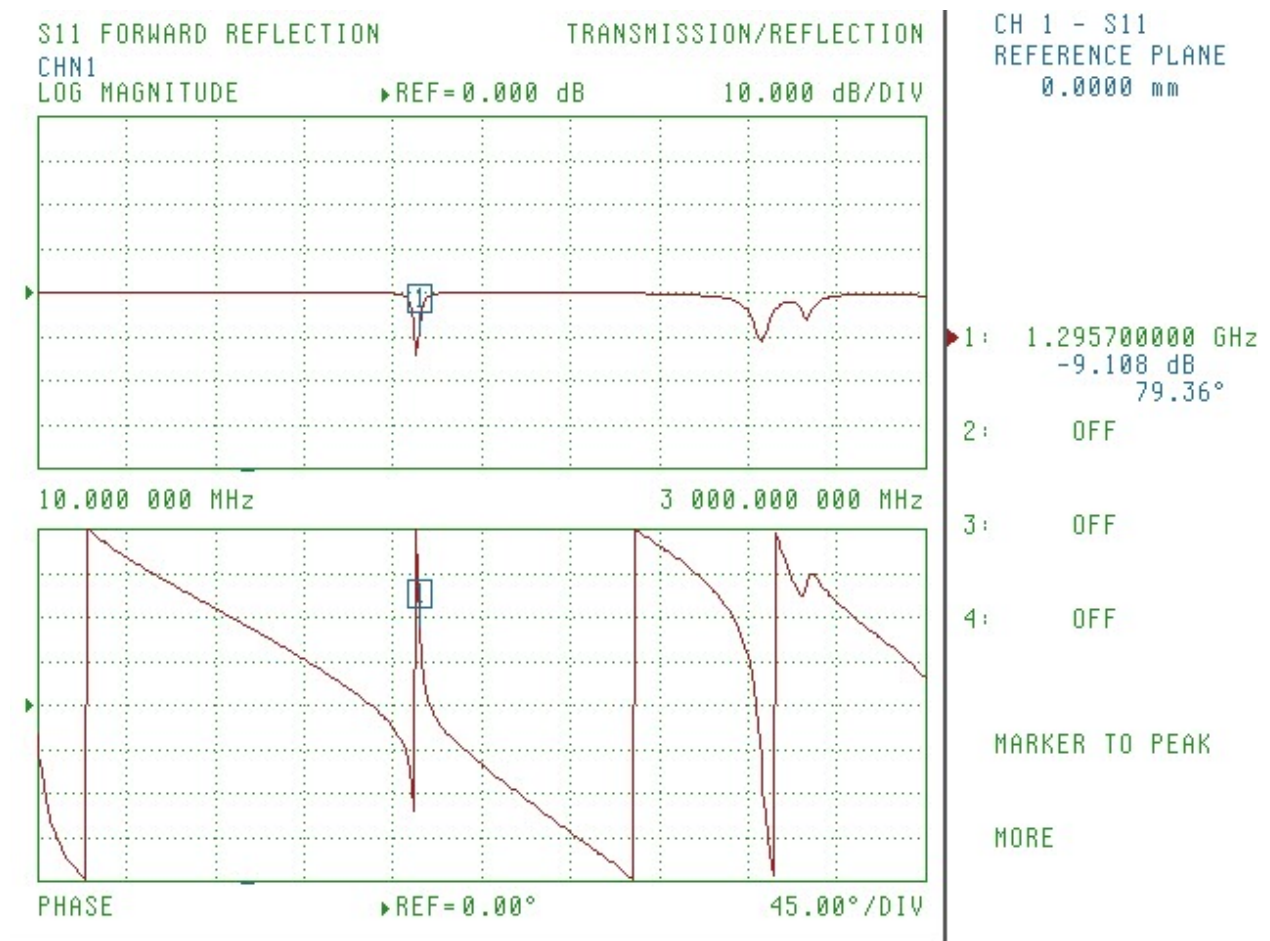


Figure 3.34: Second prototype of patch antennas.

With sufficient efficiency achieved, the antenna is tested in the chamber. The radiation patterns are seen in Figures 3.35 and 3.36. The antenna gain is close to the simulation results; 5.8 dBi and 5.2 dBi are very close. The sidelobes of the simulation are not as visible relative to real life. Another aspect to note is that those sidelobes are not necessarily symmetric.

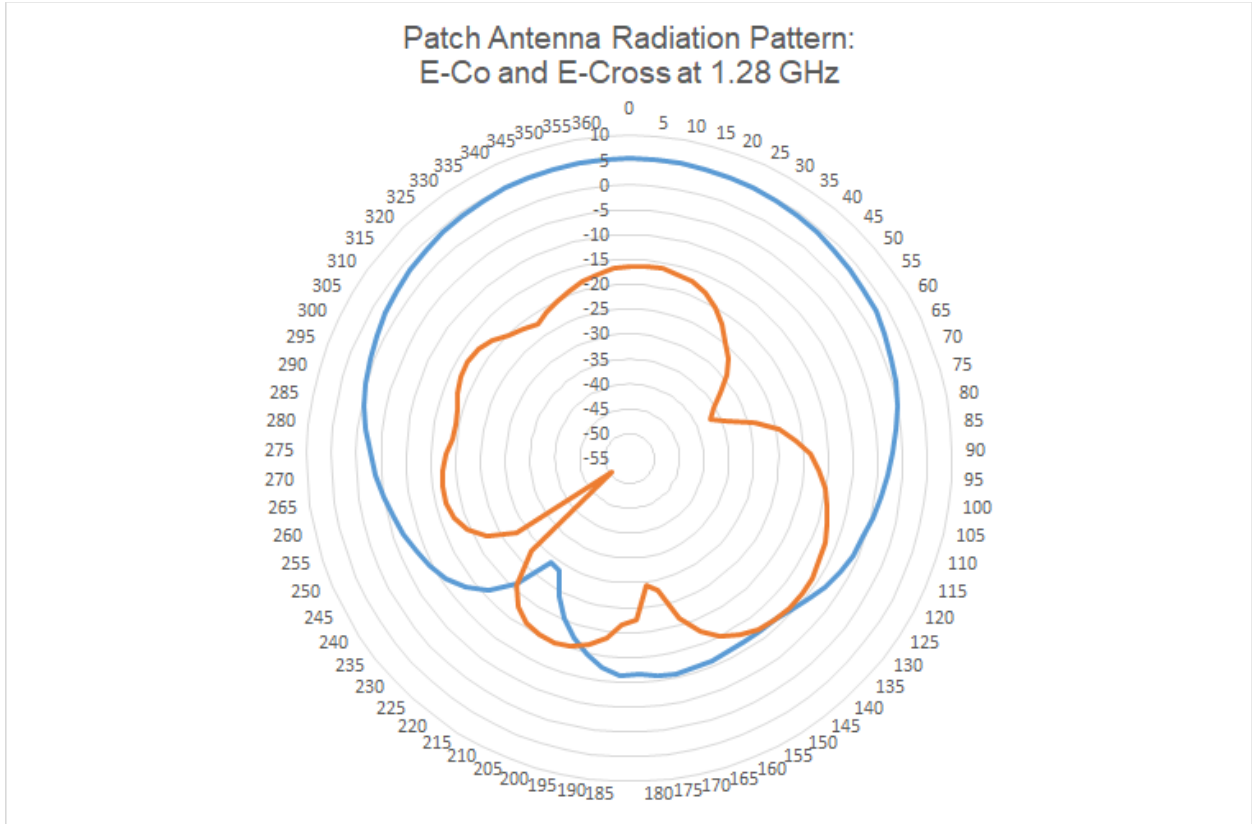


Figure 3.35: E-co is blue, E-cross is orange. 3-dB Beamwidth of E-Co is 120 degrees, max gain is 5.2 dBi.

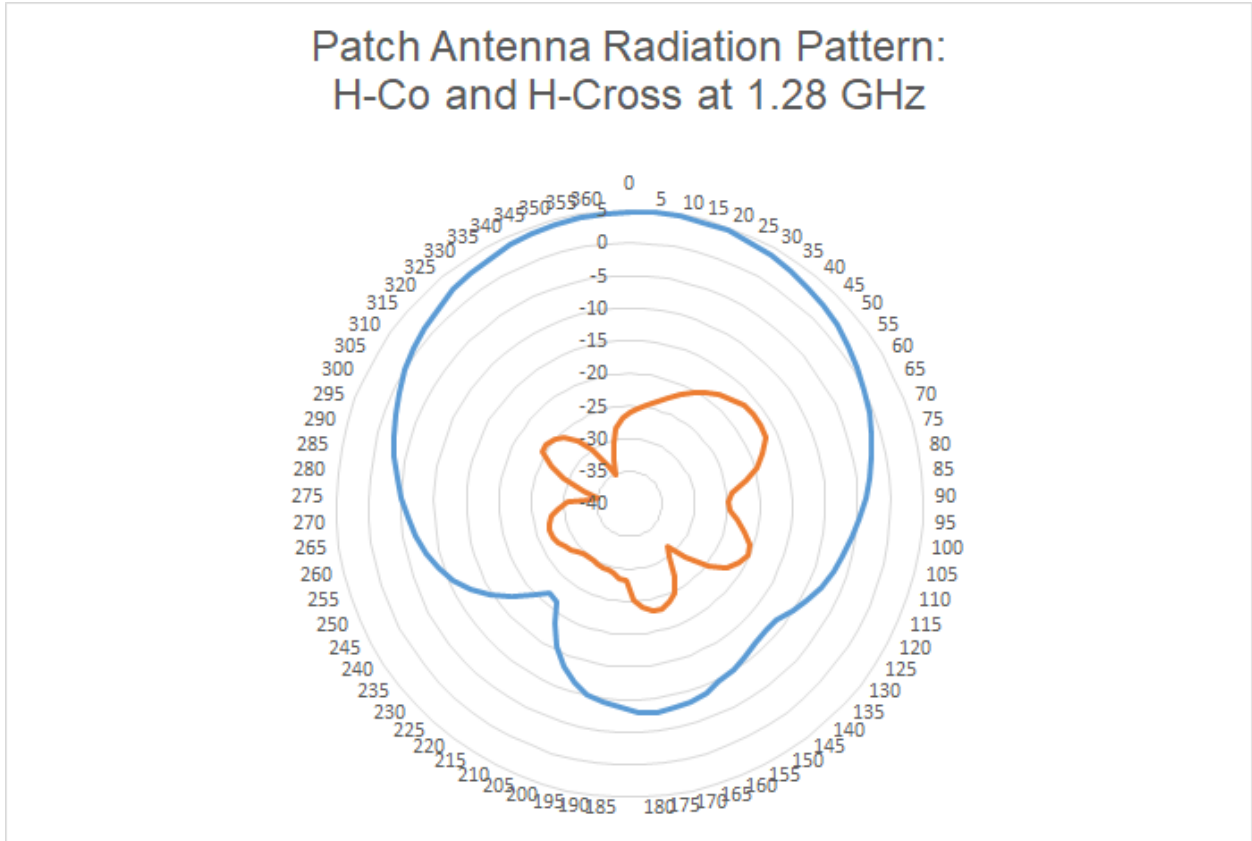


Figure 3.36: H-co is blue, H-cross is orange. 3-dB Beamwidth of H-Co is 100 degrees, max gain is 4.8 dBi.

3.4 Preamplifiers Overview and Implementation

Overview

There are many types of amplifiers, each used for different circumstances. For example, a transmitter amplifier may require high gain and a high power limit before distortion occurs. On the other hand, preamplifiers require as low as possible noise figure to preserve the quality of the signal. The purpose of a preamplifier is to convert a weak incoming signal into an output signal that is adequate for further processing and noise-tolerant. An ideal preamplifier would have as low as possible noise figure, matched input and output impedance with respect to the

system, high IP3, as well as high gain. The input and output impedance are matched to prevent reflections at the input and output of the amplifier, while a high IP3 is required to minimize the effects of distortion provided by the amplifier. A high-gain amplifier may offset the effects of noise; however, note that high-gain amplifiers may be too costly depending on the application. Below shows Friis' noise equation to determine the overall noise figure of cascaded elements. The noise of passive components is approximately equal to the loss of the component. This equation is especially useful for determining signal-to-noise before the digital processing units.

$$F_{total} = F_1 + \frac{F_2 - 1}{G_1} + \frac{F_3 - 1}{G_1 G_2} + \frac{F_4 - 1}{G_1 G_2 G_3} + \dots + \frac{F_n - 1}{G_1 G_2 \dots G_{n-1}}$$

Equation 3.6: Friis Noise Equation

Note that in designing a receiver, this equation needs to be taken into account with more consideration. However, for the purposes of the MIMO project, the only noise one would need to account for is at the antenna and after the pre-amplifier. The contribution to noise in the VSA is unknown.

Implementation

The Mini-Circuits amplifier ERA-3+ is selected due to its packaging type. Surface-mount technology (SMT) may require layout and a surface-mount soldering station, both which may require more time and additional resources. Unlike the common SMT-packaged amplifiers commonly used in industry, the ERA-3+ comes in a Micro-X packaging, which is convenient for dead-bug style prototyping. The benefit of dead-bug style prototyping is that a simple copper clad board and soldering iron will produce the platform for the circuit. Figures 3.37 through 3.39 display the characteristics of the ERA-3+, along with the physical implementation requirements.

Drop-In Monolithic Amplifier

DC-3 GHz

Product Features

- DC-3 GHz
- Single voltage supply
- Internally matched to 50 ohms
- Unconditionally stable
- Low performance variation over temperature
- Transient protected
- Aqueous washable
- Protected By US Patent 6,943,629



ERA-3+

CASE STYLE: VV105

+RoHS Compliant

The +Suffix identifies RoHS Compliance. See our web site for RoHS Compliance methodologies and qualifications

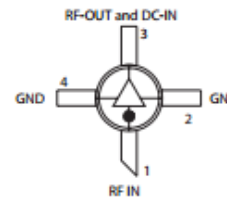
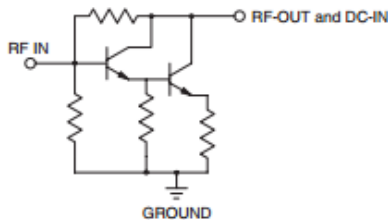
Typical Applications

- Cellular/ PCS/ 3G Base Station
- CATV, Cable Modem & DBS
- Fixed Wireless & WLAN
- Microwave Radio & Test Equipment

General Description

ERA-3+ (RoHS compliant) is a wideband amplifier offering high dynamic range. It has repeatable performance from lot to lot. It is enclosed in a Micro-X package. ERA-3+ uses Darlington configuration and is fabricated using InGaP HBT technology. Expected MTBF is 10,000 years at 85°C case temperature.

simplified schematic and pin description



Function	Pin Number	Description
RF IN	1	RF input pin. This pin requires the use of an external DC blocking capacitor chosen for the frequency of operation.
RF-OUT and DC-IN	3	RF output and bias pin. DC voltage is present on this pin; therefore a DC blocking capacitor is necessary for proper operation. An RF choke is needed to feed DC bias without loss of RF signal due to the bias connection, as shown in "Recommended Application Circuit".
GND	2,4	Connections to ground. Use via holes as shown in "Suggested Layout for PCB Design" to reduce ground path inductance for best performance.

Notes

- A. Performance and quality attributes and conditions not expressly stated in this specification document are intended to be excluded and do not form a part of this specification document.
 B. Electrical specifications and performance data contained in this specification document are based on Mini-Circuits' applicable established test performance criteria and measurement instructions.
 C. The parts covered by this specification document are subject to Mini-Circuits' standard limited warranty and terms and conditions (collectively, "Standard Terms"); Purchasers of this part are entitled to the rights and benefits contained therein. For a full statement of the Standard Terms and the exclusive rights and remedies thereunder, please visit Mini-Circuits' website at www.minicircuits.com/MICLStore/terms.jsp



www.minicircuits.com P.O. Box 350166, Brooklyn, NY 11235-0003 (718) 934-4500 sales@minicircuits.com

REV. N
M151107
ERA-3+
150716
Page 1 of 4

Figure 3.37: ERA-3+ Datasheet 1/3

Electrical Specifications at 25°C and 35mA, unless noted

Parameter		Min.	Typ.	Max.	Units	Cpk
Frequency Range*		DC		3	GHz	
Gain	f=0.1 GHz	21	23.4	24.4	dB	≥ 1.5
	f=1 GHz	—	21	—		
	f=2 GHz	17.6	18.7	20.7		
	f=3 GHz	15.4	16.4	18.5		
Magnitude of Gain Variation versus Temperature (values are negative)	f=0.1 GHz	—	0.0045	0.009	dB/°C	
	f=1 GHz	—	0.0051	0.010		
	f=2 GHz	—	0.0059	0.012		
	f=3 GHz	—	0.0064	0.013		
Input Return Loss	f=0.1 GHz		30		dB	
	f=1 GHz		19			
	f=2 GHz		18			
	f=3 GHz		18			
Output Return Loss	f=0.1 GHz		21		dB	
	f=1 GHz		17			
	f=2 GHz		17			
	f=3 GHz		17			
Reverse Isolation	f=2 GHz	21	24	—	dB	
Output Power @ 1 dB compression	f=0.1 GHz	—	12.5	—	dBm	≥ 1.5
	f=1 GHz	—	12.1	—		
	f=2 GHz	9	12.5	—		
	f=3 GHz	—	10.5	—		
Saturated Output Power (at 3dB compression)	f=0.1 GHz		13.6		dBm	
	f=1 GHz		13.3			
	f=2 GHz		13.1			
	f=3 GHz		12.1			
Output IP3	f=0.1 GHz	24	27	—	dBm	≥ 1.5
	f=1 GHz	24	27	—		
	f=2 GHz	23	26	—		
	f=3 GHz	21	24	—		
Noise Figure	f=0.1 GHz		2.7		dB	≥ 1.5
	f=1 GHz		2.6			
	f=2 GHz		2.8			
	f=3 GHz		2.9			
Group Delay	f=2 GHz		80		psec	
Recommended Device Operating Current			35		mA	
Device Operating Voltage		3.0	3.2	3.4	V	≥ 1.5
Device Voltage Variation vs. Temperature at 35mA			-2.3		mV/°C	
Device Voltage Variation vs. Current at 25°C			3.6		mV/mA	
Thermal Resistance, junction-to-case ¹			181		°C/W	

*Guaranteed specification DC-3 GHz. Low frequency cut off determined by external coupling capacitors.

Absolute Maximum Ratings

Parameter	Ratings
Operating Temperature*	-45°C to 85°C
Storage Temperature	-65°C to 150°C
Operating Current	75mA
Power Dissipation	330mW
Input Power	13dBm

Note: Permanent damage may occur if any of these limits are exceeded.

These ratings are not intended for continuous normal operation.

¹Case is defined as ground leads.

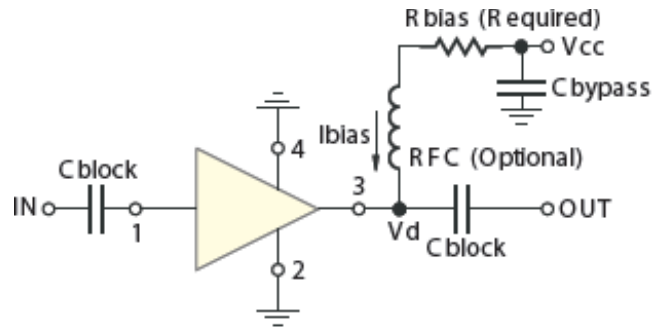
*Based on typical case temperature rise 5°C above ambient.

Notes

- A. Performance and quality attributes and conditions not expressly stated in this specification document are intended to be excluded and do not form a part of this specification document.
- B. Electrical specifications and performance data contained in this specification document are based on Mini-Circuits' applicable established test performance criteria and measurement instructions.
- C. The parts covered by this specification document are subject to Mini-Circuits standard limited warranty and terms and conditions (collectively, "Standard Terms"); Purchasers of this part are entitled to the rights and benefits contained therein. For a full statement of the Standard Terms and the exclusive rights and remedies thereunder, please visit Mini-Circuits' website at www.minicircuits.com/WCLStore/terms.jsp



Figure 3.38: ERA-3+ Datasheet 2/3



Materials List

- 2x 0.1 μ F
- 1x 1 μ F
- 1x 10 μ H
- 2x 215 Ω
- Semi-Rigid Coax Cables
- SMA Connectors
- Copper Clad board

R BIAS	
Vcc	"1%" Res. Values (ohms) for Optimum Biasing
7	107
8	133
9	162
10	191
11	221
12	251
13	280
14	309
15	340
16	365
17	392
18	422
19	453
20	475

Figure 3.39: ERA-3+ Layout and Materials List 3/3

With a schematic shown in Figure 3.39, the first prototype is implemented, shown in Figure 3.40. With a supply voltage of 10 volts, the measured scattering parameters are displayed in Figure 3.41.



Figure 3.40: ERA-3+ first prototype implementation.

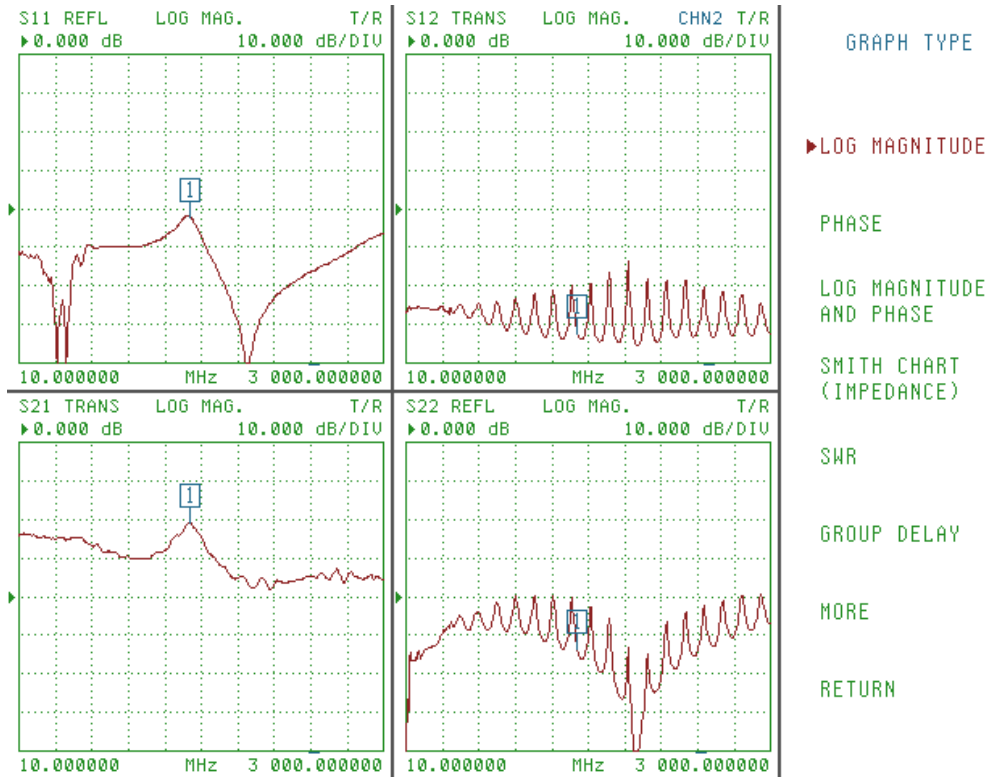


Figure 3.41: ERA-3+ characterization of the first prototype, $V_{cc}=10$ V. Multiple ERA-3+ were constructed. It is not as clean as the one shown in Figure 3.43. Note that this vector network analyzer measures from 10 MHz to 3 GHz.

The results in Figure 3.41 indicate that the lead lines are too long, creating resonances at certain frequencies while blocking out others. A different layout minimizing length is shown in Figure 3.42.



Figure 3.42: ERA-3+ second prototype implementation underway; only the semi-rigid coax cables need to be soldered on.

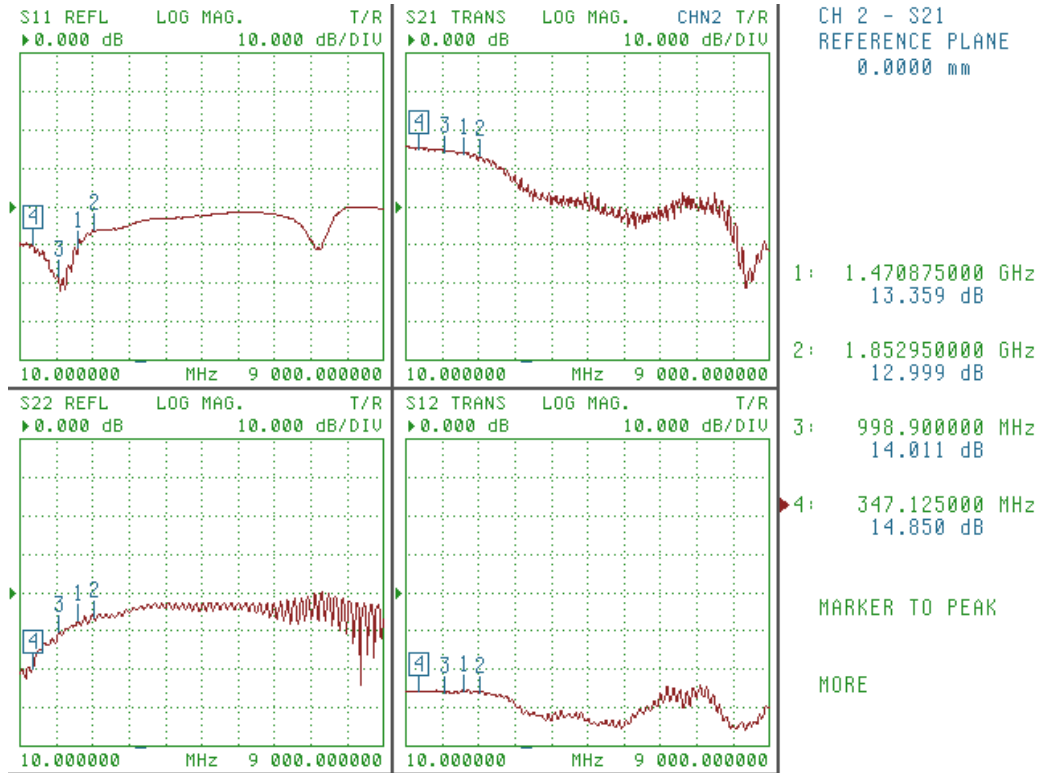


Figure 3.43: ERA-3+ second characterization, $V_{cc}=7$ V. The physical implementation is shown in Figure 3.42. Note that this vector network analyzer measures from 10 MHz to 9 GHz, unlike the one shown in Figure 3.41.

In higher frequency circuits, cleaner-laid out circuits matter more, due to wavelengths matching physical dimensions of circuits. This may create unwanted reflections, as seen in a comparison of Figure 3.41 vs Figure 3.43.

Two amplifiers were successfully created, while others gain; the gain is between 12-13 dB with a voltage set at 7 volts. The noise figure could not be measured using the vector network analyzers. Crude methods such as observing the noise floor rise could be used but may not give 0.1 dB accuracy. It is expected based on the datasheet that the noise figure is around 2.7 dB. The amplifiers are used on the receiver end after the antennas.

Chapter 4: Test Data

4.1 SISO

SISO Experiment 1:

Purpose:

Evaluate a SISO test case to compare later on to MISO, SIMO, and MIMO test cases.

Procedure

The purpose of this experiment is to set a standard and collect data to later compare to other cases. The data of interest is the channel matrix, and a metric related to signal-to-noise. The setup is shown in Figure 4.1 and 4.2. The Figures 4.3 through 4.6 display the data collected.

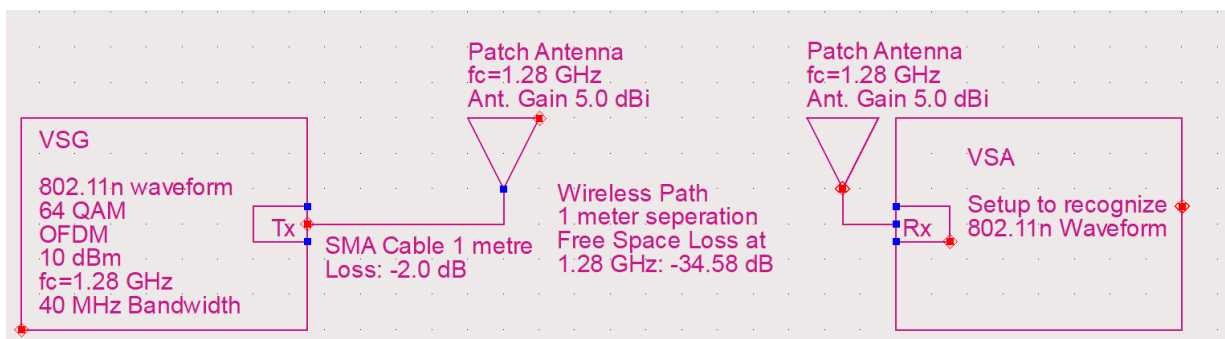


Figure 4.1: Experiment 1 Setup and Loss Analysis

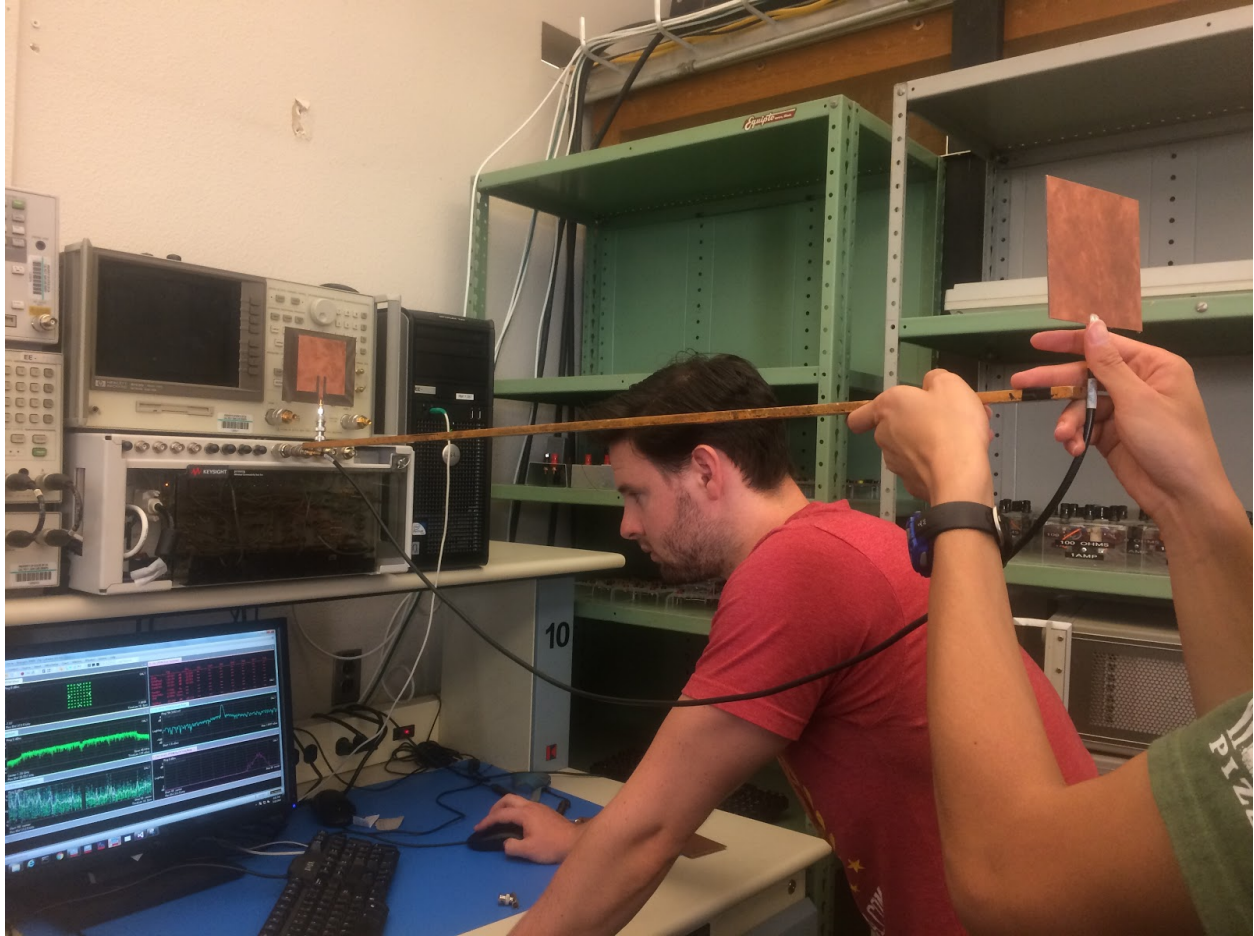


Figure 4.2: Physical Setup

Data



Figure 4.3: An instance of the IQ diagram, spectrum analyzer view, error vector spectrum are displayed.

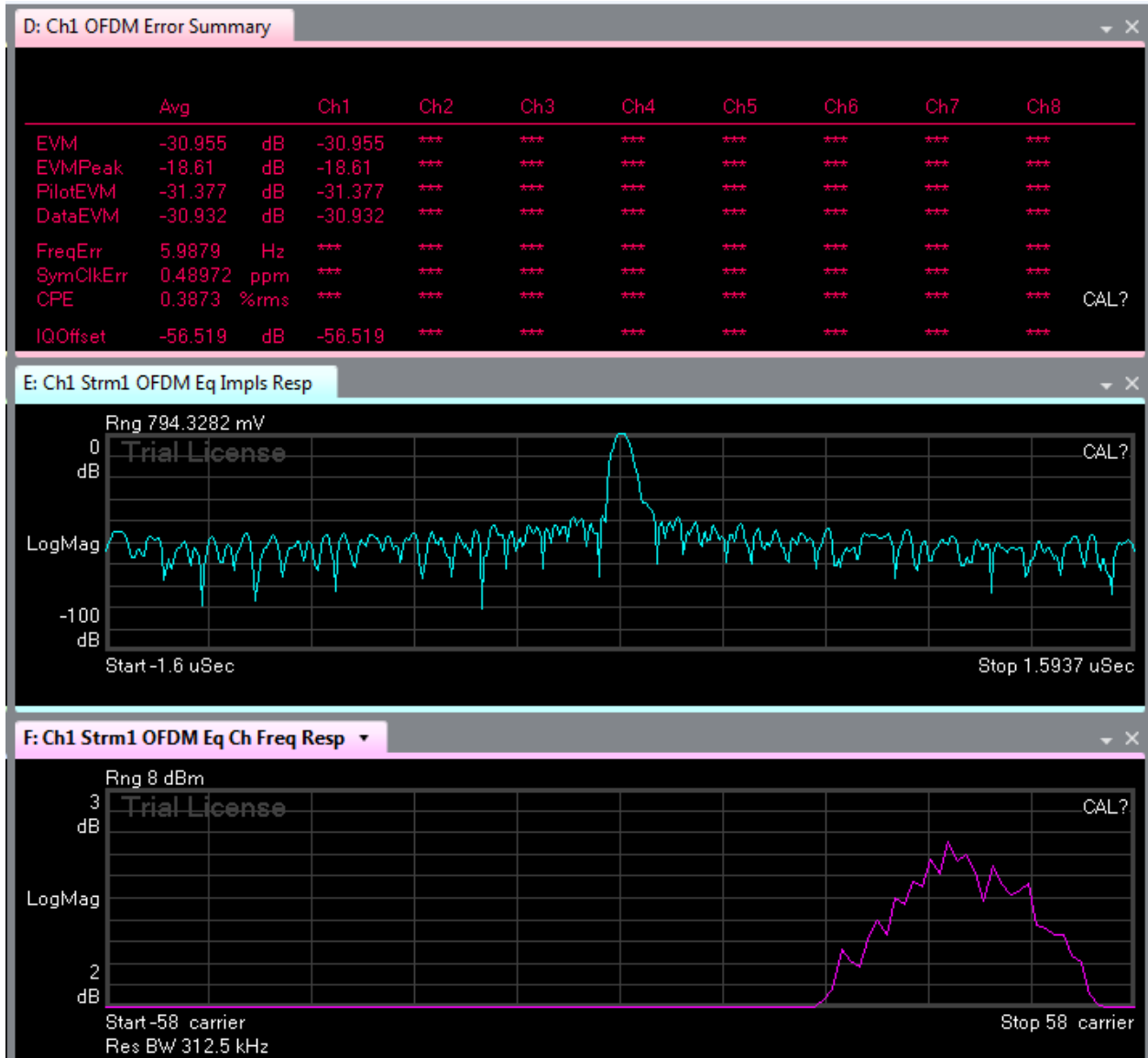


Figure 4.4: An instance of error vector summary, impulse response, and channel frequency response are displayed. The error vector magnitude reads -30.955 dB.

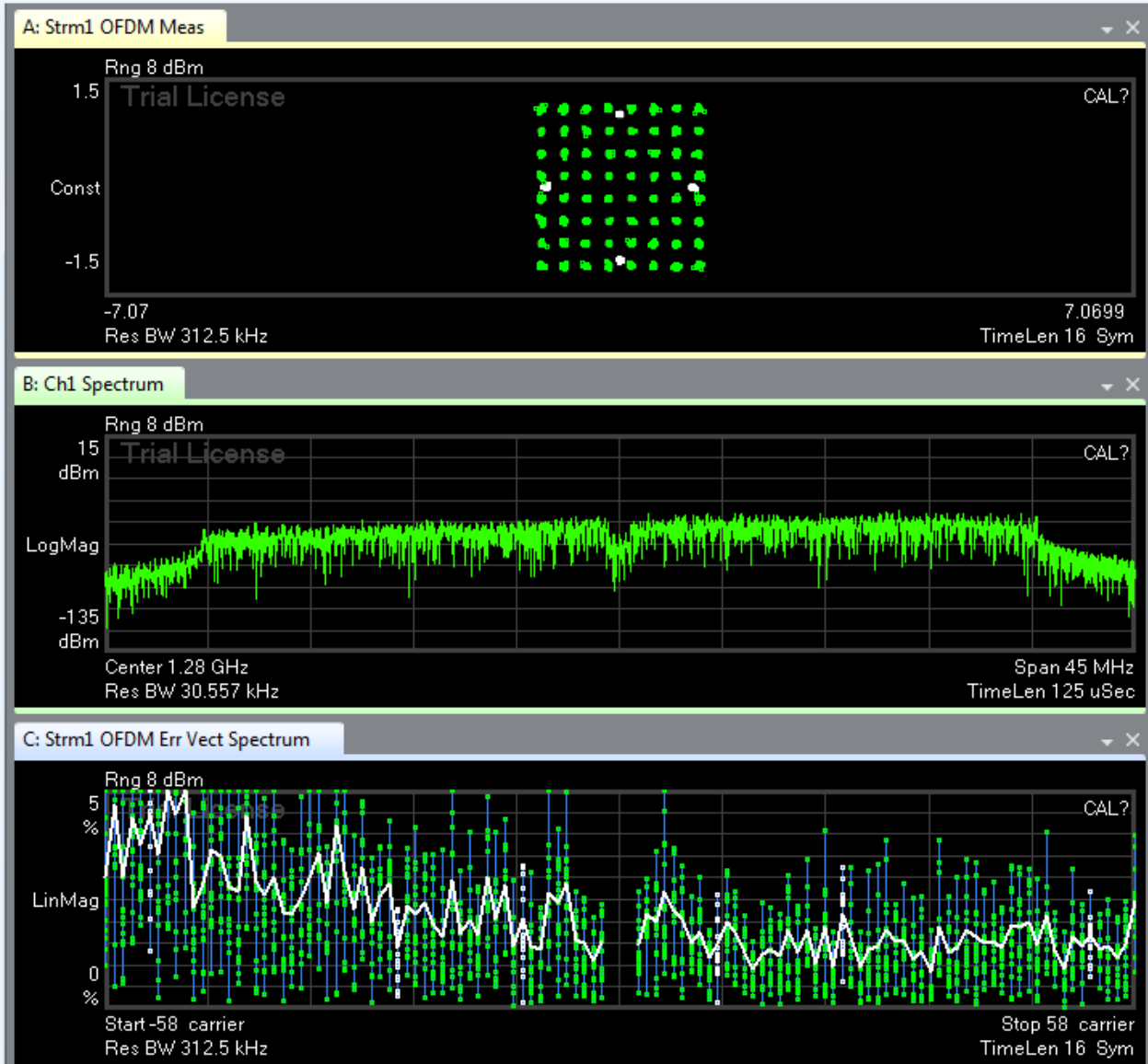


Figure 4.5: A second instance of the IQ diagram, spectrum analyzer view, error vector spectrum are displayed.



Figure 4.6: The second instance of error vector summary, impulse response, and channel frequency response are displayed. The error vector magnitude reads -32.47 dB.

Discussion

The SISO test case data is collected for comparison to higher input-output orders. Error vector magnitude is directly related to signal-to-noise ratio. Imagine noise as the error vector; the larger the noise, the larger the error vector. In a log scale, a larger EVM is not sought for. The

data collected suggests that for a SISO case, the EVM is -30.955 dB to -32.47 dB for the set conditions of 1 meter and 10 dBm for a MIMO signal. This metric can be compared to MISO, SIMO, and MIMO cases to understand the effect of increasing spatial diversity and verifying the Shannon Capacity trend.

SISO Experiment 2: Relationship between EVM and SNR

Purpose

Evaluate the relationship between error vector magnitude and signal-to-noise ratio.

Procedure

The objective of this experiment is to understand the error vector magnitude metric and its relationship to signal-to-noise ratio. The antennas are separated from 1 to 6 meters to mimic loss, resulting in lower signal-to-noise ratios. The setup is seen in Figure 4.7. The data collected is seen in Figures 4.8 through 4.13.

$$EVM = \text{sqrt}[1/10^{(SNRdB/10)}] \times 100 (\%)$$

Equation 4.1: EVM-SNR theoretical equation

The theoretical error vector magnitude can be determined from signal-to-noise ratio as seen in the above equation.

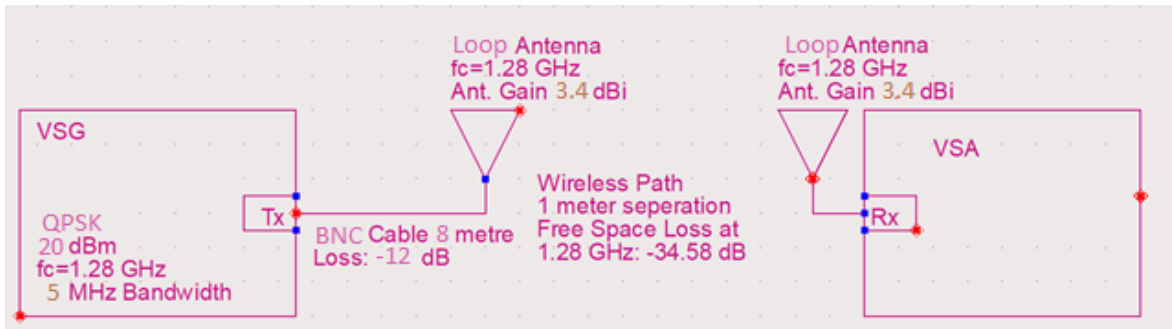


Figure 4.7: Setup for EVM and SNR experiment.

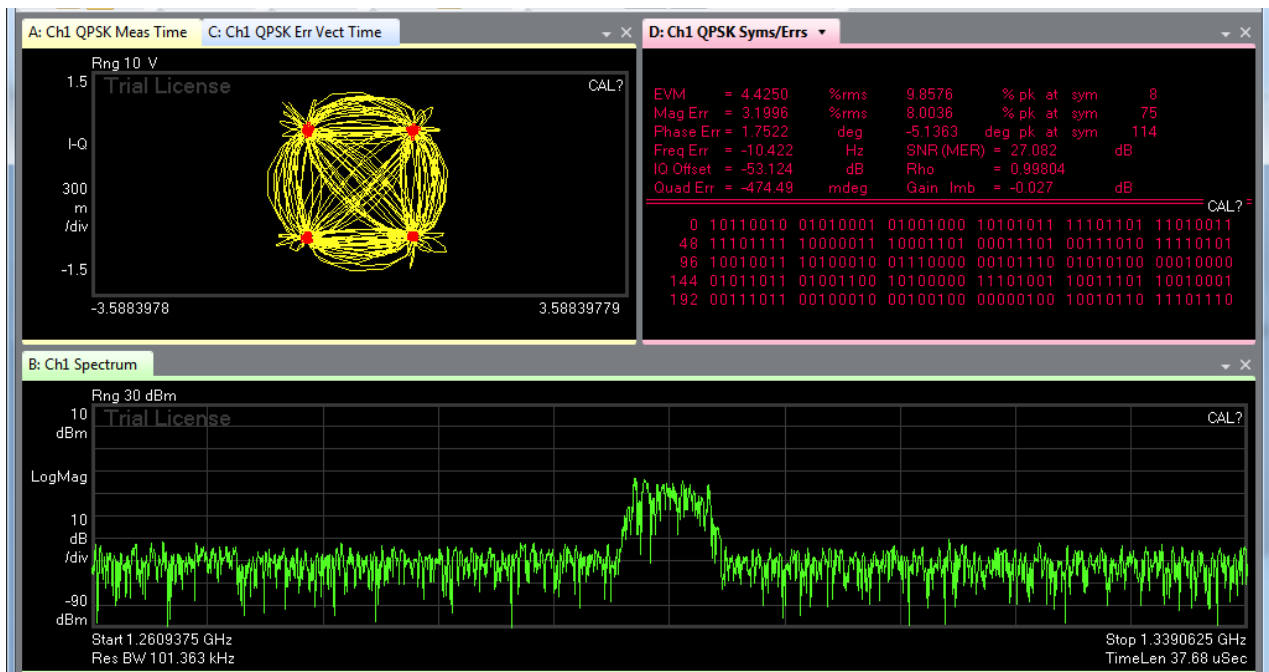


Figure 4.8: QPSK 5 MHz bandwidth, center frequency at 1.28 GHz at 1 meter separation.

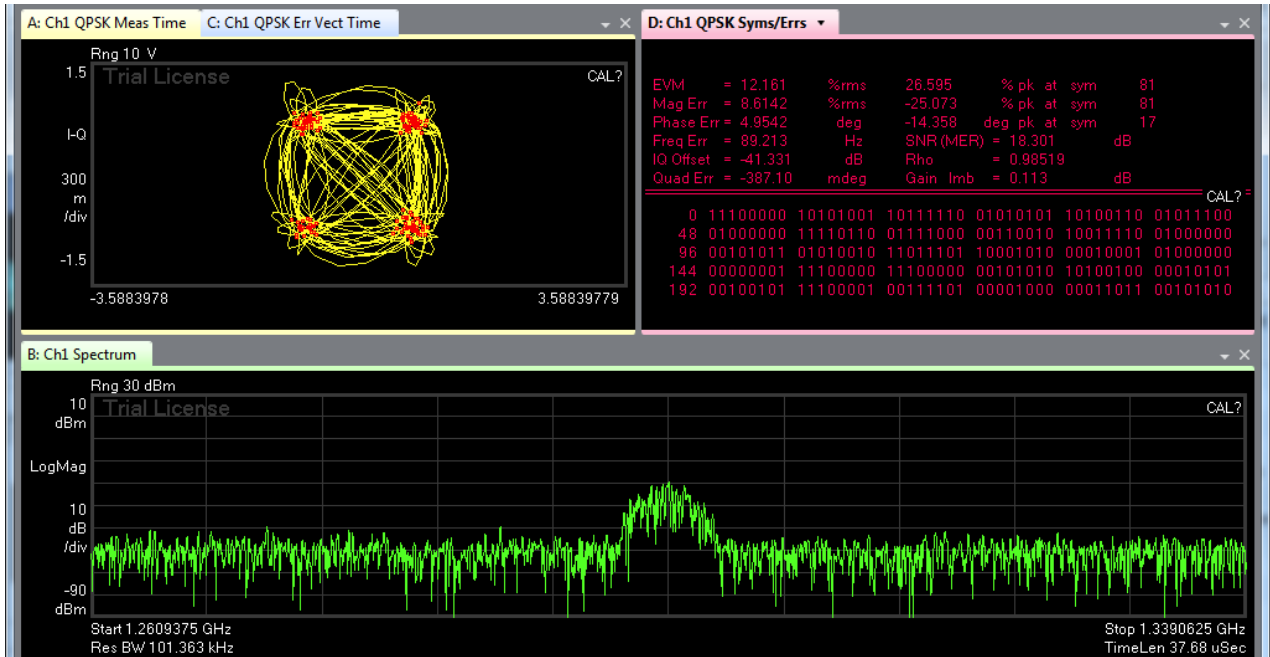


Figure 4.9: QPSK 5 MHz bandwidth, center frequency at 1.28 GHz at 2 meter separation.

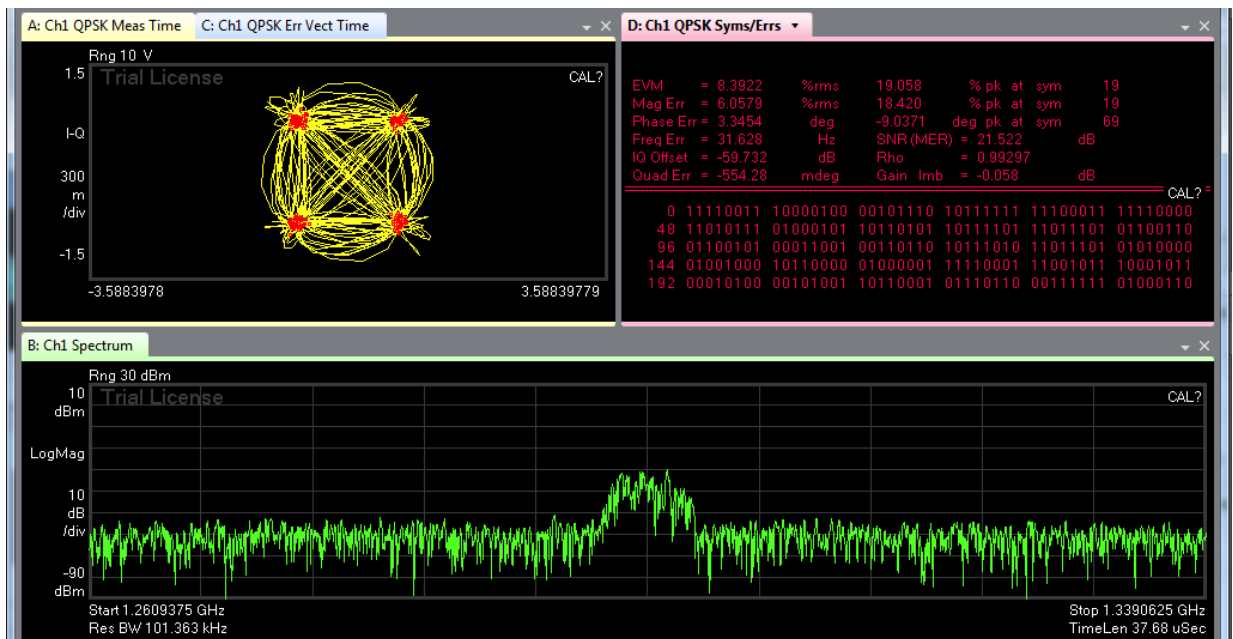


Figure 4.10: QPSK 5 MHz bandwidth, center frequency at 1.28 GHz at 3 meter separation.

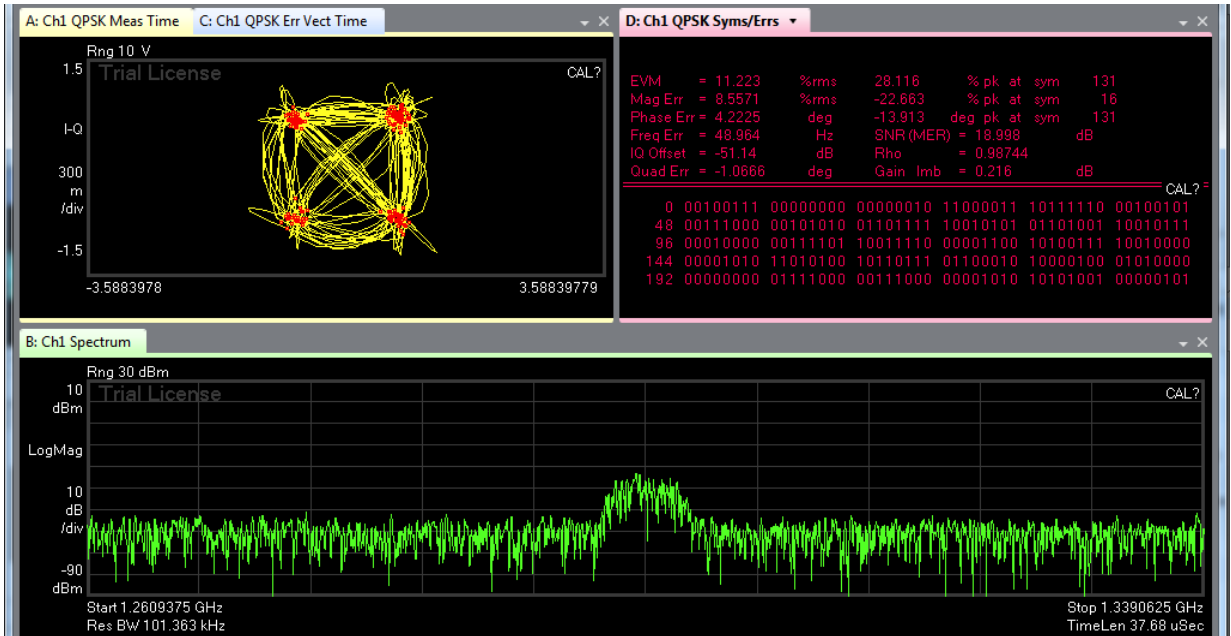


Figure 4.11: QPSK 5 MHz bandwidth, center frequency at 1.28 GHz at 4 meter separation.

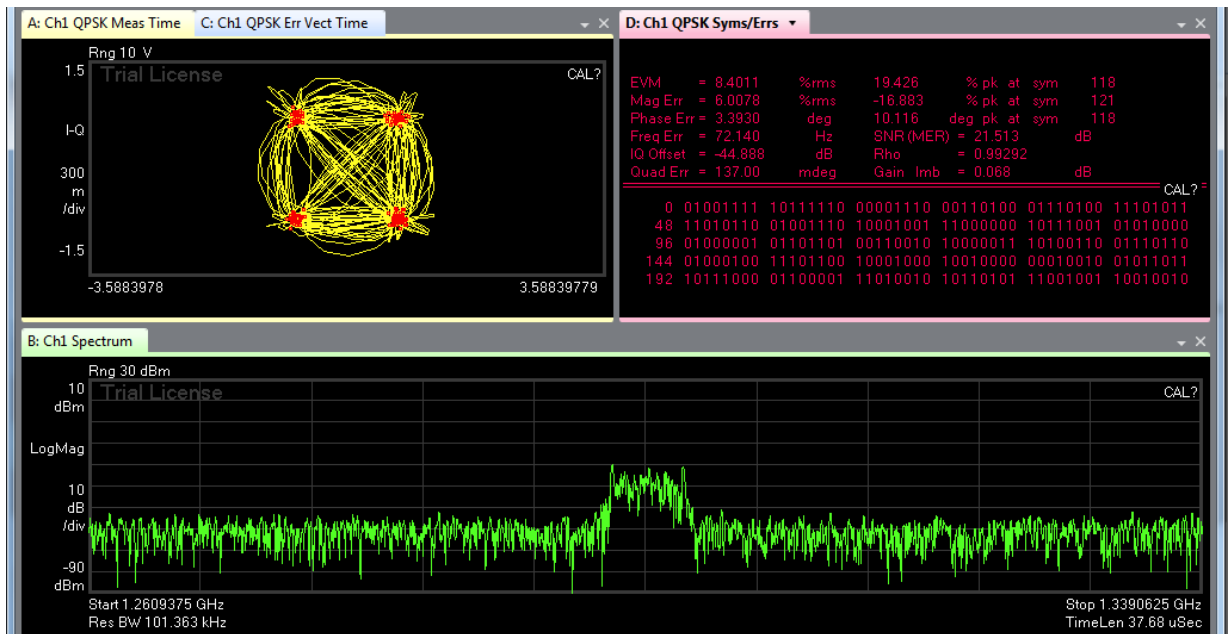


Figure 4.12: QPSK 5 MHz bandwidth, center frequency at 1.28 GHz at 5 meter separation.

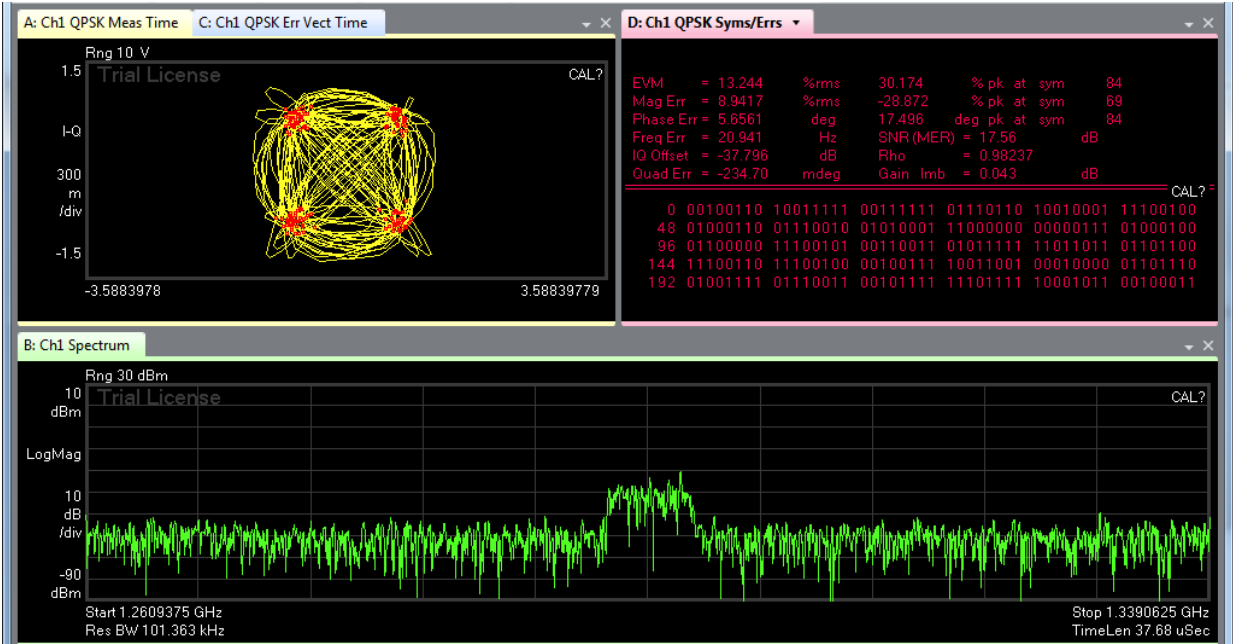


Figure 4.13: QPSK 5 MHz bandwidth, center frequency at 1.28 GHz at 6 meter separation.

Table 4.1: Compiled data of SNR-EVM experiment

Distance (m)	SNR (dB)	EVM (%)
1	27.082	4.425
2	12.161	18.301
3	8.3922	21.522
4	11.223	18.998
5	8.4011	21.513
6	13.244	17.56

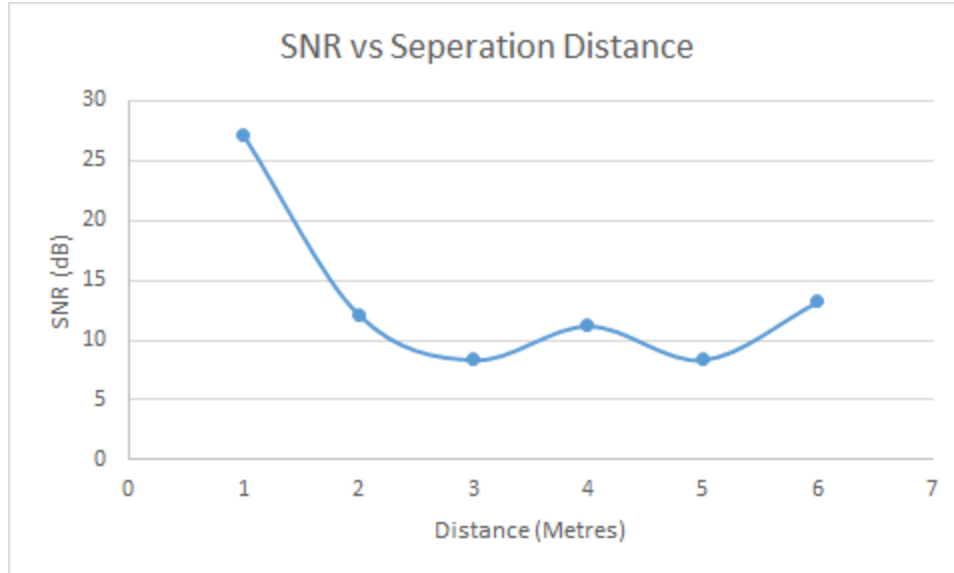


Figure 4.14: SNR versus distance.

The expected result is that signal-to-noise ratio decreases as distance increases. The expected result does not match the experiment. After 3 meters, the SNR stays at a consistent level between 8 and 13 dB.

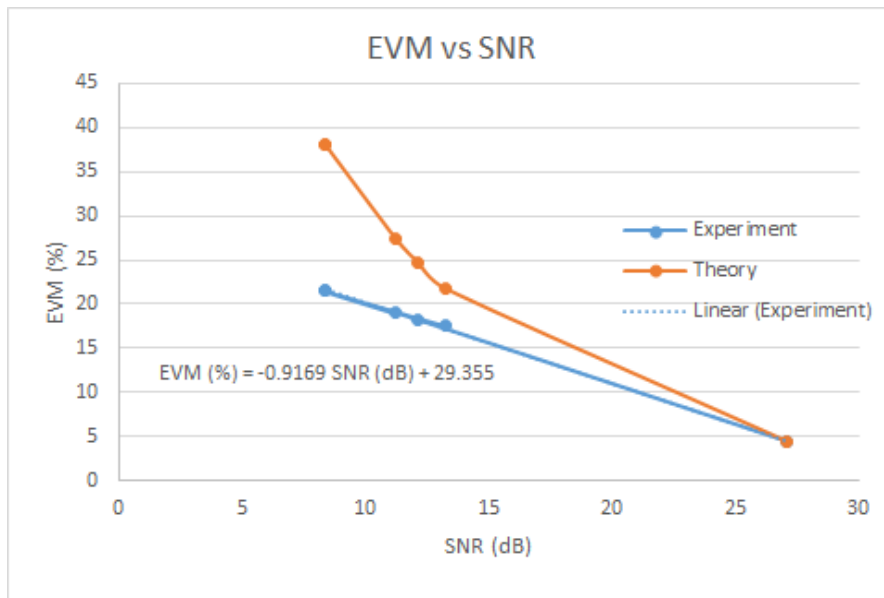


Figure 4.15: EVM versus SNR, comparing theory to experimental equation displayed earlier.

Discussion

The data shown in Table 4.1 is graphed in Figure 4.14 and 4.15 to display the relationships and trends in data. The goal of this test was to understand the relationship between EVM and SNR. The experiment displayed lower EVM for a lower SNR than when compared with the theoretical equation, surprisingly. The general trend still holds true: increasing SNR decreases EVM in general. At higher SNRs, the EVM converges, as seen in Figure 4.15.

The distance versus signal-to-noise ratio did not meet expectations or predictions. As distance increased, the SNR started to stay at the same level, seen in Figure 4.14. Perhaps larger magnitudes of distance separation are needed to demonstrate the expended trend of a lower SNR. The experiment had a linear sweep of distance. A logarithmic sweep of distance (1 m, 10 m, 100 m) could be a better method of setting up an improved experiment. However, cable lengths may be a limiter in this situation.

SISO Experiment 3: Effects of modulation on EVM and SNR

Purpose

Evaluate the effects of increasing modulation on error vector magnitude and signal-to-noise ratio.

Procedure

The objective of this experiment is to understand the error vector magnitude metric and its relationship to increasing modulation. The antennas are separated from 3 meters constantly,

while the generator generates different modulation types. The setup is seen in Figure 4.16 to 4.18. The data collected is seen in Figures 4.19 through 4.26.

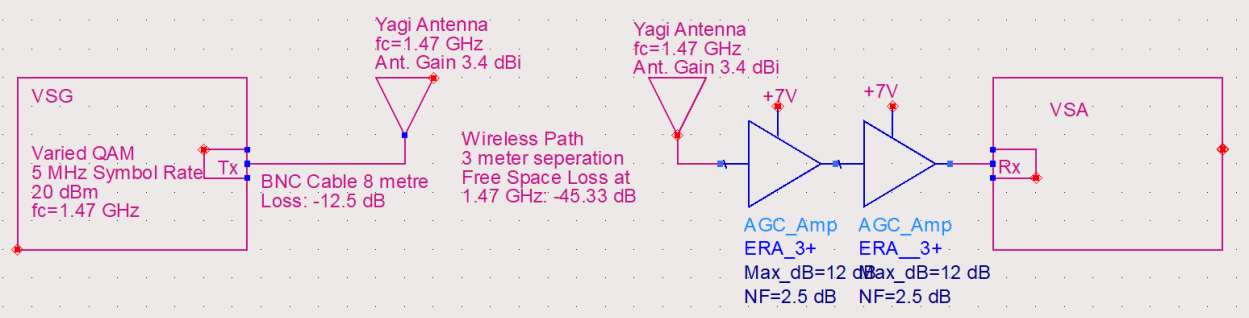


Figure 4.16: Modulation experiment setup



Figure 4.17: Modulation experiment physical setup

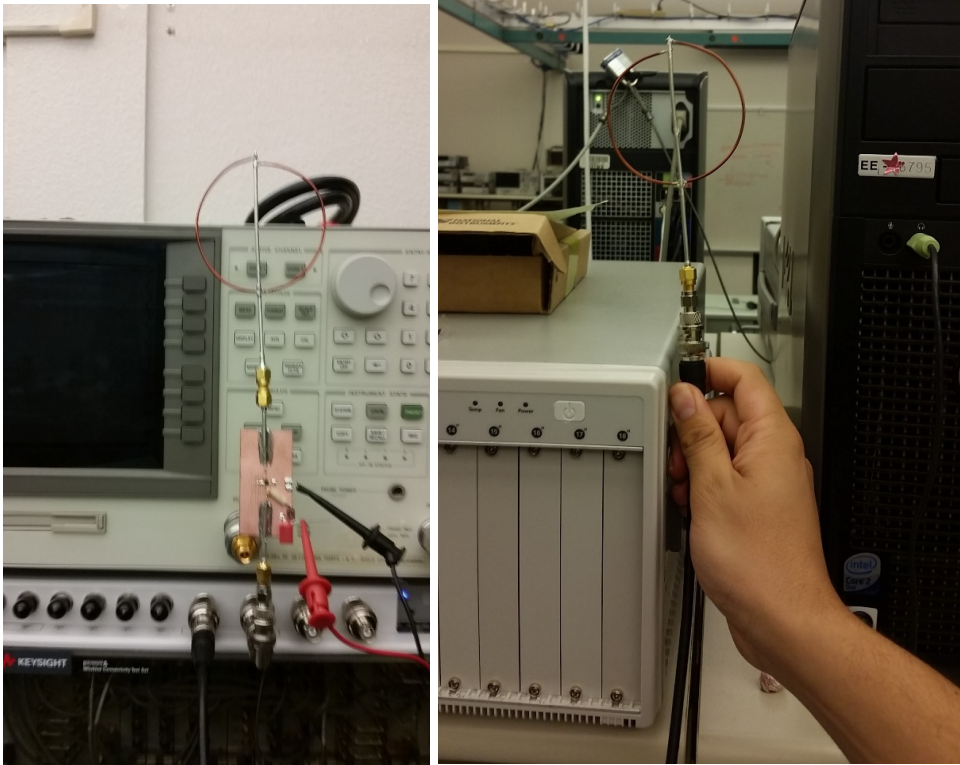


Figure 4.18: Transmitter and receiver, along with amplifier

Data

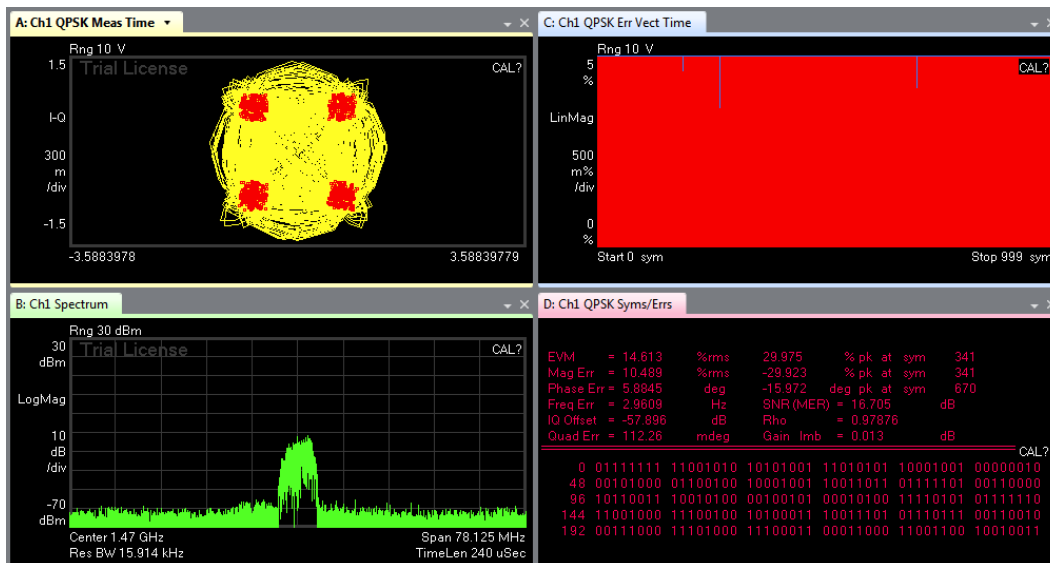


Figure 4.19: QPSK test case

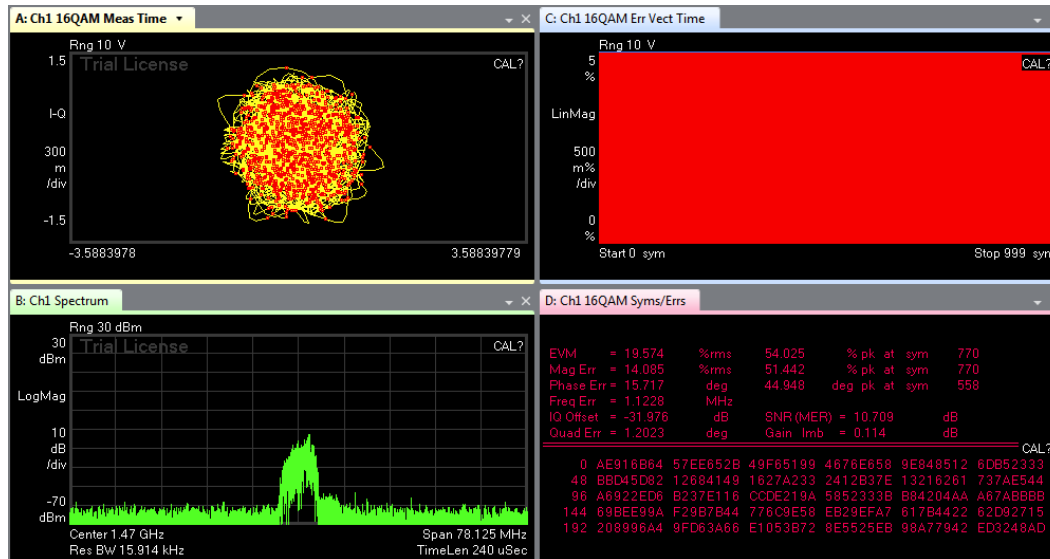


Figure 4.20: 16 QAM test case

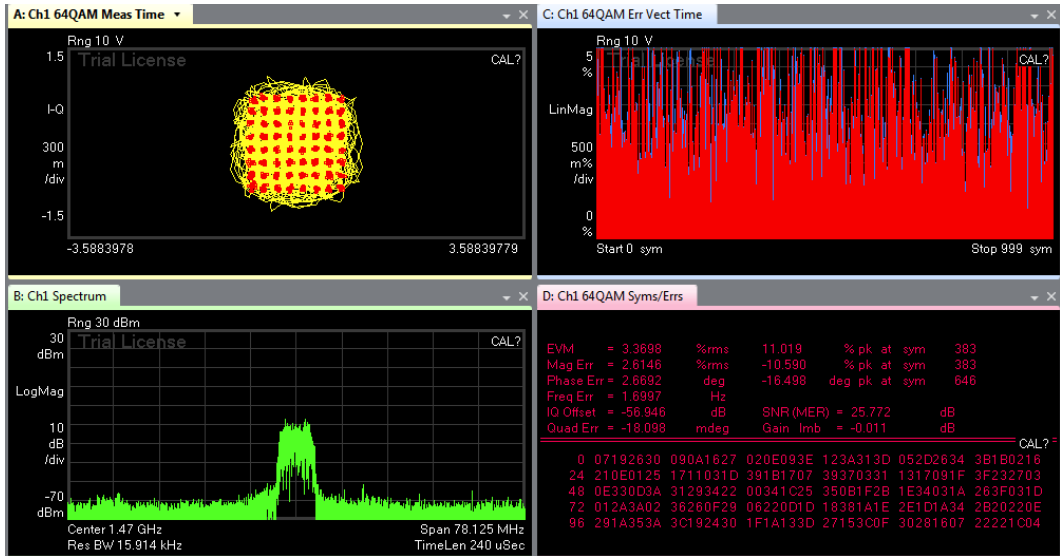


Figure 4.21: 64QAM test case

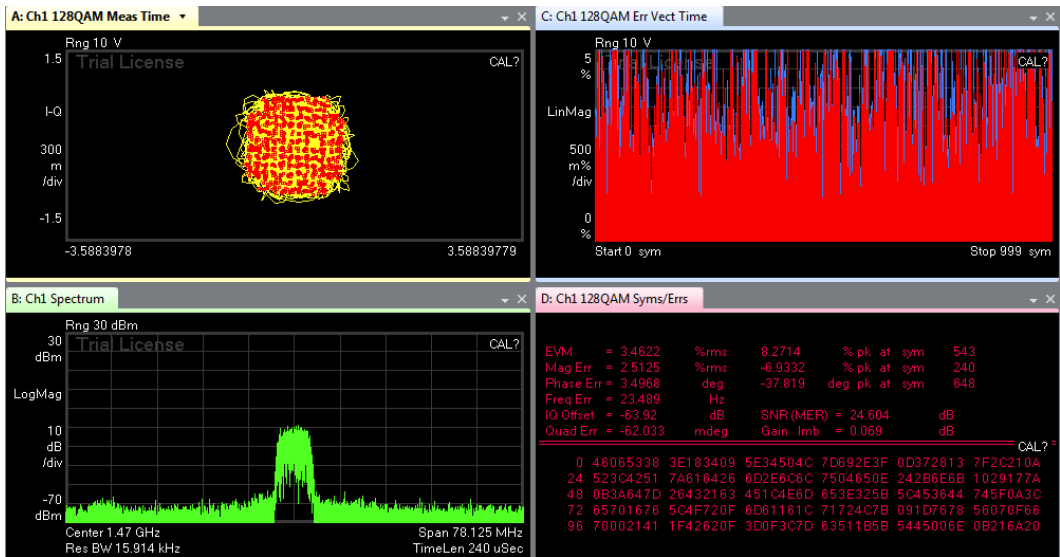


Figure 4.22: 128 QAM test case

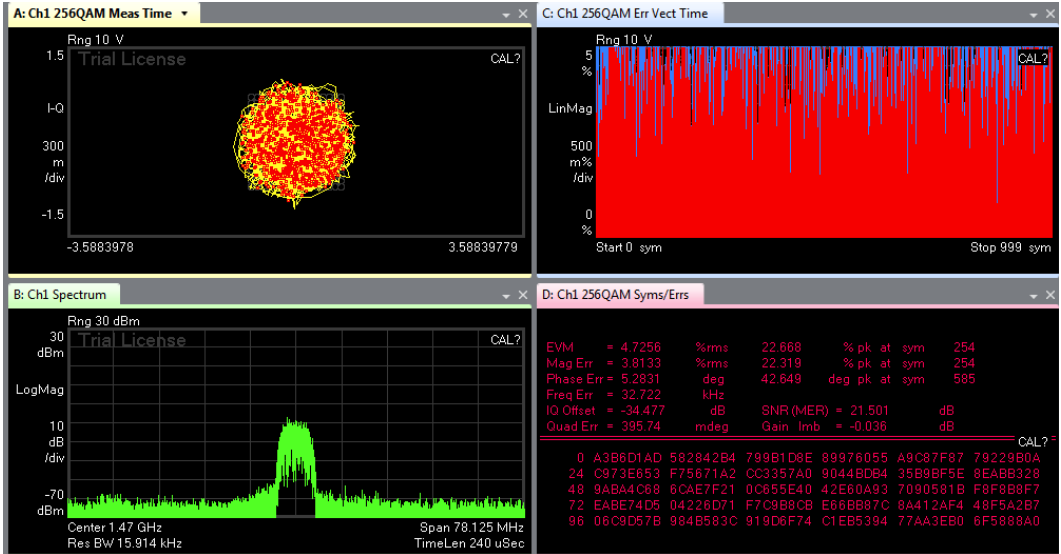


Figure 4.23: 256 QAM test case

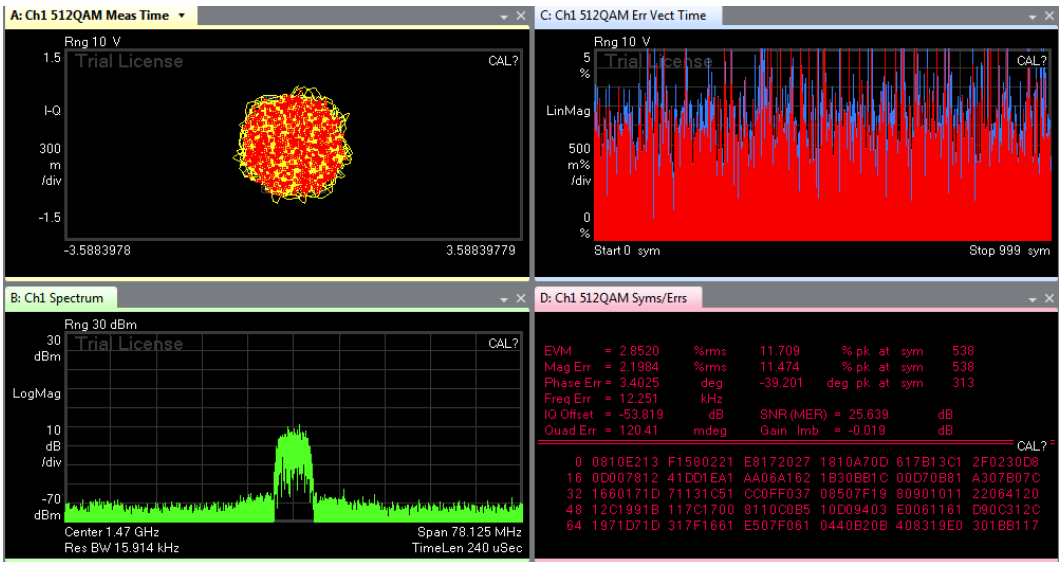


Figure 4.24: 512 QAM test case

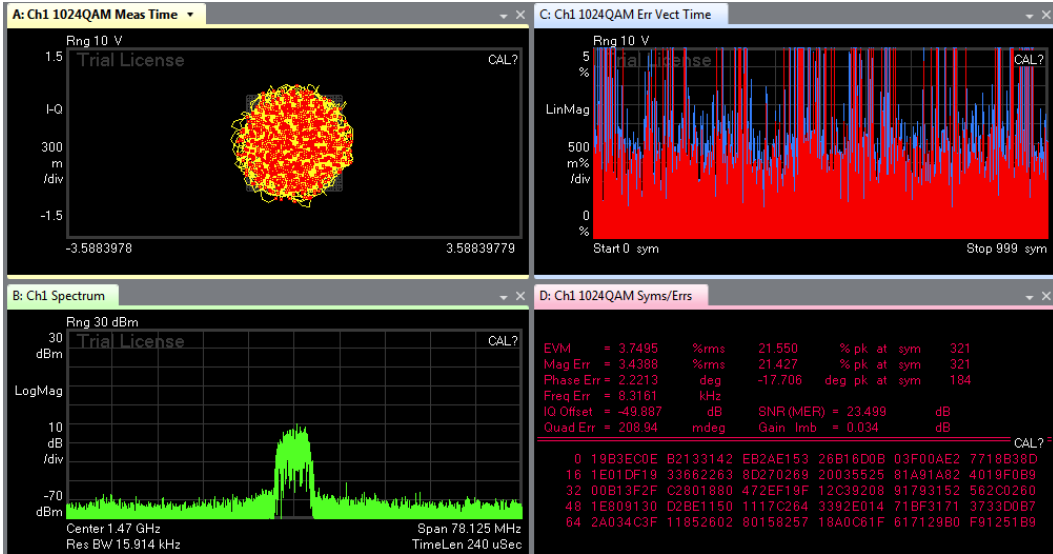


Figure 4.25: 1024 QAM test case

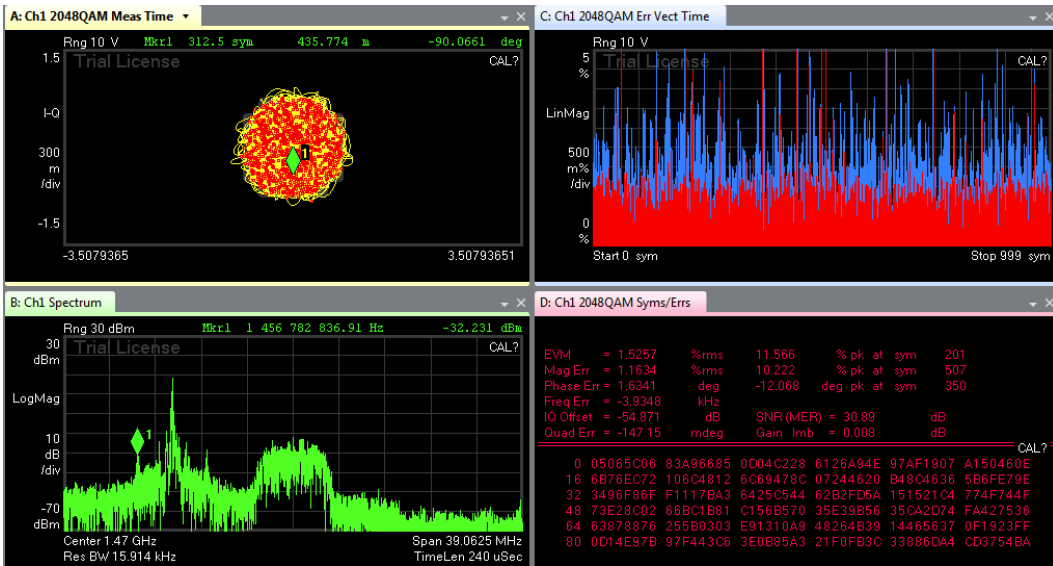


Figure 4.26: 2048 QAM test case

Table 4.2: Compiled results

QAM (symbols)	EVM (%)	SNR (dB)
4	14.613	16.705
16	19.574	10.709
64	3.3698	25.772
128	3.4622	24.604
256	4.7256	21.501
512	2.852	25.639
1024	3.7495	23.499
2048	1.5257	30.89
4096	1.7533	29.669

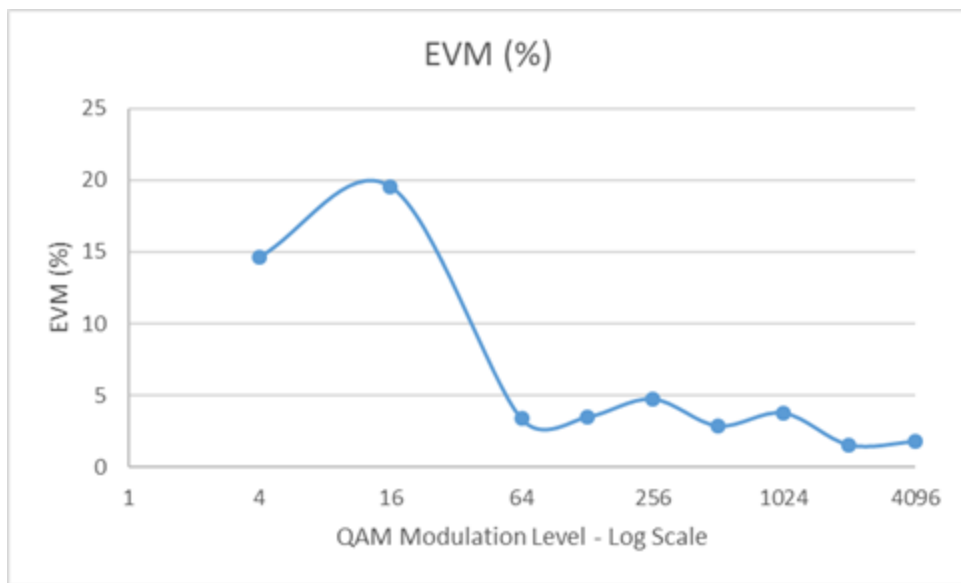


Figure 4.27: EVM vs QAM Modulation relationship.

Note that this is misleading based on how the vector signal analyzer determines EVM. The trendline should be increasingly worse EVM.

Discussion

The goal of this test was to see how the increasing the modulation of a SISO system affects the EVM and SNR. Looking at the graph in Figure 4.27, the maximum EVM occurs at approximately 16 QAM and after decreases sharply. Originally it was believed that increasing the QAM modulation would increase the EVM, but upon closer inspection the experimental trend is valid. Looking at 16 QAM constellation diagram in Figure 4.20 has a very chaotic pattern, where the points are not lined up with the expected position. When 16 QAM is compared to 64 QAM there is a very stark difference in clarity. The 64 QAM constellation shown in Figure 4.21 had point almost exactly on the expected spots, thus the 64 QAM case had a better EVM than the 16 QAM case. After the 64 QAM case the 128 QAM was tested and had a worse EVM, which is expected, but when higher modulations were tested the trend failed. When looking at the constellation diagrams for the 256 to 4096 cases (Figure 4.23 to Figure 4.26) the constellation diagrams are just as messy and chaotic as the 16 QAM case, but the EVM was better than the 16 QAM case.

This suggests that the EVM for the higher cases of modulation is not an accurate way to measure the performance of the SISO system. The reason the EVM may fail is because the error is determined by the distance from the experimental point to the closest expected constellation point. In cases above 128 QAM the points are far closer together, which provides more points to be closer to the experimental point than for lower modulations such as 16QAM. Since the points are closer together the error distances is significantly smaller and thus the ratio of error to the constellation point difference to the origin is extremely smaller than lower QAM cases. The SNR is inversely proportional to the EVM so SNR should be worse at higher QAM

modulations, but since the SNR was calculated from the experimental data the SNR will have the same faults at higher frequencies. Thus modulation used in future tests should only be with modulations less than 128 QAM to prevent misconceptions about EVM.

4.2 MISO

Purpose:

Evaluate a MISO test case to compare later on to MISO, SIMO, and MIMO test cases.

Procedure

The purpose of this experiment is to set a standard and collect data to later compare to other cases. The data of interest is the channel matrix, and a metric related to signal-to-noise.

To perform our MISO test, we drove each VSG with the WLAN_11n_64QAM_40MHz.wfm waveform using the C# program. The next step was to change the setup of the 89600 software such that it could read the waveform we are sending. Once the setup was complete we then adjusted the center frequency to allow for the program to run.

Once both VSGs and the VSA were being driven we then separated the transmit antennas and receive antennas by a length of 1 meter, shown in Figures 4.28 and 4.29. . The data was recorded in the following section, Figures 4.30 through 4.33 .

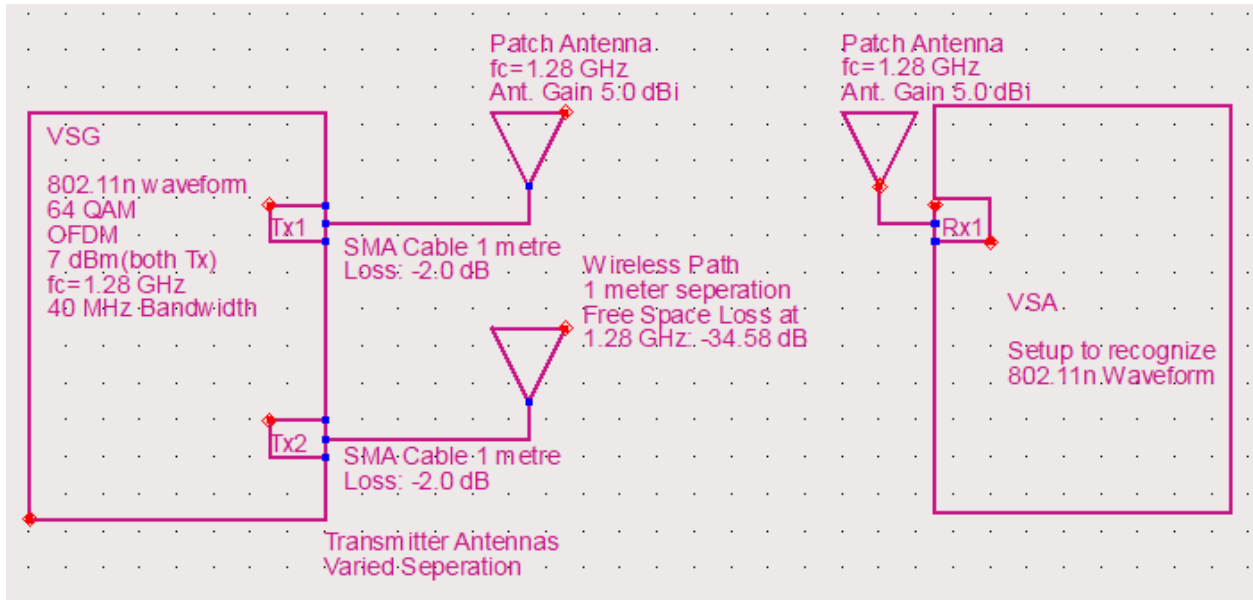


Figure 4.28: MISO experimental setup



Figure 4.29: MISO experiment physical setup

Data



Figure 4.30: MISO 10 cm horizontal separation case. EVM is -30.932 dB.



Figure 4.31: MISO 40 cm horizontal separation case. EVM is -33.848 dB.



Figure 4.32: MISO no separation case where antennas are back-to-back, front antenna is 1 m away from receivers' centroid. EVM is -31.551 dB.



Figure 4.33: MISO 16 cm separation case where antennas are back-to-back, front antenna is 1 m away receivers centroid. EVM is -20.421 dB.

Table 4.3: Compiled MISO cases and EVM

Case	Distance	EVM (dB)
Horizontal	10 cm	-30.932
	40 cm	-33.848
Vertical	0 cm	-31.551
	16 cm	-20.421

Discussion

The MISO cases demonstrated better signal-to-noise ratio, based on configurations. Examining the horizontal cases, the separation distance effects the error-vector-magnitude. With a meter distance to the receiver held constant, increasing horizontal separation distance between the transmit antennas resulted in better signal received at certain points. In the experiment, 40 cm separation resulted in an EVM of -33.848 dB, whereas the close distance of 10 cm resulted in -30.932 dB, as tabulated in Table 4.3. Different separation distances resulted in EVM around -30 dB as well. Separation distances greater than half a meter started to exhibit a decay, rising to -20 dB for instance. Overall, this method of spatial diversity may prove cheaper and more effective than controlling power and phase (in beamforming), as long as the number of array elements is low and cost of mechanical parts does not outweigh the cost of variable amplifiers and phase shifters.

The back-to-back cases explores the effect of another patch antenna back lobe on the transmit signal. For the back-to-back case of 0 cm separation, the error vector magnitude was comparable to the horizontal cases between 10 and 40 cm; the error vector magnitude was below -30 dB. For the case of 16 cm, or approximately $\frac{3}{4}$ of the wavelength, the EVM suffered, dropping to -20 dB. This experiment demonstrates that in a MIMO system with multiple patch

antennas facing different directions, the back lobe of the radiation may affect other patch antennas unintentionally in a negative manner.

4.3 SIMO

Purpose:

Evaluate a SIMO test case to compare later on to MISO, SIMO, and MIMO test cases.

Procedure

The purpose of this experiment is to set a standard and collect data to later compare to other cases. The data of interest is the channel matrix, and EVM, a metric related to signal-to-noise. The physical setup is shown in Figures 4.34 and 4.35.

To perform the SIMO test, we drove one VSG with the WLAN_11n_64QAM_40MHz.wfm waveform using the C# program. The next step was to change the setup of the 89600 software such that it could read the waveform we are sending. Once the setup was complete we then adjusted the center frequency to allow for the program to run.

Once the VSG and both VSAs were being driven we then separated the transmit antenna and receive antennas by a length of 1 meter. The data was recorded in the following section, seen in Figures 4.36 and 4.37.

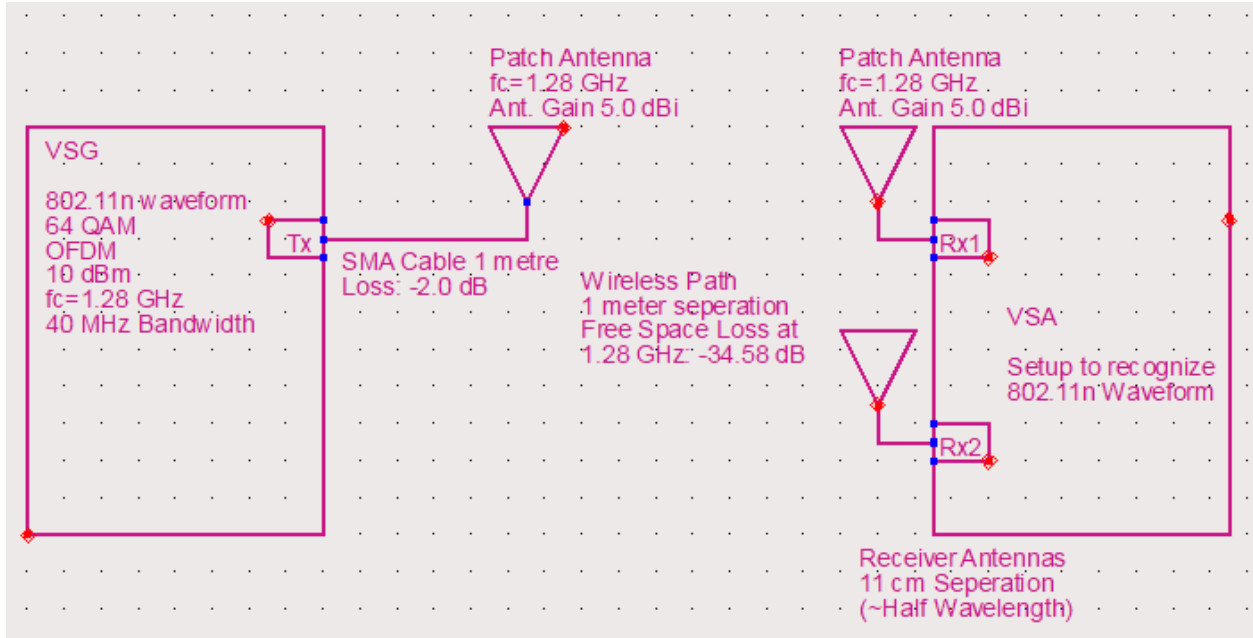


Figure 4.34: MISO experimental setup

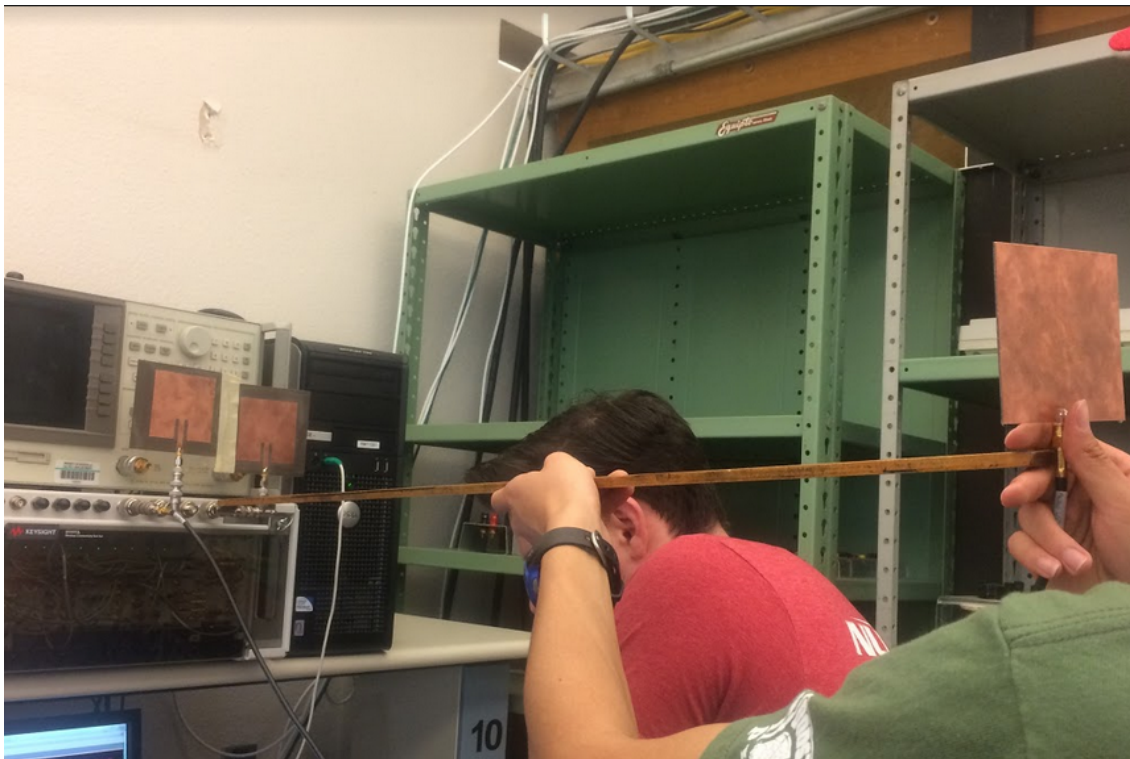


Figure 4.35: MISO experiment physical setup

Data



Figure 4.36: SIMO test case results. IQ diagram, spectrum analyzer view, error vector spectrum are displayed.

Both received signals were about the same power, with the second spectrum slightly lower. The IQ diagram shown was clean, suggesting that EVM measurement error would not occur from overlap.

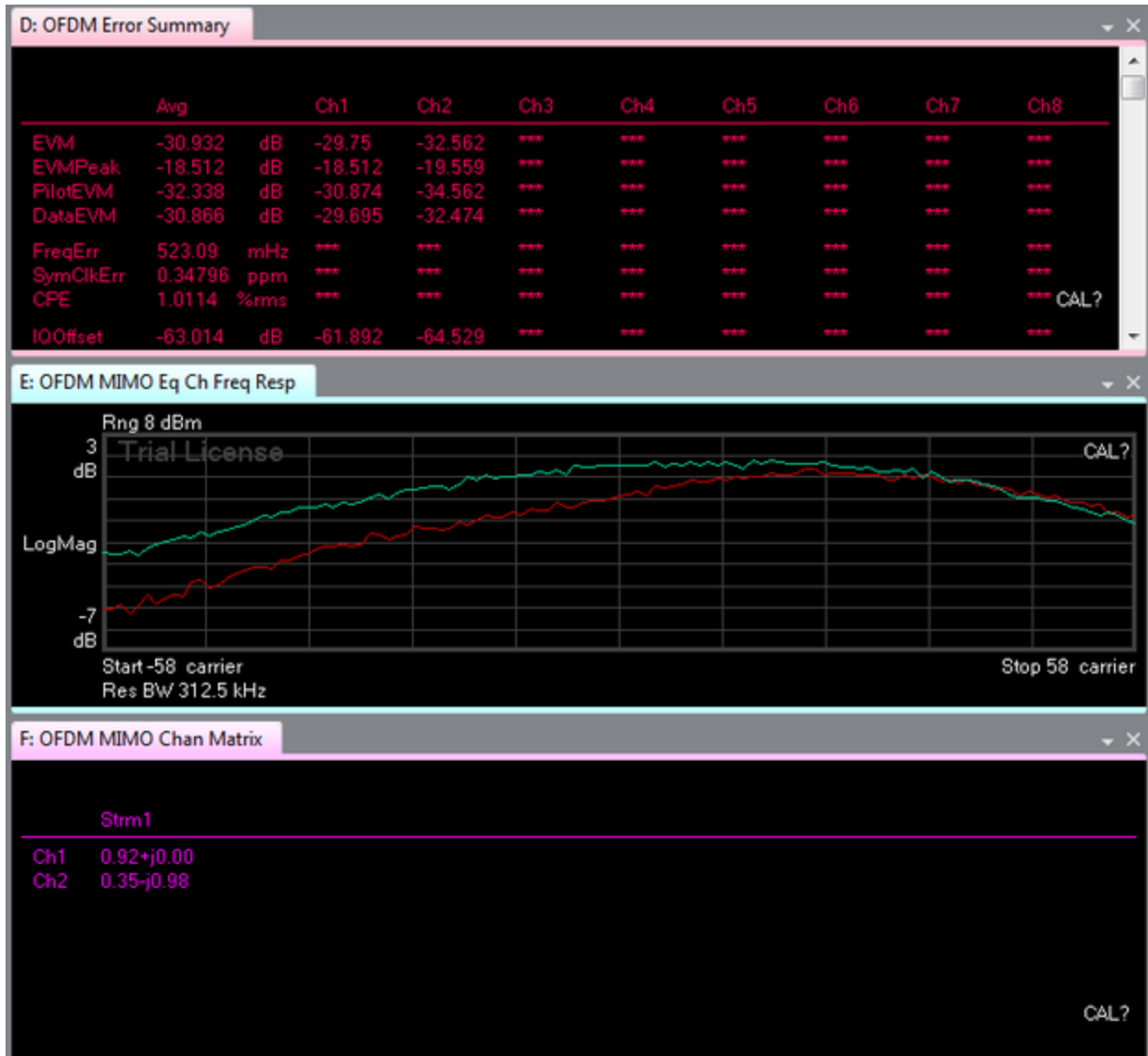


Figure 4.37: SIMO test case results. Error vector summary, impulse response, and channel frequency response are displayed. The error vector magnitude reads -30.932 dB.

The channel frequency response differed, with one channel being more even across the board, while the other attenuated lower carriers more. This could be dependent on the antenna

bandwidth. Perhaps one antenna's center frequency was slightly different by a few megahertz, causing higher carriers to have the highest channel frequency response, rather than the center. The error vector magnitude for one channel was slightly better. This is perhaps due to less multipath for that antenna, or even less lossy wires before entering the demodulation of inside the VSAs.

Discussion

The error vector magnitude of -30.932 dB, as seen in Figure 4.37, is comparable to the SISO case. This makes sense, as there is no spatial diversity on the transmitter side. Although the results for SISO and SIMO were similar, note that SIMO has a superior worst-case. For example, if multipath or a jammer disabled the quality of the signal going into one antenna, the second antenna could still potentially pick up a usable signal in the case of SIMO. For SISO, the receiver under the same conditions may not be able to render a usable signal.

4.4 2x2 MIMO

Purpose:

The purpose of this portion of the experiment was to implement and test a 2x2 MIMO system. This was done by running the C# program via Microsoft's Visual Studio.

Procedure:

To perform our MIMO test, we drove each VSG with the WLAN_11n_64QAM_40MHz.wfm waveform using the C# program. The next step was to change the setup of the 89600 software such that it could read the waveform we are sending. Once the setup was complete we then adjusted the center frequency to allow for the program to run.

Once both VSGs and both VSAs were being driven we then separated the transmit antennas and receive antennas by a length of 1 meter, seen in Figure 4.38. The data was recorded in the following section, seen in Figures 4.39 through 4.43.

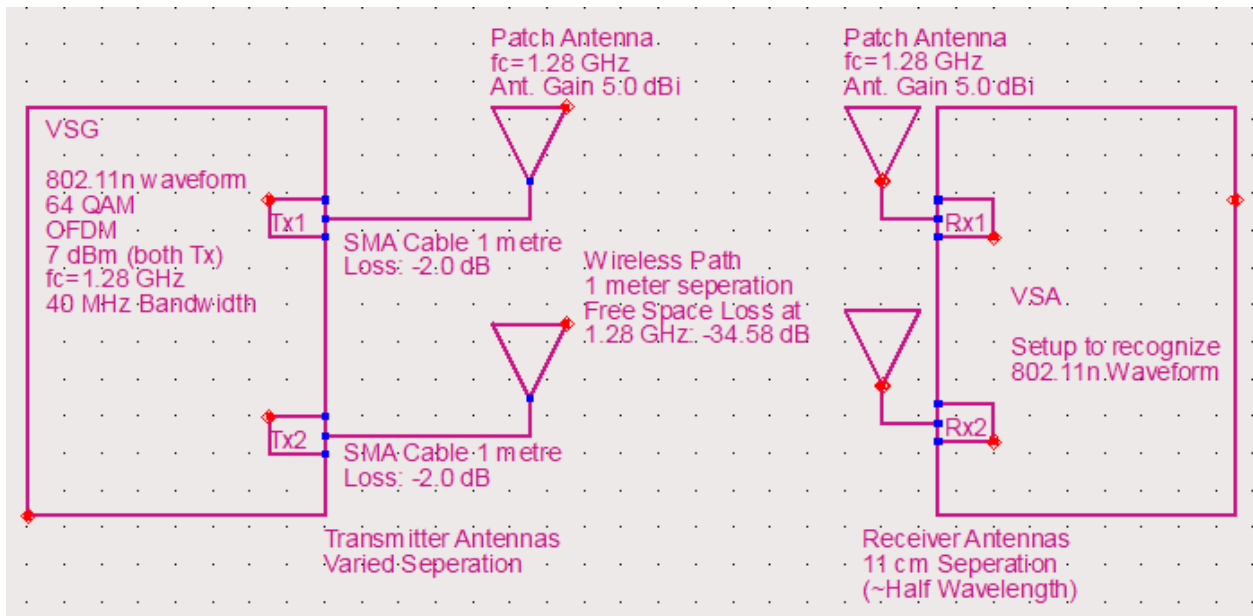


Figure 4.38: MIMO experimental setup

Data:

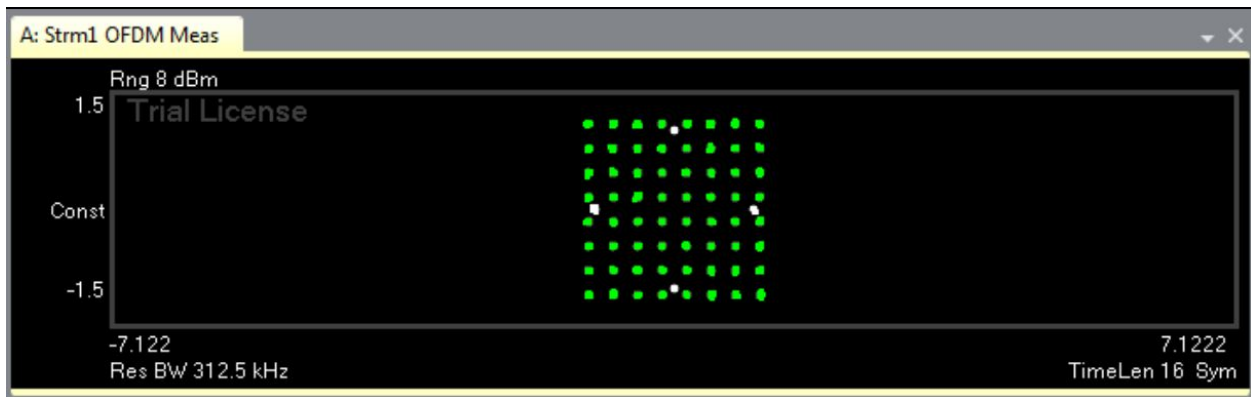


Figure 4.39: 802.11n OFDM 64 QAM Constellation Diagram

Figure 4.39 shows the WLAN 802.11n 64 QAM constellation diagram for a 2x2 MIMO system with a modulation frequency of 1.28 GHz. This particular constellation diagram appears to be rather clean. The constellation points are tightly knit, in other words, the demodulated symbols are rather close to the predetermined reference points.

	Avg		Ch1	Ch2	Ch3	Ch4	Ch5	Ch6	Ch7	Ch8
EVM	-32.989	dB	-31.311	-35.761	***	***	***	***	***	***
EVMPeak	-20.109	dB	-20.109	-24.265	***	***	***	***	***	***
PilotEVM	-33.813	dB	-32.854	-35.047	***	***	***	***	***	***
DataEVM	-32.947	dB	-31.239	-35.804	***	***	***	***	***	***
FreqErr	-1.5511	Hz	***	***	***	***	***	***	***	***
SymClkErr	-1.5383	ppm	***	***	***	***	***	***	***	***
CPE	0.5668	%rms	***	***	***	***	***	***	***	***
IQOffset	-55.101	dB	-52.148	-70.917	***	***	***	***	***	***

Figure 4.40: OFDM Error Summary

Figure 4.40 shows the OFDM error summary for our WLAN signal. We can immediately notice that the EVM of channel 2 is lower than that of channel 1; both VSG 1 and VSG 2 are outputting the same signal and no diversity coding is taking place, so this difference in channel EVM can most likely be attributed to antenna orientation as well as signal interference.

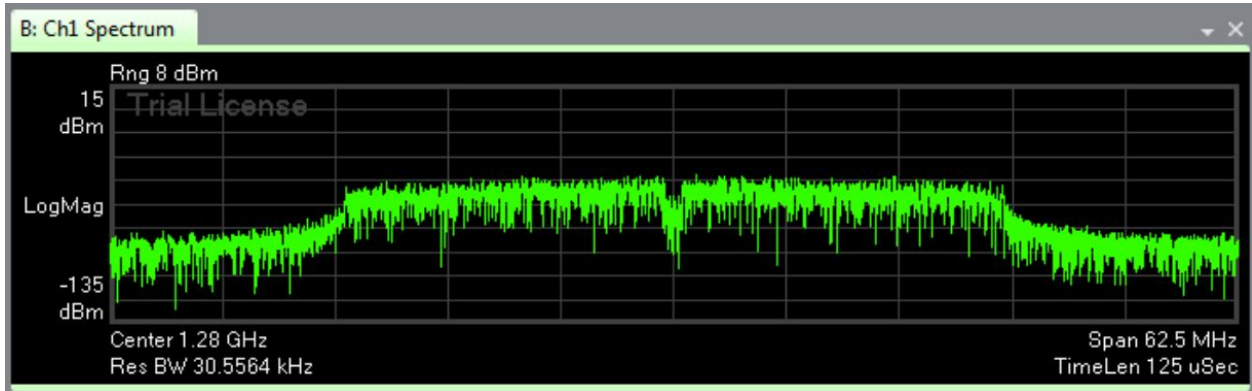


Figure 4.41: Channel 1 Spectrum

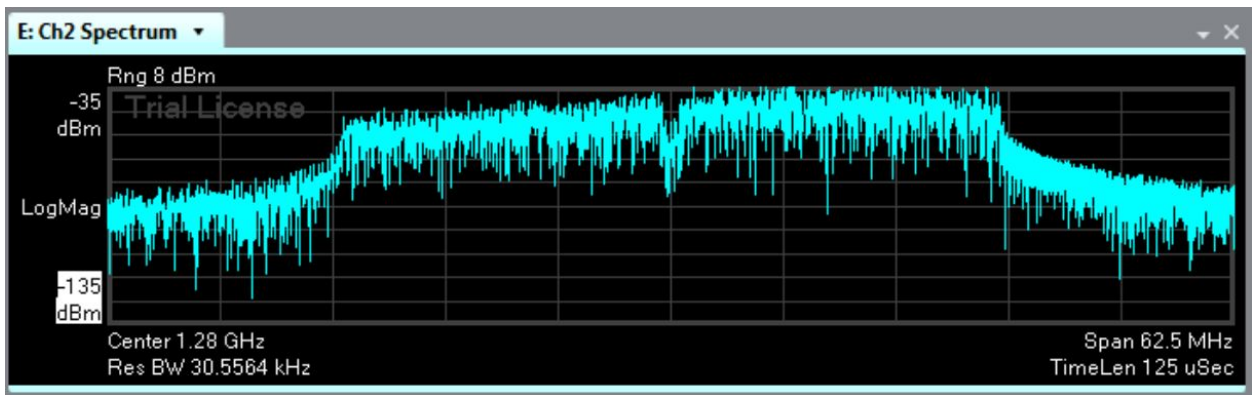


Figure 4.42: Channel 2 Spectrum

Figures 4.41 and 4.42 show the spectrums of channel 1 and channel 2. We can immediately see that both spectrums look very similar to each other. However, the upper sideband of channel 2 spectrum appears to be higher than its lower sideband. This deviation in sideband flatness is not seen in channel 1 spectrum.

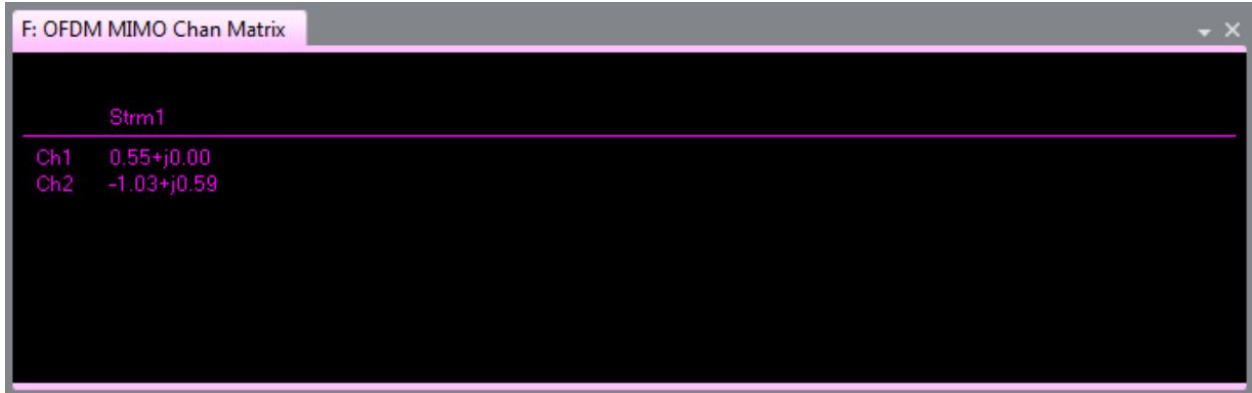


Figure 4.43: OFDM MIMO Channel Information Matrix

Figure 4.43 shows the channel information for stream 1. There were some issues with getting the 89600 software to receive and display data from stream 2. Stream 2 corresponds to the secondary incoming signals. Knowing this we can say that $h_{11}=0.55+j0.00$ and $h_{22}=-1.03+j0.59$ with h_{12} and h_{21} having unknown values.

Table 4.4: Compiled cases of EVM: SISO through MIMO

Case	In/Out	EVM (dB)	Ch1	Ch2	SNR
SISO	1x1	-30.955			27.255
SIMO	1x2	-30.932	-29.75	-32.562	27.232
MISO	2x1	-30.932			27.232
MIMO	2x2	-32.989	-31.311	-35.761	29.289
Adjacent antenna separation is 10 cm.					

$$SNR = - [3.7 + 20 * \log_{10} (EVM / 100\%)] \text{ for 64 QAM}$$

Equation 4.2: EVM-SNR theoretical equation, 64 QAM specific

Discussion:

Table 4.4 shows the compiled results for every single case. The equation underneath the table is specific for 64 QAM and is used to determine the SNR. The transmitter and receiver distance is kept constant at 1 meter, while the antenna separation for input or output are close to half a wavelength, at 10 cm. SNR is about the same for SISO, SIMO, and MISO. Note that for SIMO the second channel has a lower EVM, resulting in a higher SNR; however, the EVM column only takes into account the average of the two. The MIMO case has 2 dB higher signal power than noise relative all the other cases. While this may seem small, keep in mind that 2 dB greater in SNR for the same amount of input power will result in lower bit-error rate, allowing for faster and more robust communication. Also note that MIMO is an improvement over SIMO. Individually looking at the two channels, the EVM was lower for both channel 1 and channel 2 in the MIMO case by 2 to 3 dB. Although not intuitive from the data, MISO is a better case than SISO.

Although the results based on SNR look the same, MISO's worst case is better than SISO's worst case. For example, if one transmitter antenna was blocked physically, another antenna could send the signal. This could not be said about SISO. Real life examples where this situation may occur includes birds building nests around antennas, degrading the signal integrity of that antenna. Combining both SIMO and MISO produce the best case overall. The conclusion drawn from this data is that increasing spatial diversity results in a better signal overall.

Chapter 5: Conclusion and Recommendations

Originally, the plan was to create and test the beam forming capabilities of a 2x2 MIMO system. Unfortunately, due to the hardware not configuring correctly beamforming tests could not be performed. Instead EVM measurements were taken across SISO, SIMO, MISO, and MIMO configurations and compared to validate MIMO has a better SNR rate than any other configuration that was tested. The SNR rates for the SISO, MISO, SIMO, and MIMO tests are 27.255 dB, 27.232 dB, 27.232 dB, and 29.289 dB. These results show that MIMO had a 2 dB higher SNR and the SIMO and MISO tests had a similar performance to the SISO system. The performance of the communication systems demonstrated that increasing spatial diversity would generate a more robust received signal. The project also provided insight on the limits of using EVM with different levels of QAM. SISO testing revealed that any level higher than 128 QAM produces undesired results, so as a result the 802.11 n reference signal only used 64 QAM as its modulation.

Unlike the Keysight equipment, the antennas were created without too much difficulty. The main problem that arose was when the patch antenna dimensions got mixed up during milling. This resulted in the antennas not operating at the desired 1.3 GHz frequency. At first, conductive tape was added to the patch antennas to try and fix the erroneous dimensions, but this resulted in inconsistent return loss measurements in the antennas. The problem was addressed by remilling four new patch antennas with correct dimensions. The new antennas transmitted at 1.28 GHz, which is only a 1.5% error. Having a relatively small error is a success especially since the Keysight equipment can send signals at 1.28 GHz.

This project provides a solid base for future projects pertaining to MIMO. Future projects could include beamforming, investigations into more complex configurations such as 3x3 MIMO and 4x4 MIMO, and observing the effects a jammer signal has on the different communication systems. The background concepts discussed in this report provide a solid basic understanding of the key concepts of MIMO a person need to know before performing any MIMO experiments. The discussions on how to configure the VSAs and VSGs, build and characterize antennas, and how to use signal studio to communicate to the VSAs and VSGs are also integral concepts which form the base of a majority of future MIMO projects. Finally the collection of Keysight M9381A VSG and M9391A VSA will be very useful for future projects since they explain how to run basic tests and how to configure multiple chassis and the limitations for higher order MIMO system testing.

Appendix A: Senior Project Analysis

Advisor: Dr. Dennis Derickson

1. Summary of Functional Requirements:

As stated previously, this project is to build several unique communication systems and test them. The results of these test will be recorded, analyzed, and compiled into a final research report. Our findings will provide insight primarily to cellular service providers who may use our results to design the optimal method for cellular communication.

2. Primary Constraints:

The first challenge faced in this project was the understanding of digital communications. Digital Communications is considered to be a rather abstract concept and can be quite hard to grasp. Another aspect of this project that will prove to be difficult is understanding which MIMO implementations are the most important to analyze. MIMO designs are already in existence and being used today; determining ways to better these systems is a difficult task.

3. Economic:

Target of \$200 budget for the construction of all systems. Construct the hardware with materials available in the lab, and order the rest from vendors. Materials available in the lab include coaxial connectors, coaxial cables, wires, and some amplifiers. With the modulation and demodulation of the signal taken care of by the VSA and VSG, we will aim to construct the RF path. The ordered parts include amplifiers, an empty paint can and connectors. Since this is a research project, students will be unpaid. The main people that will benefit from our product are not the consumer, but whichever company uses our research to develop MIMO. Fortunately, our project will be primarily be done on the VSGs and VSAs in the Networks Lab. We will need to implement discrete hardware components such as antennas and amplifiers. The cost for these external components will be quite small.

4. If Manufactured on a Commercial Basis:

Our final product is not something that a typical consumer would purchase, however, how it is implemented may have a very large effect on the common consumer. In 2015, a total of 403

million smartphones were purchased; the total number sold increased by 9.7% in the fourth quarter of that year. Currently the average production cost for smartphones is \$220, the implementation of MIMO will raise that cost slightly (the main difference is adding antennas).

5. Environmental:

Lead-free designs will be used in the construction of the MIMO hardware. The European market disallows anything with Lead inside the design; if the product were to include lead, our customer base will disclude the entire European communications market. Furthermore, the power of the antennas will not exceed more than 1 watt for each transmission antenna. This is to comply with the Federal Communications Commission's standards.

6. Manufacturability:

The manufacturing process for smartphones has already been developed quite some time ago. If MIMO were to be implemented in the common modern phone, the manufacturing process would change very little. As stated in the previous section, the main change for cellular devices would be the increase in antennas. The manufacturing process would need to be adjusted such that the implementation of additional antennas could be accommodated. This change in process does not pose much of a threat to achieving MIMO integration into cellular devices.

7. Sustainability:

The designs will involve hardware that is not the newest but not obsolete either. This will ensure that hardware such as power amplifiers will be available to purchase over the course of 5 to 10 years. An upgrade that we could implement are multi-frequency amplifiers, this could allow for

the design to last longer when put into a cell phone. Upgrading the system would be a step that our customers would take. They would choose alternative ways to use MIMO.

8. Ethics:

There are a few ethical dilemmas that this MIMO research can encounter. The first covers the thought of 'who can this research be sold to?': Many people believe that MIMO is the future for digital communications. Depending on how MIMO is implemented, we may be encouraging a monopoly for cellular service providers. If a cellular service provider uses our research to implement the best method for digital communications, many consumers would change their provider to that company. Economic monopoly has been a major ethical issue for quite some time. Depending on how successful MIMO is, many companies that cannot compete will lose customers.

Eventually, most of the companies will cease to exist which will result in thousands of unemployed people. We are well aware that the concept of a monopoly is illegal, however there are many 'loopholes' that companies take advantage of. One of our potential customers are several branches of the military. When selling to the government, one often faces many ethical dilemmas due to the secrecy of the government. On one hand 'could our research assist in saving lives?' on the other hand 'will our research be put to unethical use that will lead to the loss of innocent lives?'

9. Health and Safety:

The implementation of MIMO poses little to no health threats. Even though MIMO itself does not directly pose any threats, cell phones still do. There have been many studies linking cell phone

use to an increased risk of certain types of cancer. Many people are concerned with the radio waves that come with cell phones. The increased number of antennas may facilitate an increase in the intensity of these radio wave, however, this is unlikely. As a safeguard, the research will comply with FCC standards of no more than one Watt of power delivered to the transmit antenna. Higher power may be detrimental to the health of living organisms around the RF device. For example, radiation from WiFi bands have been found to have negative effects on the body, such as altered brain tissue and lower sperm count.

10. Social and Political:

The implementation of MIMO should be in accordance to the Federal Communications Commission's standards. This means that the research will utilize amateur radio bands, and avoid bands not available to the public. Violating the FCC standards may result in heavy fines. The social analysis is that cellular providers are able to view this research equally. For companies that already use a MIMO implementation in their system, this may be seen as detrimental to their business, as competitors may gain insight to MIMO technology. For cellular companies that have not utilized MIMO, this will provide valuable knowledge to their research and development groups. For researchers, this MIMO research may confirm their theoretical MIMO models and prove to be beneficial to the research community.

11. Development:

At the conclusion of the project a working understanding of the basic principles of characterizing the performance of different communication system was obtained. To put these principles into use a greater understanding of antennas, how to configure the Keysight PXIe vector signal

analyzers and vector signal generators, and how to use the 89600 VSA and signal studio programs to transmit and analyze a received modulated WiFi signal was necessary. Specifically the project required understanding on how to build a patch and a can antenna, as well as how to determine the transmitting frequencies. Also to gether the radiation patterns an understanding of how to use the anechoic chamber was also acquired. To generate the testing configuration of the Keysight PXIe vector signal analyzers and vector signal generators a greater understanding of how the VSA and VSG are connected both internally and externally was acquired. Also how to use Visual Studio to open drivers and control the individual VSA and VSG signals was also obtained. Finally, good communication, problem solving, and time management skills were also improved.

12. Bill of Materials:

#	Part/Process	Description	Quantity	Price	Cost
1	ACX1230-ND	Connector SMA JACK, 50 OHM	4	\$4.68	\$18.72
2	ERA-3+	TB, ERA-3, VV105,50 OHM /ROHS	4	\$1.80	\$7.20
3	Patch Antenna Milling Process	IEEE Milling	8	\$8.00	\$64.00
4	Copper Tape	Copper Tape	1	\$16.00	\$16.00
5	Empty Quart Paint Can	Cantenna can	1	\$11.75	\$11.75
				Total:	\$116.92

Appendix B: References

MIMO Resources

[1] Langton Charan and Bernard Sklar. (2011). *Tutorial 27 -Finding MIMO* [Online]. Available

FTP:<http://complextoreal.com/wp-content/uploads/2013/01/mimo.pdf>

[2] D. Tse and P. Viswanath, <https://people.eecs.berkeley.edu>, 2005. [Online]. Available:

https://people.eecs.berkeley.edu/~dtse/Chapters_PDF/Fundamentals_Wireless_Communication_chapter7.pdf. [Accessed: 07- Jun- 2017].

[3] J. Proakis and M. Salehi, "Digital Transmission on Fading Multipath Channels - National Instruments", *Ni.com*, 2017. [Online]. Available: <http://www.ni.com/white-paper/14931/en/>.

[Accessed: 07- Jun- 2017].

[4] C. McKell, "https://polylearn.calpoly.edu/AY_2016-2017/pluginfile.php/328798/mod_resource/content/0/MIMO%20and%20Info%20Theory.pdf", 186-C102, 2016.

[5] "Singular Value Decomposition (SVD) tutorial", *Web.mit.edu*, 2017. [Online]. Available:

http://web.mit.edu/be.400/www/SVD/Singular_Value_Decomposition.htm. [Accessed: 07- Jun- 2017]

[6] C. Beard and W. Stallings, *Wireless Communication Networks and Systems*. 2016, p. 9, 22, 40, 93-146, 156, 236-250, and 282.

<http://study.com/academy/lesson/stretching-compression-of-logarithmic-graphs.html>

[7] "MIMO", en.wikipedia.org, 2017. [Online]. Available:

<https://en.wikipedia.org/wiki/MIMO> [Accessed: 02-October-2016].

[8] "Convolutional Code", en.wikipedia.org, 2017. [Online]. Available:

https://en.wikipedia.org/wiki/Convolutional_code [Accessed: 25-May-2017].

- [9] "Multipath Propagation", en.wikipedia.org, 2017. [Online]. Available:
https://en.wikipedia.org/wiki/Multipath_propagation [Accessed: 03-October-2016].
- [10] "Fading", en.wikipedia.org, 2017. [Online]. Available:
<https://en.wikipedia.org/wiki/Fading> [Accessed: 28-May-2017].
- [11] "Rayleigh Distribution", en.wikipedia.org, 2017. [Online]. Available:
https://en.wikipedia.org/wiki/Rayleigh_distribution [Accessed: 05-June-2017].
- [12] "Rayleigh Fading", en.wikipedia.org, 2017. [Online]. Available:
https://en.wikipedia.org/wiki/Rayleigh_fading [Accessed: 05-June-2017].
- [13] "Rice Distribution", en.wikipedia.org, 2017. [Online]. Available:
https://en.wikipedia.org/wiki/Rice_distribution [Accessed: 05-June-2017].
- [14] "Rician Fading", en.wikipedia.org, 2017. [Online]. Available:
https://en.wikipedia.org/wiki/Rician_fading [Accessed: 05-June-2017].
- [15] Charan Langton. (2013). *Tutorial 22 -Orthogonal Frequency Division Multiplexing* [Online].
Available FTP:<http://complextoreal.com/wp-content/uploads/2013/01/ofdm2.pdf>

Keysight and VSA/VSG resources

- [16] "Vector Signal Analyzer", en.wikipedia.org, 2017. [Online]. Available:
https://en.wikipedia.org/wiki/Vector_signal_analyzer [Accessed: 07- Jun- 2017].
- [17] I. Poole, "Vector Signal Generator | VSG Generator | Radio-Electronics.Com",
Radio-electronics.com, 2017. [Online]. Available:
http://www.radio-electronics.com/info/t_and_m/generators/vector-signal-generator-vsg.php.
[Accessed: 07- Jun- 2017].
- [18] "Intermediate Frequency", en.wikipedia.org, 2017. [Online]. Available:
https://en.wikipedia.org/wiki/Intermediate_frequency [Accessed: 07- Jun- 2017].

[19]"Keysight Technologies M9381A PXIe Vector Signal Generator 1 MHz to 3 GHz or 6 GHz Data Sheet", *Literature.cdn.keysight.com*, 2017. [Online]. Available:

<http://literature.cdn.keysight.com/litweb/pdf/5991-0279EN.pdf>. [Accessed: 07- Jun- 2017].

[20]"Keysight Technologies M9391A PXIe Vector Signal Analyzer 1 MHz to 3 GHz or 6 GHz Data Sheet", *Literature.cdn.keysight.com*, 2017. [Online]. Available:

<http://literature.cdn.keysight.com/litweb/pdf/5991-2603EN.pdf>. [Accessed: 07- Jun- 2017].

[21]"Keysight LTE/LTE-A Multi-Channel Reference Solution Startup Guide",

Literature.cdn.keysight.com, 2017. [Online]. Available:

<http://literature.cdn.keysight.com/litweb/pdf/Y1299-90001.pdf?id=2413851>. [Accessed: 07- Jun- 2017].

[22]"Keysight LTE/LTE-A Multi-Channel Reference Solution User's Guide",

Literature.cdn.keysight.com, 2017. [Online]. Available:

<http://literature.cdn.keysight.com/litweb/pdf/Y1299-90005.pdf?id=2655403>. [Accessed: 07- Jun- 2017].

[23]"Keysight M9391A PXIe Signal Analyzer & M9381A PXIe Vector Signal Generator 1 MHz to 3 GHz or 6 GHz Startup Guide", *keysight.com*, 2017. [Online]. Available:

http://edownload.software.keysight.com/Modular/M938XA/2.1/M9391_and_M9381_StartupGuide.pdf?__gda__=1496885723_d25bf157871f111fb6d27d15da2cd2b8&fileExt=.pdf. [Accessed: 07- Jun- 2017].

[24]"Keysight M9391A Pxi Vector Signal Analyzer & M9381A PXIe Vector Signal Generator

Programming Guide", *www.keysight.com*, 2017. [Online]. Available:

http://edownload.software.keysight.com/Modular/M938XA/2.1/M9391_and_M9381_ProgrammingGuide.pdf?__gda__=1496884677_697c82329541458461f97c9851df42a1&fileExt=.pdf.

[Accessed: 07- Jun- 2017].

Antenna and Preamplifier Resources

[25] P. Bevelacqua, "The Antenna Theory Website", *Antenna-theory.com*, 2017. [Online]. Available:

<http://www.antenna-theory.com/>. [Accessed: 07- Jun- 2017].

[26]"Satellite frequency bands", *European Space Agency*, 2017. [Online]. Available:

http://m.esa.int/spaceinimages/Images/2013/11/Satellite_frequency_bands. [Accessed: 07- Jun- 2017].

[27]I. Giangrandi, "Field regions around an antenna", *Giangrandi.ch*, 2017. [Online]. Available:

<http://www.giangrandi.ch/electronics/anttool/regions.shtml>. [Accessed: 07- Jun- 2017].

[283]"Antenna Near Field & Field Distance Calculator", *everythingRF*, 2015. [Online]. Available:

<https://www.everythingrf.com/rf-calculators/antenna-near-field-distance-calculator>. [Accessed: 07- Jun- 2017].

[29]*Wisense.files.wordpress.com*, 2017. [Online]. Available:

<https://wisense.files.wordpress.com/2014/12/isotropic-12.png?w=418&h=428>. [Accessed: 07- Jun- 2017].

Appendix C: Vector Signal Generator C# Code

Adapted from Keysight's 'Example_MIMOConsoleApp.cs' located in:

C:\Program Files (x86)\Agilent\M938x\Help\Examples

To open this code, open Visual Studio 'File' → 'Open' → 'Project/Solution...' →

'ConsoleApplication14' → 'ConsoleApplication14'

```

1  #region Specify using Directives
2  using System;
3  using System.Collections.Generic;
4  using System.Linq;
5  using System.Text;
6  using Ivi.Driver.Interop;
7  using Agilent.AgM938x.Interop;
8  using Agilent.AgM9300.Interop;
9  using Agilent.AgM9018.Interop;
10 #endregion
11
12 namespace MIMOConsoleApp
13 {
14     class Program
15     {
16         static void Main(string[] args)
17         {
18             int numChannels = 2;        // Set to "2", "3", or "4"
19             bool simulateHardware = false; // Set to "false" when connecting real hardware.
20
21             #region Create Driver Instances
22             IAgM938xEx M9381A_VSG1 = new AgM938x(); // Create VSG 1
23             IAgM938xEx M9381A_VSG2 = new AgM938x(); // Create VSG 2, Used by 2x2 MIMO
24             IAgM9300Ex M9300A_REF1 = new AgM9300(); // Create the Reference
25             IAgM9018 M9018A_CHASSIS1 = new AgM9018(); // Create Chassis
26             #endregion
27
28             try
29             {
30                 #region Initialize Driver Instances and Check for Errors
31                 bool IdQuery = true;
32                 bool Reset = true;
33                 int errorcode = -1;
34                 string message = string.Empty;
35
36                 // Resource Name Addresses
37                 string M9381A_VSG1_ResourceName = "PXI7::0::0::INSTR;PXI12::0::0::INSTR;PXI13::0::0::INSTR;PXI20::0::0::INSTR";
38                 string M9381A_VSG2_ResourceName = "PXI27::0::0::INSTR;PXI26::0::0::INSTR;PXI21::0::0::INSTR";
39                 string M9381A_VSGx_OptionString = string.Format(
40                     "QueryInstrStatus=true, Simulate={0}, M9381Setup= Model=, Trace=false", (simulateHardware ? "true" : "false"));
41
42                 string M9300A_REF1_ResourceName = "PXI20::0::0::INSTR";
43                 string M9300A_REF1_OptionString = string.Format(
44                     "QueryInstrStatus=true, Simulate={0}, M9300Setup= Model=, Trace=false", (simulateHardware ? "true" : "false"));
45
46                 string M9018A_CHASSIS1_ResourceName = "PXI15::0::0::INSTR";
47                 string M9018A_CHASSIS1_OptionString = string.Format(
48                     "QueryInstrStatus=true, Simulate={0}, M9018Setup= Model=, Trace=false", (simulateHardware ? "true" : "false"));
49
50
51
52
53
54                 // Initialize M9018A PXIe Chassis 1
55                 M9018A_CHASSIS1.Initialize(M9018A_CHASSIS1_ResourceName, IdQuery, Reset, M9018A_CHASSIS1_OptionString);
56                 Console.WriteLine("M9018A PXIe Chassis 1 - Driver Initialized");
57
58                 //Initialize M9300A PXIe Reference and clear startup messages & warnings, if any.
59                 M9300A_REF1.Initialize(M9300A_REF1_ResourceName, IdQuery, Reset, M9300A_REF1_OptionString);
60                 do
61                 {
62                     M9300A_REF1.Utility.ErrorQuery(ref errorcode, ref message);
63                     if (errorcode != 0)
64                         Console.WriteLine(message);
65                 } while (errorcode != 0);
66                 Console.WriteLine("M9300A PXIe Reference - Driver Initialized");
67
68                 //Initialize M9381A Channel 1 and clear startup messages & warnings, if any.
69                 M9381A_VSG1.Initialize(M9381A_VSG1_ResourceName, IdQuery, Reset, M9381A_VSGx_OptionString);
70                 do
71                 {
72                     M9381A_VSG1.Utility.ErrorQuery(ref errorcode, ref message);
73                     if (errorcode != 0)
74                         Console.WriteLine(message);

```

```

74         Console.WriteLine(message);
75     } while (errorcode != 0);
76     Console.WriteLine("M9381A PXIe VSG Channel 1 - Driver Initialized");
77
78     //Initialize M9381A Channel 2 and clear startup messages & warnings, if any.
79     M9381A_VSG2.Initialize(M9381A_VSG2_ResourceName, IdQuery, Reset, M9381A_VSGx_OptionString);
80     do
81     {
82         M9381A_VSG2.Utility.ErrorQuery(ref errorcode, ref message);
83         if (errorcode != 0)
84             Console.WriteLine(message);
85     } while (errorcode != 0);
86     Console.WriteLine("M9381A PXIe VSG Channel 2 - Driver Initialized");
87
88
89     #endregion
90
91
92
93     #region Route Backplane Triggers from M9300A to VSGs, EXTERNAL/ALC TRIGGER on VSGs, MASTER/SLAVE Backplane Triggers on VSAs
94
95     #region numChannels == 2
96     if (numChannels == 2)
97     {
98         // Two M9381A PXIe VSGs and Two M9391A PXIe VSAs in one M9018A PXIe Chassis
99         // /-----:-----\
100        // |           :           :           :
101        // |           :<-Bus Segment 1->:<-Bus Segment 2->:<-Bus Segment 3->:
102        // |           :           :           :
103        // |           : 1| 2--3| 4| 5| 6: 7| 8| 9|10|11|12:13|14|15-16|17|18:
104        // |           : %<---VSG1-->% %<-VSA1-->%R %<-VSA2-->% %<---VSG2-->%
105        // |           :           : e           :           :
106        // |           :           : f           :           :
107        // |           :           :           :           :
108        // /-----:-----\
109        //
110        Console.WriteLine("\nRoute Backplane Triggers for VSGs in 2x2 MIMO Chassis 1:");
111        // Route Backplane External Trigger from M9300A to each M9311A (VSG) for Playback synchronization (slot 10 to 2, 15, 7, 11)
112        M9018A_CHASSIS1.TriggerBus.Connect(0, Agilent.Ag#M9018.Interop.Ag#M9018TrigBusEnum.Ag#M9018TrigBus2To1And3);

113
114        Console.WriteLine("\tVSGs TRIG 0: Connect Bus 2 to 1 and 3: \n_
115            '\tso that the M9300A PXIe Reference can generate a \n\t\
116            'Synchronization Playback Trigger' on PXI TRIG 0 \n\t...this trigger will be received by VSG 1 and VSG 2.\n");_
117
118        // Use Default Backplane Triggers for VSG1
119        Console.WriteLine("\tVSG1 TRIG 6: Uses Bus Segment 1: 'EXTERNAL TRIGGER' M9301A to M9311A"); // (slot 5 to 2)
120        Console.WriteLine("\tVSG1 TRIG 7: Uses Bus Segment 1: 'ALC TRIGGER' M9311A to M9310A"); // (slot 2 to 4)
121
122        // Use Default Backplane Triggers for VSG2
123        Console.WriteLine("\tVSG2 TRIG 6: Uses Bus Segment 3: 'EXTERNAL TRIGGER' M9301A to M9311A"); // (slot 18 to 15)
124        Console.WriteLine("\tVSG2 TRIG 7: Uses Bus Segment 3: 'ALC TRIGGER' M9311A to M9310A"); // (slot 15 to 17)
125
126        Console.WriteLine("\nRoute MASTER/SLAVE Backplane Triggers for VSAs in 2x2 MIMO Chassis 1:");
127        // MASTER/SLAVE Backplane Triggers are used to coordinate the capture alignments on the VSA
128        M9018A_CHASSIS1.TriggerBus.Connect(1, Agilent.Ag#M9018.Interop.Ag#M9018TrigBusEnum.Ag#M9018TrigBus2To3);
129        Console.WriteLine("\tVSA1 to VSA2 TRIG 1: Connect Bus 2 to 3: MASTER to SLAVE");
130
131        M9018A_CHASSIS1.TriggerBus.Connect(2, Agilent.Ag#M9018.Interop.Ag#M9018TrigBusEnum.Ag#M9018TrigBus3To2);
132        Console.WriteLine("\tVSA2 to VSA1 TRIG 2: Connect Bus 3 to 2: SLAVE to MASTER");
133    }
134    #endregion
135
136    #endregion
137
138    #region Setting Up the M9381A PXIe VSGs for WLAN Rx Testing
139    // These commands are sent to each VSG Driver, "Apply" or "PlayArb" methods start them playing on real hardware.
140
141    Console.WriteLine("\nSet each M9381A PXIe VSG to the following settings:");
142
143    M9300A_REF1.ReferenceBase2.ProgrammableOutputTrigger2.Destination = Ag#M9300TriggerEnum.Ag#M9300TriggerPXITrigger0;
144    M9300A_REF1.Apply();
145    Console.WriteLine("\tGenerate a 'Playback Synchronization Trigger' _
146        '\n\tfrom the M9300A PXIe Reference, on PXI TRIG 0, \n\tso that each M9381A PXIe VSG starts waveform playback.");_
147
148    // Configure all M9381A PXIe VSGs to listen for an External Trigger on PXI TRIG 0.
149    if (!simulateHardware)
150    {
151        Console.WriteLine("\nConfigure the 'External Trigger' on the _
152            '\n\tbackplane PXI TRIG 0 line to deliver a \n\t'Synchronization Playback Trigger' \n\tfrom the M9300A PXIe Reference.");_

```

```

153 M9381A_VSG1.Triggers.ExternalTrigger.Configure(true, 0.01, 0.5, AgM938xTriggerSlopeEnum.AgM938xTriggerSlopePositive,
154 AgM938xTriggerEnum.AgM938xTriggerPXITrigger0, AgM938xTriggerTerminationEnum.AgM938xTriggerTermination500hm, 10000,
155 AgM938xTimeoutModeEnum.AgM938xTimeoutModeTimeoutAbort);
156 Console.WriteLine("\t...to VSG 1");
157 M9381A_VSG2.Triggers.ExternalTrigger.Configure(true, 0.01, 0.5, AgM938xTriggerSlopeEnum.AgM938xTriggerSlopePositive,
158 AgM938xTriggerEnum.AgM938xTriggerPXITrigger0, AgM938xTriggerTerminationEnum.AgM938xTriggerTermination500hm, 10000,
159 AgM938xTimeoutModeEnum.AgM938xTimeoutModeTimeoutAbort);
160 Console.WriteLine("\t...to VSG 2");
161 }
162
163 Console.WriteLine("\nConfigure the 'External Trigger' on the \n\backplane PXI TRIG 0 line to deliver a \n\t)
164 'Synchronization Playback Trigger' \n\tfrom the M9300A PXIe Reference:");
165
166
167 // Disable ALC for WLAN waveforms to achieve best Residual EVM
168 Console.WriteLine("\n\tDisable ALC for WLAN waveforms to achieve best Residual EVM:");
169 M9381A_VSG1.ALC.Enabled = false;
170 Console.WriteLine("\t... on VSG 1");
171 M9381A_VSG2.ALC.Enabled = false;
172 Console.WriteLine("\t... on VSG 2");
173
174
175 // Enable Pulse Blanking to achieve Best Off Time Rejection
176 //
177 // Note - The following commands are dependent on whether or not
178 // the waveform being used contains pulse blanking markers
179 Console.WriteLine("\n\tEnable Pulse Blanking to achieve Best Off Time Rejection:");
180 M9381A_VSG1.RF.OutputPulseMode = AgM938xOutputPulseModeEnum.AgM938xOutputPulseModePulseOnWithTrigger;
181 Console.WriteLine("\t... on VSG 1");
182 M9381A_VSG2.RF.OutputPulseMode = AgM938xOutputPulseModeEnum.AgM938xOutputPulseModePulseOnWithTrigger;
183 Console.WriteLine("\t... on VSG 2");
184
185
186
187 // Set PLL MODE to Best Wide Offset
188 Console.WriteLine("\n\tSet PLL MODE to Best Wide Offset:");
189 M9381A_VSG1.Modules.Synthesizer.PLLMode = AgM938xSynthesizerPLLModeEnum.AgM938xSynthesizerPLLModeBestWideOffset;
190 Console.WriteLine("\t... on VSG 1");
191 M9381A_VSG2.Modules.Synthesizer.PLLMode = AgM938xSynthesizerPLLModeEnum.AgM938xSynthesizerPLLModeBestWideOffset;
192 Console.WriteLine("\t... on VSG 2");

```

```

196 // Sets RF Frequency
197 Console.WriteLine("\n\nWhat is the desired Modulation Frequency in Hz?");
198 double Frequency = Convert.ToDouble(Console.ReadLine());
199 double FreqGHz = Frequency / 1e9;
200 Console.WriteLine("\n\nDesired Modulation Frequency: {0} GHz", FreqGHz);
201
202 Console.WriteLine("\n\tSet RF Frequency:");
203 M9381A_VSG1.RF.Frequency = Frequency;
204 Console.WriteLine("\t... on VSG 1 to {0}", Frequency);
205 M9381A_VSG2.RF.Frequency = Frequency;
206 Console.WriteLine("\t... on VSG 2 to {0}", Frequency);
207
208
209
210 // Sets Amplitude (Power/Level) of VSG1
211 Console.WriteLine("\n\nWhat is the desired Power Level of VSG 1? (in dBm)");
212 double LevelVSG1 = Convert.ToDouble(Console.ReadLine());
213
214 // Sets Amplitude (Power/Level) of VSG2
215 Console.WriteLine("\n\nWhat is the desired Power Level of VSG 2? (in dBm)");
216 double LevelVSG2 = Convert.ToDouble(Console.ReadLine());
217
218 Console.WriteLine("\tSet the amplitude (power/level) of the RF output signal in dBm:");
219 M9381A_VSG1.RF.Level = LevelVSG1;
220 Console.WriteLine("\t... on VSG 1 to {0} dBm", LevelVSG1);
221 M9381A_VSG2.RF.Level = LevelVSG2;
222 Console.WriteLine("\t... on VSG 2 to {0} dBm", LevelVSG2);
223
224
225 // Enables Modulation
226 // If working in simulation mode, there is no way to enable modulation and the following error will be returned:
227 // "AgM938x: Instrument model does not support this feature: get_Modulation."
228 // Use the following if statement to avoid this error during simulation mode.
229 if (!simulateHardware)
230 {
231 Console.WriteLine("\tEnable Modulation:");
232 M9381A_VSG1.Modulation.Enabled = true;
233 Console.WriteLine("\t... on VSG 1");
234 M9381A_VSG2.Modulation.Enabled = true;
235 Console.WriteLine("\t... on VSG 2");

```

```

235         Console.WriteLine("\t... on VSG 2");
236     }
237 }
238 else
239     Console.WriteLine("\tEnable Modulation:");
240
241 // Enables RF Output
242 Console.WriteLine("\tEnable RF Output:");
243 M9381A_VSG1.RF.OutputEnabled = true;
244 Console.WriteLine("\t... on VSG 1");
245 M9381A_VSG2.RF.OutputEnabled = true;
246 Console.WriteLine("\t... on VSG 2");
247
248
249 #endregion
250
251 #region Start Waveform Playback on the M9381A PXIe VSGs
252
253 // Specify a waveform file to upload and play
254 // If a Signal Studio waveform file is used, it may require a software license.
255 string ExamplesFolder = "C:\\Program Files (x86)\\Agilent\\M938x\\Example Waveforms\\";
256 //string WaveformFile = "MLAM_11ac_64QAM_160MHz.wfm";
257 Console.WriteLine("\n\nPlease specify the desired waveform \nMust come from C:\\Program Files (x86)\\Agilent\\M938x\\Example Waveforms\\ \nWaveform:");
258 string WaveformFile = Console.ReadLine();
259 string ArbFileName = ExamplesFolder + WaveformFile;
260 string mWaveformHandle = "Mod Waveform";
261
262
263 // Upload a waveform file
264 // If working in simulation mode, there is no way to upload a waveform file and the following error will be returned:
265 // "AgM938x: Instrument model does not support this feature: get_Modulation."
266 // Use the following if statement to avoid this error during simulation mode.
267 if (!simulateHardware)
268 {
269     Console.WriteLine("\n\nUpload the following waveform file: \n\t{0}", WaveformFile);
270     M9381A_VSG1.Modulation.IQ.UploadArbAgilentFile(mWaveformHandle, ArbFileName);
271     Console.WriteLine("\t...to VSG 1");
272     M9381A_VSG2.Modulation.IQ.UploadArbAgilentFile(mWaveformHandle, ArbFileName);
273     Console.WriteLine("\t...to VSG 2");
274 }
275 }
276 else
277     Console.WriteLine("\n\nUpload the following waveform file to each VSG: \n\t{0}", WaveformFile);
278
279
280 System.Threading.Thread.Sleep(100);
281 bool continuous = true;
282
283 // Play a waveform file
284 if (continuous == true)
285 {
286     // If working in simulation mode, there is no way to upload/play a waveform file and the following error is returned:
287     // "AgM938x: Validation error - The name Mod Waveform is not in the uploaded ARB waveform catalog"
288     // Use the following if statement to avoid this error during simulation mode.
289     if (!simulateHardware)
290     {
291         Console.WriteLine("\nPlay the uploaded waveform file:");
292         M9381A_VSG1.Modulation.PlayArb(mWaveformHandle, AgM938xStartEventEnum.AgM938xStartEventExternalTrigger);
293         Console.WriteLine("\t...using VSG 1");
294         M9381A_VSG2.Modulation.PlayArb(mWaveformHandle, AgM938xStartEventEnum.AgM938xStartEventExternalTrigger);
295         Console.WriteLine("\t...using VSG 2");
296         System.Threading.Thread.Sleep(100);
297     }
298     else
299         Console.WriteLine("\nPlay the uploaded waveform file on VSGs.");
300 }
301
302 // Generate a sync pulse on the M9300 reference module, on PXI TRIG 0
303 M9300A_REF1.ReferenceBase2.ProgrammableOutputTrigger2.GenerateTrigger();
304
305 // -----
306 // Once a waveform is playing, continue with the section:
307 // "Use 89600 VSA Software to Control the M9391A PXIe VSAs and Perform Transmitter Tests"
308 Console.WriteLine("\n\nProceed to the next section of the Programming Guide:");
309 Console.WriteLine("...and \Use 89600 VSA Software to Control all M9391A PXIe VSAs\");
310 #endregion
311

```



```

311     }
312 }
313 catch (Exception ex)
314 {
315     Console.WriteLine("\nExceptions for the drivers:\n");
316     Console.WriteLine(ex.Message);
317 }
318 finally
319 {
320     #region Close Driver Instances
321     Console.WriteLine("\n\nPress Enter to Stop Playing Waveforms and Close Drivers");
322     Console.ReadLine();
323     {
324         if (M9381A_VSG2 != null && M9381A_VSG2.Initialized)
325         {
326             M9381A_VSG2.Close();
327             Console.WriteLine("M9381A PXIe VSG Channel 2 - Closed");
328         }
329         if (M9381A_VSG1 != null && M9381A_VSG1.Initialized)
330         {
331             M9381A_VSG1.Close();
332             Console.WriteLine("M9381A PXIe VSG Channel 1 - Closed");
333         }
334         if (M9300A_REF1 != null && M9300A_REF1.Initialized)
335         {
336             M9300A_REF1.Close();
337             Console.WriteLine("M9300A PXIe Reference - Closed");
338         }
339         if (M9018A_CHASSIS1 != null && M9018A_CHASSIS1.Initialized)
340         {
341             M9018A_CHASSIS1.Close();
342             Console.WriteLine("M9018A PXIe Chassis 1 - Closed");
343         }
344     }
345 }
346 #endregion
347
348

```

```

348
349
350     Console.WriteLine("\nDone - Press Enter to Exit");
351     Console.ReadLine();
352 }
353 }
354 }
355 }
356 }
357 }
358

```